Design of inhaled insulin dry powder formulations to bypass deposition in the human extrathoracic region and enhance lung targeting

Keith Try Ung

A thesis submitted in fulfillment
of the requirements for a degree
of Doctor of Philosophy

Faculty of Pharmacy the
University of Sydney

2016

Preface

The work described in this thesis was carried out at Novartis Pharmaceuticals Corp. in San Carlos, California USA, under the supervision of Dr. Nagaraja Rao (Novartis, San Carlos, CA) and Professor Hak-Kim Chan (Faculty of Pharmacy, University of Sydney). This thesis has not been submitted for a degree at any other university. Full acknowledgement has been made where the work of others has been cited or used. A list of publications is included in support of this thesis.

Keith Try Ung

Abstract

The effectiveness of aerosol drug delivery to the lungs depends on both the drug formulation and device. Currently marketed inhalation drug products often deliver no more than 15 – 30% of the packaged dose to the lung, either due to losses in the inhaler device, or deposition in the patient's mouth-throat. This poses a significant challenge in the development of inhalation drugs, as it can dictate higher nominal doses in order to compensate for losses, and can result in increased systemic exposure for drugs that are orally bioavailable and, in some instances, increases in local and systemic side effects (e.g., for inhaled corticosteroids). In addition, large extrathoracic region losses can lead to increased variance in dose delivery to the lung. The goal of this research was to demonstrate that for dry powder inhalers, improved targeting to the lungs may be achieved by tailoring the micromeritic properties of the particles (e.g., size, density, and rugosity) to reduce deposition in the mouth and throat to negligible levels, thereby maximizing the total dose delivered to the lung.

Spray drying is becoming more widely used in the manufacture of dry powder formulations for inhalation, as it provides a way to tailor particle properties so that they are more readily dispersed and efficiently delivered to the lung. One focus of this research was to use co-solvent spray drying to produce dry powder formulations of insulin (a model compound) with varying micromeritic properties, and relate the powder properties to *in vitro* aerosol dose delivery performance with inhaler devices. It is shown here that insulin particle size and density can be modulated by adding small amounts of ethanol (<10% v/v) to the aqueous solution feedstock of insulin, together with varying spray drying process parameters such as solids content and air-to-liquid ratio (ALR). Spray dried insulin powders covering a range of

particle size and density have been tested with dry powder inhalers to identify a particle design space where dose delivery to the lung is greatly enhanced.

A second focus of this research has been to develop an *in vitro* methodology for comparative assessments of the dose delivery performance of inhaled drugs. The conventional approach was to use cascade impactors to measure aerodynamic particle size distributions (APSD) of aerosolized drugs, and interpret the size distribution data to draw conclusions about dose delivered to the lung. While the cascade impactor approach is widely used as a "quality control" test to differentiate batches of the same product, it is not well suited for comparative performance assessments of inhalation drug products of different designs, or under different use conditions. The methodology developed here provides a more direct measure of dose delivery performance for such applications. It uses an idealized anatomical model of an adult human mouth and throat (the "Alberta idealized throat", AIT) to more realistically estimate the "total lung dose" (TLD) that is delivered from an inhalation drug product, under conditions that are relevant to clinical use. The utility of the AIT in performance assessment of inhalation drug products is demonstrated here by studying the sensitivity of different types of dry powder inhalers that includes key patient-use parameters such as peak inspiratory flow-rate (PIFR) and ramp-up rate of the inspiratory flow.

Finally, the AIT approach is also used to assess the dose delivery performance of the prototype insulin powders with two types of DPIs. *In vitro* test results with the AIT suggest that a remarkably high degree of potential lung targeting can be achieved with engineered powders, almost completely bypassing deposition in the extrathoracic region. Under the most favorable conditions tested, a TLD of ~96% is achieved, i.e., ~98% of the delivered dose in the inhaler is delivered past the mouth and throat and to the lung.

Table of contents

Acknowledgments

I sincerely thank Professor Hak-Kim Chan and associate supervisor Dr. Nagaraja Rao for their guidance and mentorship through my candidature. My personal thanks go to Dr. Andrew R Clark and Dr. Jeffrey G Weers for their encouragement and continued support to allow all my research projects to be conducted at Novartis San Carlos, California site. And, countless colleagues and friends (without naming names) at Novartis who kindly provided their invaluable time to assist with data and publications review. Lastly, it would not have been possible to accomplish my research work without Novartis Pharmaceuticals Corp. financial support through the Novartis Tuition Reimbursement Program and available resources (equipment and materials access) at the San Carlos, California site.

I want to extend my thanks to my beautiful wife and two children for their patience, support, and encouragement for the past years to allow me to concentrate on my research work. I also would like to conclude this chapter of my life and dedicate this thesis to my grandmother and Aunt Jean for raising me from the age of 5 years old, after I lost my parents and siblings during the Cambodian Civil War from 1970 – 1975. In this life, it was unfortunate they never had an opportunity to meet my children and witness one of my life accomplishments.

Publications

Original articles

Ung TK, Rao N, Weers JG, Clark AR, and Chan H-K. *In vitro* assessment of dose delivery performance of engineered dry powders for inhalation. *Aerosol Sci. & Tech*. 2014; **48**: 1099 – 1110.

Ung TK and Chan H-K. Effects of ramp-up of inspired airflow on in vitro aerosol dose delivery performance for certain dry powder inhalers. *Eur. J. Pharm. Sci*. 2016; **84**: 46 – 54.

Ung TK, Rao N, Weers JG, Huang D, and Chan H-K. Design of spray dried insulin microparticles to bypass deposition in the extrathoracic region and maximize total lung delivery. *Int. J. Pharm.* 2016; **511**: 1070 – 1079.

Other Publications during the Candidature

Weers JG, Clark AR, Rao N, **Ung K**, Haynes A, Khindri SK, Sheryl A, Perry SA, Machineni S, and Colthorpe P. *In vitro–in vivo* correlations observed with indacaterol-based formulations delivered with the Breezhaler®. *J. Aerosol Med.* 2015; **28**: 1 – 13.

Haynes A, Ament B, Heng C, Le J, **Ung K**, Rao R, Malcolmson R, Weers J, Pavkov R, Heuerding S, and Geller DE. "In-vitro Aerosol Delivery Performance of Tobramycin Powder for Inhalation (TOBI® Podhaler®) Using Inspiratory Flow Profiles from Cystic Fibrosis Patients" Poster presented at the North American Cystic Fibrosis Conference, Salt Lake City, Utah, USA, October 17 – 19 (2013).

Weers JG, **Ung K**, Le J, Rao N, Ament B, Axford G, Maltz D, and Chan L. Dose Emission Characteristics of Placebo PulmoSphere® Particles Are Unaffected by a Subject's Inhalation Maneuver. *J. Aerosol Med.* 2013; **26**: 56 – 68.

Ung TK, Axford G, Chan L, Glusker M, Le J, Maltz D, Rao N, and Weers JG. Effect of powder release kinetics on the performance of a dry powder inhaler. *Resp. Drug Delivery*. 2012; **3**: 627 – 630.

Weers JG, Maltz DS, **Ung K**, Chan L, Glusker M, Ament B, Le J, Rao N, and Axford G. Minimizing Human Factors Effects through Inhaler Design. *Resp. Drug Delivery*. 2012; pp. 217 – 226.

List of Figures

List of Tables

Abbreviations

AIT	Alberta Idealized Throat
ANOVA	Analysis of Variance
DD	Delivered Dose
DPI	Dry Powder Inhaler
EDF	Emitted Dose Fraction
FPM	Fine Particle Mass
GSD	Geometric Standard Deviation
HPLC	High Performance Liquid Chromatography
IPS2	Inhalation Profile Simulator 2
kPa	Kilopascal
LC	Label Claim
L/min	Liters per Minute
NGI	Next Generation Impactor
pMDI	Pressurized Metered Dose Inhaler
Q	Volumetric Flow-Rate
MMAD	Mass Median Aerodynamic Diameter
ms	Millisecond
R	Flow Resistance
SD	Standard Deviation
TLD	Total Lung Dose
URT	Upper Respiratory Tract
VMD	Volume Median Diameter

Chapter 1

Introduction

1.1 Aim

This thesis aims to provide a clear understanding on the design of engineered particles for use in inhaled drug products such as dry powder inhalers (DPIs) to control unwanted deposition in the extrathoracic region, and enhance targeting of the lung. Deposition in the mouth-throat poses a significant challenge to the effectiveness of an inhaled drug, as it can dictate higher nominal doses, and can result in increased systemic exposure for drugs that are orally bioavailable and, in some instances, increases in local and systemic side effects (e.g., for inhaled corticosteroids). For inhaled drugs, improved targeting to the lungs may be achieved by tailoring the micromeritic properties of the particles (e.g., size, density, rugosity) to minimize extrathoracic region deposition and maximize the total lung dose. Aerosol drug deposition in the mouth and throat is governed to a large extent by inertial impaction, and depends on a complex interplay between inhaler, formulation, and patient. For DPI products, the ability to fluidize and disperse dry powder agglomerates is dependent on the ratio of inter-particle cohesive forces (e.g., van-der Waal's) to the hydrodynamic forces (e.g., drag and lift forces). The counteraction of hydrodynamic to inter-particle cohesive forces can be achieved by engineering particles of low density and large particle size to facilitate powder fluidization and dispersion during aerosolization (Dunbar et al., 1998; Geldart, 1973). Particles with low density and relatively large geometric diameter change the force balance in favor of the hydrodynamic forces over the cohesive forces, enabling easier dispersion of

particle agglomerates entrained in the airflow within the inhaler device. Weers et al. (2007) and Edwards et al. (1997 & 1998) have demonstrated that low density and large diameter particles prepared by spray drying processes can enhance delivery efficiency for inhaled drugs. However, even for these advanced formulations, despite having low density particles (<0.4 g/cm^3) and large equivalent optical diameter (>2.5 μm), it is estimated that >15% of delivered dose is still deposited in the mouth-throat, e.g., for PulmoSphere™ powder formulations (Ung et al., 2014; Weers et al., 2015). This thesis explores an alternative spray drying approach focused on a particle design space centered around small particle size and low density particles. It is shown that this spray drying approach, wherein the drug is processed using a co-solvent solution feedstock, may be used to prepare dry powder formulations for inhalation that reduce extrathoracic region losses to negligible levels, and greatly improve delivery efficiency to the lung.

1.2 Spray drying

Spray drying is a continuous process that converts a liquid solution to a dry powder by atomizing the solution into a hot and dry environment. The atomized droplets evaporate in the drying chamber, resulting in dry powder particles carried by drying air. These particles are then collected by separating them from the gas stream using collection devices such as a cyclone or bag filter. The ability to process dry heat-sensitive materials is one of the reasons that this process has drawn wide acceptance from food to pharmaceutical industries (Snyder et al., 2008). It has been used for producing such goods as instant coffee, dried milk and

laundry detergent to pharmaceutical inhaled medicines (Exubera®, Pfizer; Tobi®, Novartis; Aridol®, Pharmaxis).

Figure 1.1 provides an overview illustration of a typical spray drying process used for manufacturing inhaled drugs. A liquid feedstock (solution or emulsion) containing the active pharmaceutical ingredient (API) with excipients as needed is pumped through an air-assisted atomizer nozzle and is atomized into small liquid droplets. Particle formation takes place when droplets in the heated airflow rapidly evaporated inside the drying chamber. The dry particles pass through a cyclone chamber where the separation of air and particles occurs. The exhaust gas carrying ultra-fine particles is filtered through a HEPA filter; while the desired dried particles settle downstream of the cyclone into a collector vessel, where they form a bulk powder. The formulated bulk powder manufactured in this manner may be further processed, e.g., filled into blisters or capsules for use with delivery devices such as dry powder inhalers.

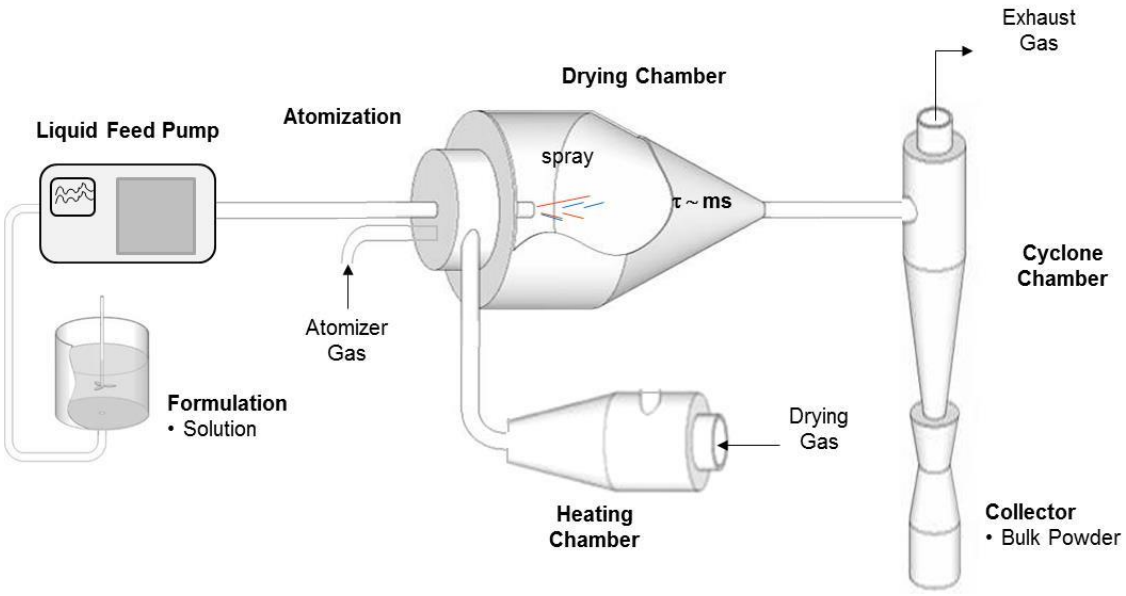

Figure 1.1 Overview schematic layout of a spray drying process.

1.2.1 Pharmaceutical particle engineering by spray drying

Particle engineering approaches based on spray drying have long been used to affect micromeritic properties of particles for pharmaceutical applications, and an excellent review of these techniques is presented in Vehring et al. (2007). These approaches include the use of shell forming excipients such as leucine or tri-leucine, or co-solvent feedstock systems, which in combination with feedstock composition, atomization, and drying parameters can be used to control the surface composition and morphology of the particles, e.g., by introducing rugosity (Lechuga-Ballesteros et al., 2008; Vanbever et al., 1999; Chew et al., 2005). For small molecules, a spray drying approach based on emulsion-based feedstocks has been used to produce porous low density particles and large particle size, with the marketed product Tobi® Podhaler® being an example (Geller et al., 2011). Low density and large diameter particles (i.e., >5 μm) of biologics like insulin have been prepared by spray drying using an ethanol-water co-solvent based feedstock (Edwards et al., 1997 & 1998; Vanbever et al., 1999). Ethanol-water co-solvent feedstocks have also been used to tailor particle morphology by spray drying of small molecules like budesonide (Boraey et al., 2013). In these previous studies, feedstocks with relatively large volume fractions of ethanol were used (>50% v/v). In contrast, this thesis explores a co-solvent spray drying approach where relatively small amounts of organic solvents added to water can be used to modulate particle morphology. This approach has been used to prepare engineered dry powder formulations of insulin (as a model compound) for use in dry powder inhalers.

1.3 Dry powder inhalers

The present work is focused on improving the delivery performance of engineered powder formulations intended for use with a class of inhalation delivery devices known as dry powder inhaler (DPI). The commercial introduction of dry powder inhalers began in 1949 with the launching of the Aerohaler® for the delivery of Norisodrine®, isoprenaline sulphate, by Abbot Laboratories (Clark, 1995). DPIs gradually became more commonly available as an alternative to other aerosol drug delivery systems (i.e., pressurized metered dose inhaler and nebulizer) used for administration of inhalation therapy. Today, there are more than two dozen marketed DPI products for local and systemic delivery (Islam et al., 2008). Depending on the design and functionality, DPIs may be categorized in numerous ways, e.g., active *versus* passive, unit dose *versus* multi-dose, etc. Passive DPIs rely on a patient's breath to fluidize and disperse the dry powder formulation. Such DPIs have a flow resistance that is characteristic of their design, and use various design elements coupled with inspiratory airflow to fluidize and disperse the bulk powder, and deliver it to the patient's airway. Two DPIs with different working principles were used to assess the performance of spray dried insulin powders investigated in this thesis research. These are the Simoon, a blister-based unit dose inhaler (Maltz et al., 2008; Ung et al., 2012; Weers et al., 2013), and the T-326, a capsule-based unit-dose inhaler (Geller, 2011; Maltz et al., 2011). **Figure 1.2** presents photographs and schematic drawings of the two DPIs. In addition, in developing the test methodology for assessing dose delivery performance, comparative assessments for several other marketed DPI products (**Figure 1.3**) were also conducted. The following section provides some background on the development of the test methodology.

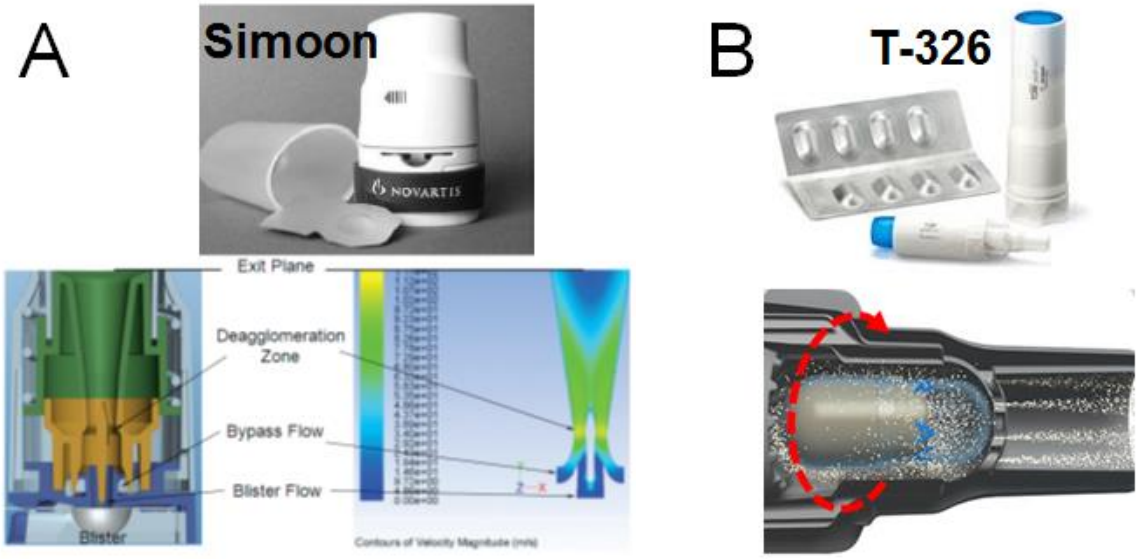

Figure 1.2 (A) Simoon and (B) T-326 inhaler used for *in vitro* aerosol performance evaluation of engineered particles.

Figure 1.3 Marketed DPI products evaluated in this thesis are (A) HandiHaler®, (B) Diskus®, (C) Twisthaler®, (D) Breezhaler®, (E) Podhaler®, and (F) Flexhaler®.

1.4 *In vitro* methods for assessing the aerosol dose delivery performance of inhaled drugs

In general, *in vitro* aerosol performance assessment of inhaled drug products is primarily focused on two attributes, i.e., the delivered dose (DD), and the aerodynamic particle size distribution (APSD). The DD test (also known as the emitted dose, ED) measures the "quantity" and consistency of aerosol dose delivered from the inhaler. The APSD is a measure of the "quality" of the delivered aerosol dose, as particle size is a key factor determining the efficiency of delivery to the lung. Particles with aerodynamic diameters in the range 1 – 5 μm are considered favorable for inhalation drug delivery.

The test set-up and methodology for measuring the DD and APSD generally follow the guidance in the Pharmacopeia (e.g., USP General Chapter <601>). DD measurements are relatively simple to perform and use a filter, typically with a spacer tube (e.g., DUSA) to collect and assay the dose emitted by the inhaler. APSD measurements are performed using cascade impactors (e.g., Next Generation Pharmaceutical Impactor), which rely on the principle of inertial impaction to classify airborne particles into different aerodynamic size fractions.

Passive DPIs rely on a patient's breath to fluidize and disperse the dose, and are typically tested under standard conditions using a square-wave airflow profile generated with a timer-controlled vacuum source. Use studies with DPIs have shown that human subjects can generate inhaler pressure drops of 1 – 10 kPa and airflow volumes of 1 – 3 L during an inhalation maneuver (Al-Ahowair et al., 2007; Clark et al., 1992). During testing, the inhaler is actuated with airflow at a pre-determined pressure drop and sampled flow volume that are

within the range observed in human use (e.g., 4 kPa pressure drop, and 2 L of sampled airflow through the inhaler and dose sampling apparatus). These standardized tests are intended primarily for quality control, e.g., for batch release, stability testing, and for comparing batch-to-batch variance of a given product under the same test conditions. While the APSD test is essentially a measure of particle size, it is sometimes used to derive estimates of dose delivered to the lung. A widely used approach, for example, is to designate the aerosol mass below a certain cut-off size (e.g., fine particle fraction <5 μm) as representing the lung dose. Such an approach is reasonable for rank order comparisons of batches of a given inhaled drug product tested under identical conditions. It is less suited for comparing inhaled drug products under different conditions, or when comparing different types of products, such as different types of formulations. For this purpose, a different approach is clearly needed, such as considering the process by which the dose emitted by the inhaler device is depleted on its way to the lung.

There are other reasons why the aerodynamic particle size data obtained by cascade impactors may not be predictive of the lung dose. Rader et al. (1985) used computer modeling to estimate the effect of ultra-Stokesian drag and particle interception on impaction in cascade impactor. They conclude based on their numerical analysis, that the cascade impactor approach could under estimate the aerodynamic particle size for large diameter and low density particles that are characteristic of certain types of engineered particle formulations (e.g., PulmoSphere™ formulations comprised of large, porous, and low density particles). For such formulations, aerosols delivered from a DPI remain agglomerated to a certain degree, and therefore are likely to be susceptible to non-ideal impaction effects.

As shown by Stahlhofen (1989), depletion of the aerosol dose occurs by deposition in the human mouth-throat, and is governed not just by the particle size, but by a parameter combining the particle size and flow-rate, i.e., the inertial impaction parameter (d^2Q) where d is the aerodynamic diameter (μm) and Q is volumetric airflow (L/min). One approach to use impactor data for predictive purposes is to factor in the flow-rate as well as particle size, e.g., by using a d^2Q cut-off for defining the "fine particle fraction" representative of the lung dose. A simple and potentially more direct approach to estimating lung dose in humans is to simulate the deposition in the extrathoracic region using an anatomical throat model. While several such models have been used in the past, one of the best characterized models is an idealized replica of the adult human upper-respiratory-tract (URT) known as the Alberta Idealized Throat (AIT) model (DeHaan et al., 2001; Stapleton et al., 2000). This thesis demonstrates that a methodology based on the AIT provides a simpler and more direct approach to assess product performance, especially when comparing different drug products (i.e., device and formulation) and technology platforms (i.e., engineered particles and carrier-based formulations).

1.4.1 Method for determining in vitro total lung dose

In vitro estimates of total lung dose (TLD) were measured using an anatomical throat model, i.e., the Alberta Idealized Throat (AIT), which represents the mouth and throat airway of an average human adult. The AIT was developed and characterized by Finlay and coworkers at the University of Alberta, Canada. They combined medical imaging technology (e.g., CT/MRI scans) and particle aerodynamics data to construct an idealized upper airway model whose aerosol deposition characteristics matched the average *in vivo* deposition data (DeHaan et al., 2001; Stapleton et al., 2000). For determination of *in vitro* TLD, the test

inhaler was coupled to the inlet of the AIT model, and the dose penetrating through the model was collected downstream on a filter. A suitable wetting agent was used for coating the interior walls of the AIT model to prevent particle re-entrainment. The dose collected on the filter was assayed to determine the TLD.

1.4.2 Method for measuring aerosol emission kinetics

While the AIT approach is primarily focused on measuring the degree of dispersion of the delivered dose, it is often useful to measure the kinetics of powder fluidization and emptying of the dose from the DPI. In the present research, aerosol clearance from the inhaler was characterized using a custom designed laser photometer (**Figure 1.4**) based on a commercially available laser sensor (Keyence Corp., model LX2-13W, US), which includes a laser sheet generator and an array detector. The laser photometer is configured as an aerosol flow cell whose cross-section is illuminated by the laser sheet. The presence of aerosol causes obscuration of the sheet laser and is detected by a photo-detector. The photo-detector's response is linear with obscuration (i.e., laser intensity). The intensity of the transmitted light is directly proportional to the particle concentration, which is related by Beer's law equation.

$$C_v \propto [-ln\left(\frac{V}{V_0}\right)]$$

Where C_v is the aerosol concentration, V is the baseline corrected photo-detector response in the presence of the aerosol, and V_0 is the corresponding photo-detector response in the absence of aerosol.

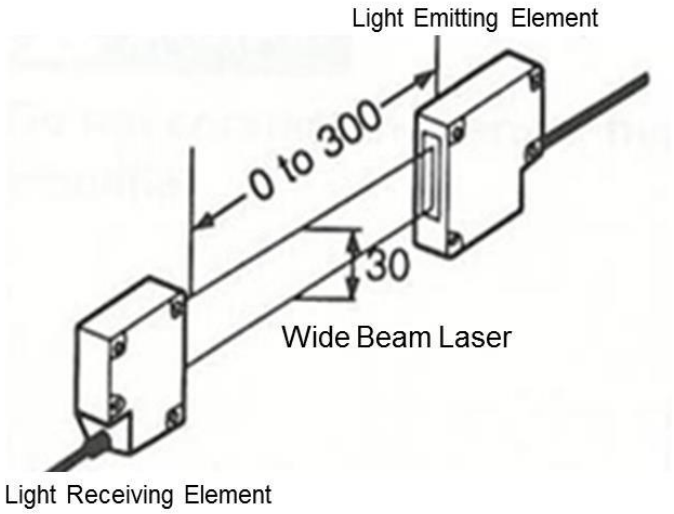

Figure 1.4 Drawing of the laser sensor used for measuring the kinetics of aerosol clearance (Keyence model LX2-13(W)), dimension in millimeters.

1.5 Structure of the thesis

The structure of the thesis is as follows. **Chapter 2** presents an initial exploration of the co-solvent spray drying approach for tailoring particle properties of insulin particles for inhalation. Several organic solvents were screened for their ability to modulate the density of insulin particles, and thereby affect aerosol delivery performance with a T-326 inhaler. Based on this pilot study, ethanol was selected as the organic solvent for further study of co-solvent spray drying of engineered particles, and their performance in DPIs.

Chapters 3 and **4** are focused on the development of an *in vitro* methodology that is well suited for comparative assessment of aerosol delivery performance of different types of inhaled drug products. The methodology developed is centered on the use of the Alberta Idealized Throat model to determine a total lung dose. The ability of the AIT to assess the

performance of inhaled drug products is demonstrated here, by evaluation of different types of DPIs, including those based on formulations of engineered particles as well as lactose carrier blends.

Chapter 5 brings together the two primary aspects of this work, i.e., co-solvent spray drying of engineered particles and *in vitro* inhaler performance assessment, to demonstrate that it is feasible to tailor the properties of insulin inhalation powders to reduce extrathoracic region losses to negligible levels, thereby enhancing dose delivery to the lungs, and enabling a high degree of lung targeting.

Chapter 6 presents concluding remarks and suggestions for further work. A significant finding in this thesis is that engineered particles formed by spray-drying can target a preferred range of micromeritic properties in order to achieve maximum total lung delivery. It is shown here that using small amounts of co-solvent addition to aqueous solution feedstock spray dried insulin bulk powder properties can be modulated in a direction more favorable for aerosol delivery performance. However, no attempt has been made to develop a theoretical framework to explain these findings, particularly the mixed morphology of wrinkled and oval particles associated with the powder samples from co-solvent spray drying. This is partly due to lack of solubility data for insulin in various co-solvent mixtures, which is essential to modeling of particle formation.

1.6 References

1. Al-Ahowair RAM, Tarsin WY, Assi KH, Pearson SB, Chrystyn H. Can all Patients with COPD use the Correct Inhalation Flow with all Inhalers and does Training Help? *Resp. Med.* 2007; **101**: 2395 – 2401.

2. Altounyan REC. Inhibition of experimental asthma by a new compound-sodium cromoglycate. *Intal. Acta Allergol.* 1967; **22**: 87 – 489.

3. Boraey MA, Hoe S, Sharif S, Miller DP, Lechuga-Ballesteros D, Vehring R. Improvement of the dispersibility of spray-dried budesonide powders using leucine in an ethanol–water co-solvent system. *Powder Technol.* 2013; **236**: 171 – 178

4. Chew NYK and Chan H-K. Use of solid corrugated particles to enhance powder aerosol performance. *Pharm. Res.* 2011; **18**: 1570 – 1577.

5. Chew NYK, Tang P, Chan H-K, and Raper JA. How Much Particle Surface Corrugation Is Sufficient to Improve Aerosol Performance of Powders? *Pharm. Res.* 2005; **22**: 148 – 152.

6. Clark AR and Hollingworth AM. The Relationship between Powder Inhaler Resistance and Peak Inspiratory Conditions in Healthy Volunteers – Implications for In Vitro Testing. *J. Aerosol Med.* 1993; **6**: 99 – 110.

7. Clark AR. Medical Aerosol Inhalers: Past, Present, and Future. *Aerosol Sci. Technol*. 1995; **22**:374-391.

8. DeHaan WH and Finlay WH. In vitro monodisperse aerosol deposition in a mouth and throat with six different inhalation devices. *J. Aerosol Med.* 2001; **14**: 361 – 367.

9. Dunbar C, Hickey A, and Holzner P. Dispersion and Characterization of Pharmaceutical Dry Powder Aerosols. *Kona Powder and Particle J.* 1998; **16**: 7 – 45.

10. Edwards AE, Hanes J, Caponetti G, Hrkach J, Ben-Jebria A, Eskew ML, Mintzes J, Deaver D, Lotan N, and Langer R. Large Porous Particles for Pulmonary Drug Delivery. *Sci.* 1997; **276**: 1868 – 1871.

11. Edwards AE, Ben-Jebria A, Langer R. Recent Advances in Pulmonary Drug Delivery Using Large, Porous Inhaled Particles. *J. Appl Physiol.* 1998; **85**: 379 – 385.

12. Geldhart D. Types of Gas Fluidization. *Powder Technol.* 1973; **7**: 285 – 292.

13. Geller DE, Weers J, and Heuerding S. Development of an Inhaled Dry-Powder Formulation of Tobramycin Using PulmoSphere™ Technology. *J. Aerosol Med.* 2011; **24**: 175 – 182.

14. Islam N and Gladki E. Dry Powder Inhalers (DPIs) – A Review of Device Reliability and Innovation. *Int. J. Pharm*. 2008; **360**: 1 – 11.

15. Lechuga-Ballesteros D, Charan C, Stults CLM, Stevenson CL, Miller DP, Vehring R, Tep V, and Kuo, MC. "Trileucine improves aerosol performance and stability of spray-dried powders for inhalation". *J. Pharm. Sci.* 2008; **97**: 287 – 302.

16. Maltz DS, Glusker M, Axford G, Postich M, Rao N, and Ung K. A novel passive dry powder inhaler for unit dose delivery to the deep lung. *Proc. Respir. Drug Deliv.* 2008; **3**: 669 – 674.

17. Maltz DS and Paboojian SJ. Device engineering insights into TOBI® Podhaler®: A development case study of high efficiency powder delivery to cystic fibrosis patients. *Proc. Respir. Drug Deliv. Europe.* 2011; **1**: 55 – 66.

18. Rader DJ and Marple VA. Effect of Ultra-Stokesian Drag and Particle Interception on Impaction Characteristics. *Aerosol Sci. & Tech*. 1985; **4**: 141 – 156.

19. Stahlhofen W, Rudof G, and James AC. Intercomparison of Experimental Regional Aerosol Deposition Data. *J. Aerosol Med.* 1989; **2**: 285 – 308.

20. Stapleton KW, Guentsch E, Hoskinson MK, and Finlay WH. On the suitability of κ–ε turbulence modeling for aerosol deposition in the mouth and throat: A comparison with experiment. *J. Aerosol Sci.* 2000; **31:** 739 – 749.

21. Ung TK, Rao N, Weers JG, Clark AR, and Chan H-K. *In vitro* assessment of dose delivery performance of engineered dry powders for inhalation. *Aerosol Sci. & Tech*. 2014; **48**: 1099 – 1110.

22. Vanbever R, Mintzes JD, and Wang J. Formulation and physical characterization of large porous particles for inhalation. *Pharm. Res*. 1999; **16**: 1735 – 1742.

23. Weers JG, Clark AR, Rao N, Ung K, Haynes A, Khindri SK, Sheryl A, Perry SA, Machineni S, and Colthorpe P. *In vitro–in vivo* correlations observed with indacaterol-based formulations delivered with the Breezhaler®. *J. Aerosol Med.* 2015; **28**: 1 – 13.

24. Weers JG, Ung K, Le J, Rao N, Ament B, Axford G, Maltz D, and Chan L. Dose emission characteristics of placebo PulmoSphere® particles are unaffected by a subject's inhalation maneuver. *J. Aerosol Med.* 2013; **26**: 56 – 68.

25. Weers JG, Tarara TE, and Clark AR. Design of fine particles for pulmonary drug delivery. *Expert Opin. Drug Delivery.* 2007; **4**: 297 – 313.

Chapter 2

Effect of chemical solvent addition to feedstock on the morphology of spray dried particles

2.1 Introduction

Organic co-solvents like ethanol added to aqueous based feedstocks have been used in spray drying processes to prepare particles for inhalation drug delivery. The organic co-solvent is often added to facilitate dissolution of API or excipients and modulate particle morphology in spray dried particles for inhalation (Boraey et al., 2013; Vanbever et al., 1999). Low density particles with wrinkled or porous morphology obtained with this approach are particularly useful for inhalation drug delivery applications. They also appear to be useful for both small molecules as well as biologics such as insulin. The above co-solvent spray drying approaches used relatively large fractions of the organic solvent (>50% v/v). More recently ethanol concentrations as low as 20% v/v have been studied for the purposes of pharmaceutical particle engineering (Ji et al., 2015).

One focus of this thesis research is to explore whether smaller amounts of organic solvent added to aqueous feedstocks could be used to effect changes in the morphology of spray dried particles. Such co-solvent systems could help influence processing in several ways. Co-solvents with different degrees of volatility (e.g., evaporation rates) relative to water may result in different mixture compositions within a drying droplet, thereby affecting the relative solubility of the API and excipients, and thus the kinetics of particle shell formation. It is

also known that small amounts of alcohols added to water can change feedstock solution properties such as viscosity and surface tension (Tanaka et al., 1987; Vázquez et al., 1995), which may affect the atomization and droplet formation, and potentially having an effect on particle morphology. Therefore, a screening experimental study with different organic solvents was performed to assess the feasibility of the approach and guide the selection of a co-solvent for further study. These experiments were performed using insulin as a model compound, and a formulation approach similar to the one developed for the inhaled insulin drug product Exubera (White et al., 2005), but with higher insulin content, 85%, compared to 60% insulin for Exubera.

2.2 Selection of Organic Solvents

A set of organic solvents for this study were selected based on their compatibility with pharmaceutical applications, miscibility with water, and to cover a range of boiling points. The intent was to provide feedstocks with varying properties such that a sufficiently wide range of processing conditions can be explored. **Table 2.1** lists the solvents selected for this study. Except for methanol, all of the selected organic solvents are considered class III solvents (low toxic potential for humans) according to the ICH guidance on residual solvent impurities. Methanol is considered a class II solvent (limited use recommended). Except for 1-butanol, all of the solvents are freely miscible with water. The sequence of boiling point (from high to low) is 1-butanol > 1-propanol > ethanol > methanol > acetone, however the sequence is reverse for saturated vapor pressure. Given that water has higher heat of

evaporation than the other chemical solvents used, it still remains the dominant factor during droplet drying kinetics as total aqueous solution only contains <10% of organic solvent.

Table 2.1 Summary of physical properties of pure liquid and shows an inverse relationship for boiling point temperature and saturated vapor pressure. Water is the primary solvent used in the feedstock solution.

Solute	Formula	Boiling Point [°C]	Density [g/cm^3]	MW	Solubility in Water at 25°C [g/100g]	P_{vap} at 40°C [kPa]	Diffusivity in Air at 40°C [cm^2/s]	Heat of Evaporation at 40°C [j/kg]
1-butanol	$C_4H_{10}O$	117.7	0.81	74.1	9.1	2.53	0.099	692733
Water	H_2O	100.0	1.0	18.0	n/a	7.39	0.292	2406863
1-propanol	C_3H_8O	97.3	0.81	60.1	∞	6.93	0.113	525190
Ethanol	C_2H_6O	78.4	0.79	46.1	∞	18.01	0.147	900668
Methanol	CH_4O	64.7	0.72	32.0	∞	35.43	0.177	1155065
Acetone	C_3H_6O	56.5	0.72	58.1	∞	56.52	0.117	524130

In considering the droplet drying kinetics in the co-solvent feedstock systems, the equilibrium vapor pressure of each component within the binary mixture is of interest, as it provides a driving force for evaporation. Estimates of equilibrium vapor pressure of water and organic solvent as a function of binary mixture composition for each of the solvents selected in this study were available from unpublished research (Mao, private communication, 2007), and are plotted in **Figure 2.1**, where the composition X_1 represents the mass fraction of the solvent in a binary mixture with water. These plots were derived from saturated vapor pressures data for pure liquids from Perry's Chemical Engineering Handbook (2008) and estimated activity coefficients for binary mixtures at infinite dilution

(Reid et al., 1988). The methodology was verified by comparing with published experimental data for methanol (Green and Perry, 2008). The plots indicate that for the selected set of organic solvents, the relative evaporation rates of organic solvent to water vary over a large range.

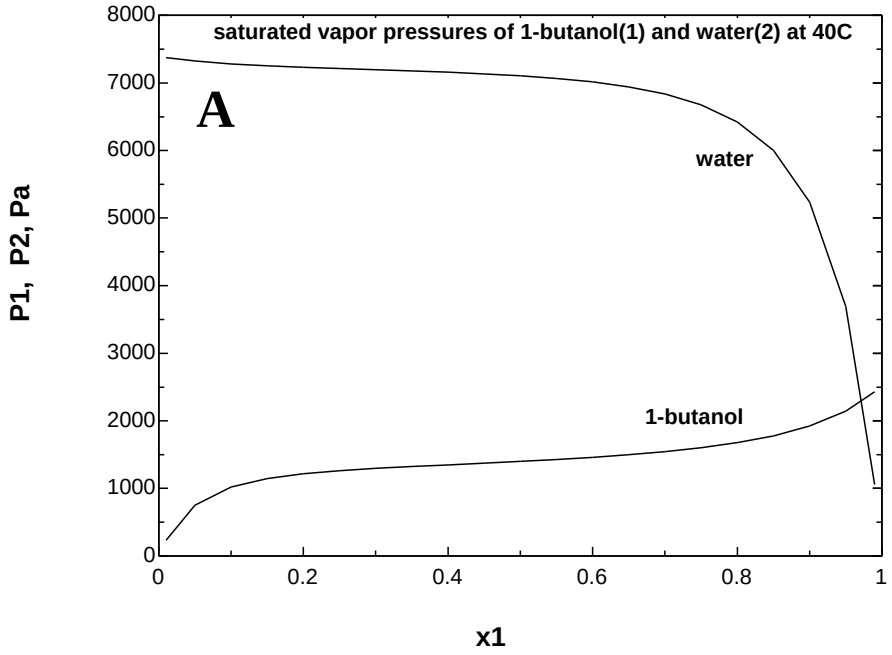

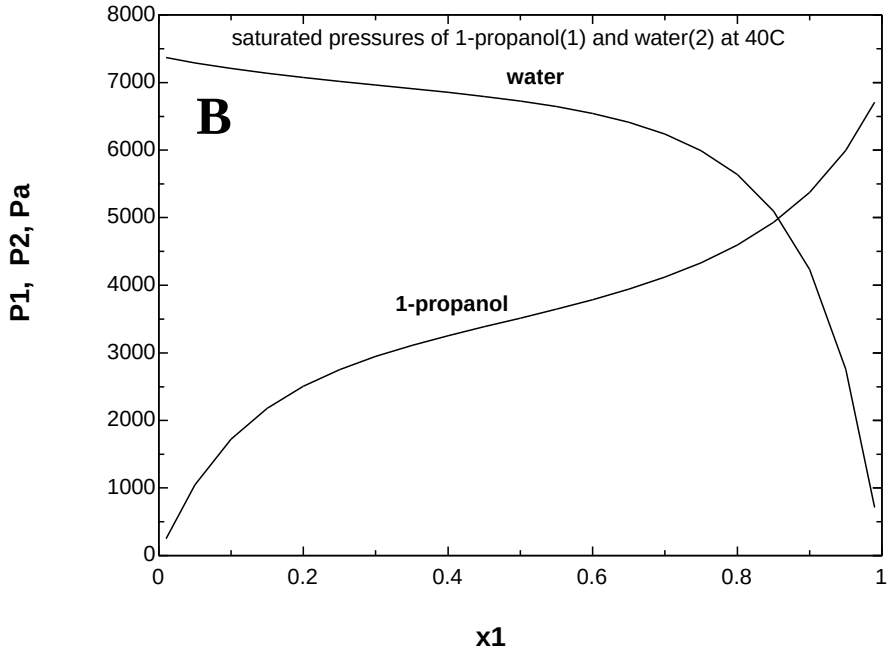

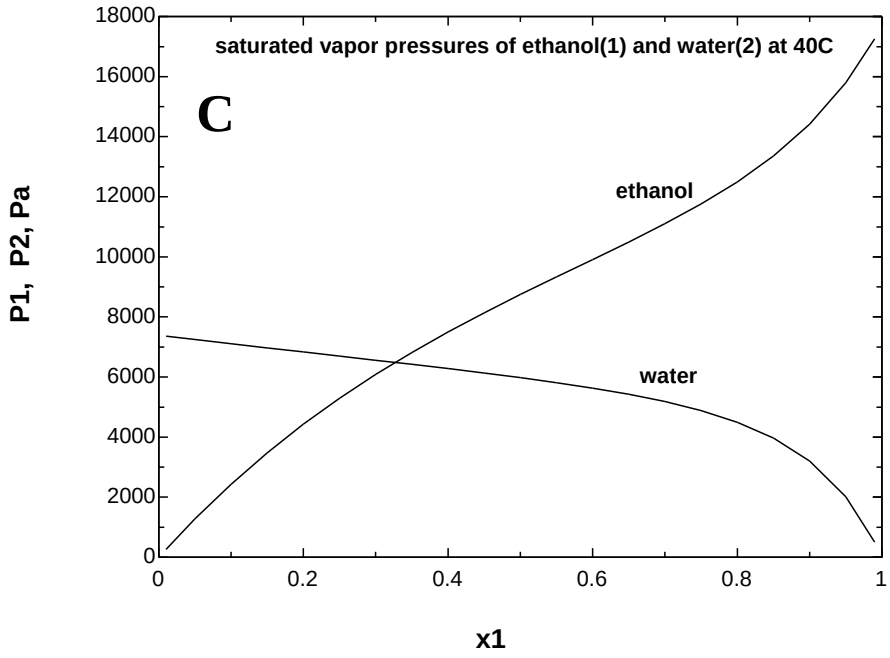
saturated vapor pressures of ethanol(1) and water(2) at 40C
C
ethanol
water
P1, P2, Pa
x1
18000
16000
14000
12000
10000
8000
6000
4000
2000
0
0
0.2
0.4
0.6
0.8
1

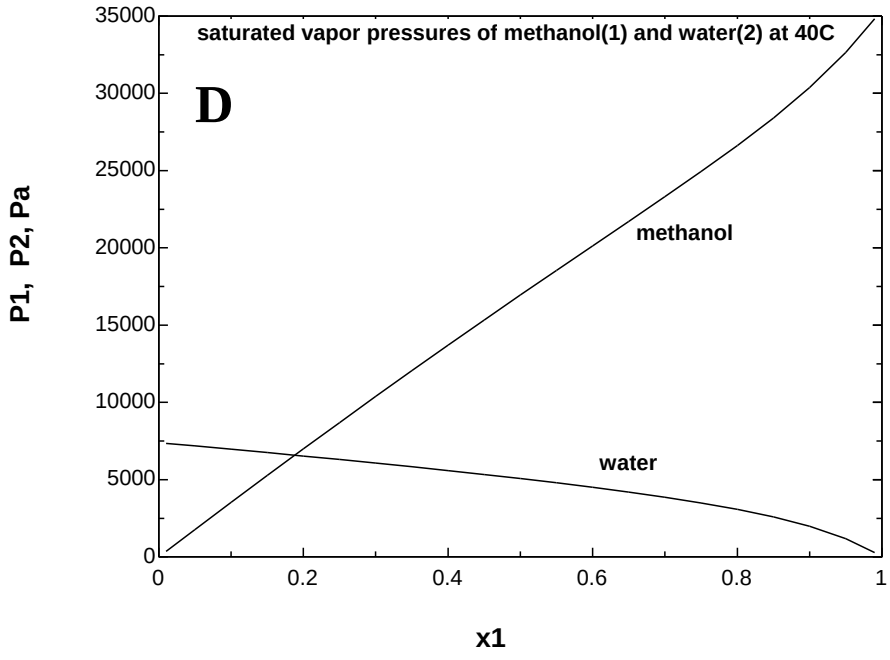
saturated vapor pressures of methanol(1) and water(2) at 40C
D
methanol
water
P1, P2, Pa
x1
35000
30000
25000
20000
15000
10000
5000
0
0
0.2
0.4
0.6
0.8
1

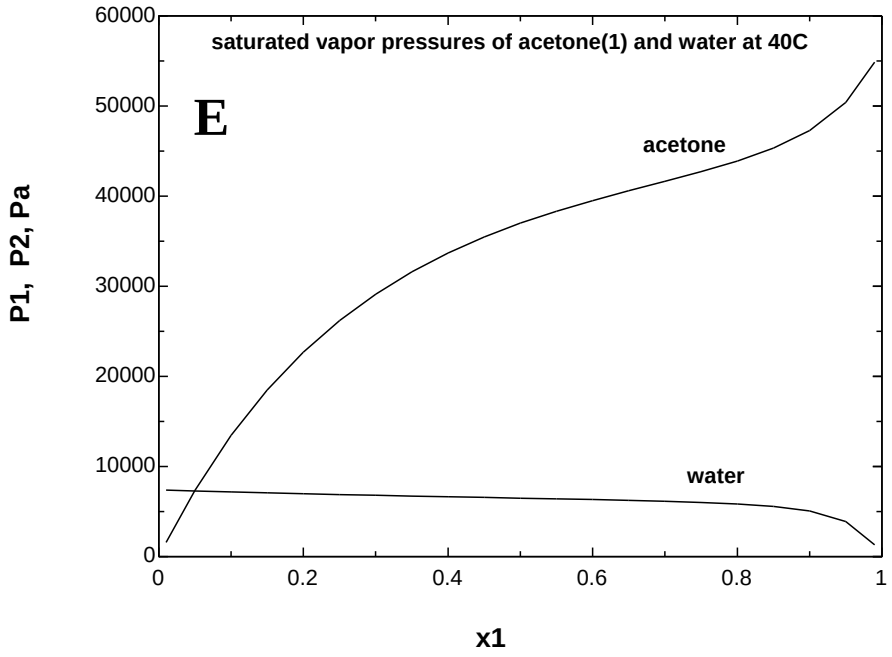

Figure 2.1 Predicted saturated vapor pressures at 40 degrees Celsius for binary liquid mixtures of selected organic solvents; (A) 1-butonal, (B) 1-propanol, (C) ethanol, (D) methanol, and (E) acetone.

Also of interest is the effect of solvent addition to properties such as surface tension, viscosity, and density as the affect droplet atomization. **Figures 2.2** and **2.3** show the effect of solvent addition on surface tension and viscosity for selected alcohols (data excerpted from Tanaka et al., 1987; Vázquez et al., 1995). Again, it is seen that a broad range of liquid properties can be obtained for the solvents selected in this study.

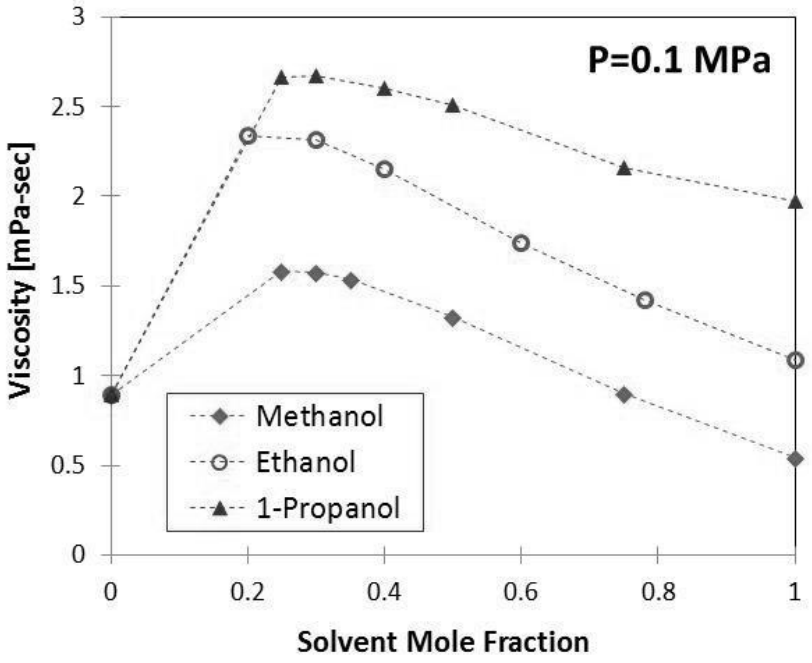

Figure 2.2 Effect of solvent addition on the viscosity of binary mixture of alcohols with water (Tanaka et al., 1987).

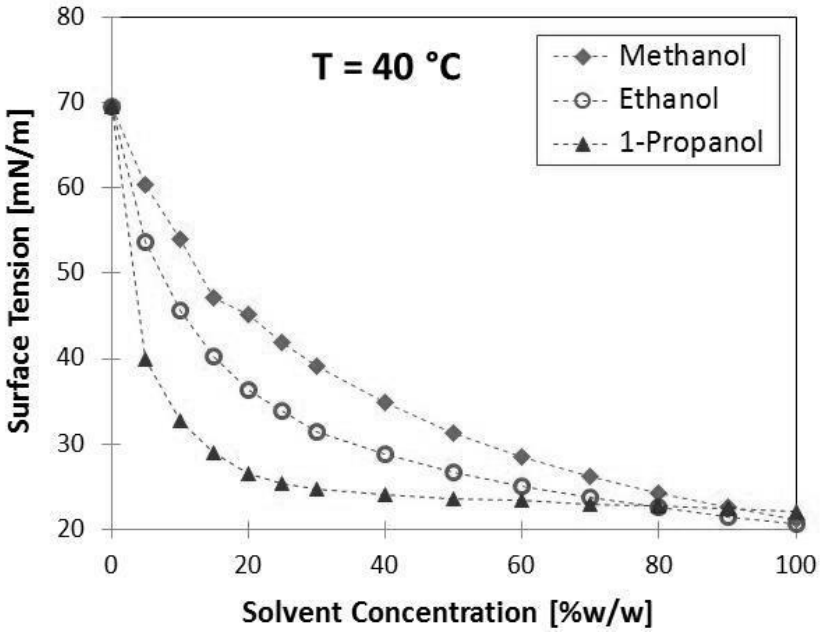

Figure 2.3 Effect of solvent addition on the surface tension of binary mixture of alcohols with water (Vásquez et al., 1995).

These solvents were used in co-solvent spray drying experiments to prepare insulin powders. Samples of the spray dried bulk powders were characterized, and then filled into capsules for aerosol delivery performance assessments with a capsule based inhaler. The materials and methods used in this study are detailed below.

2.3 Materials and Methods

2.3.1 Feedstock preparation and spray drying

The study used recombinant human insulin (P/N 10112053, Diabel GmbH & Co KG Frankfurt, Germany). The formulation comprises of 85% insulin, 10% sodium citrate, 4% mannitol, and 1% glycine. Feedstock solutions for spray drying were prepared by dissolving insulin and excipients in water or water-solvent mixtures while mixing gently on a magnetic stir plate.

This investigation used a Novartis Spray Dryer (NSD, Novartis Pharmaceuticals Corp, San Carlos, CA) a custom-built bench-scale spray drier that is similar in scale to a commercially available Büchi 191 mini spray dryer (BÜCHI Labortechnik, AG). The air-assisted atomizer nozzle is a modified version of Büchi 191 atomizer, designed to produce sprays with smaller and more uniform droplet size. The NSD dryer body and cyclone collector are fabricated out of stainless steel. The dryer body is insulated to improve temperature and relative humidity control within the process stream.

Table 2.2 presents an experimental design for spray drying insulin formulations with different solvent additions in aqueous solutions. The proposed 8% w/w of solvent addition

added to each feedstock solution will ensure alcohol is completely miscible in water forming a homogeneous solution. The spray drying process parameters were kept constant. Lot EXP-1-01 serves as a control insulin powder as the aqueous solution has no added secondary solvent where the particle morphology is primary corrugated raisin-like particles similar to Exubera formulation (White et al., 2005).

Table 2.2 Feedstock preparation for spray drying. Spray drying process parameters were kept constant; atomizer gas flow = 33 L/min, drying gas flow= 600 L/min, liquid feed rate= 4.0 mL/min, inlet temperature = 120°C.

Lot No.	Organic Co-Solvent	Alcohol Fraction [% w/w]	Water Fraction [% w/w]	Total Solids [% w/w]	Insulin Fraction [% w/w]	Sodium Citrate Fraction [% w/w]	Mannitol Fraction [% w/w]	Glycine Fraction [% w/w]
EXP-1-01	N/A	0	100	1.5	85.0	10.3	3.8	1.0
EXP-1-02	Ethanol	8	92	1.5	85.0	10.3	3.8	1.0
EXP-1-03	Methanol	8	92	1.5	85.0	10.3	3.8	1.0
EXP-1-04	Acetone	8	92	1.5	85.0	10.3	3.8	1.0
EXP-1-05	1-propanol	8	92	1.5	85.0	10.3	3.8	1.0
EXP-1-06	1-butanol	8	92	1.5	85.0	10.3	3.8	1.0

2.3.2 Determination of primary particle size of bulk powder

The primary particle size distribution of spray dried insulin powder was measured with a Sympatec HELOS Type BF Model Laser Light Diffraction Analyzer (Sympatec GmbH, Germany), the RODOS-M (OASIS) dry powder disperser, and the ASPIROS powder dosing unit. The instrument evaluation mode was set to high resolution laser diffraction (HRLD), which returns size distributions based on Fraunhofer diffraction theory. Powder samples of 5

– 15 mg of powder were placed into a 1 mL vial and loaded into the ASPIROS dosing unit set at a speed of 25 mm/s. The injector distance and primary pressure settings for the RODOS dry disperser were 4 mm and 4 bar, respectively. Measurements were performed using the R1 lens (R1: 0.1/0.18 – 35 μm). The RODOS settings were selected after confirming by experiment that they achieved essentially complete dispersion of the bulk powder down to the primary particles. Three replicate measurements were performed for each powder formulation. Results are reported here in terms of the equivalent optical diameter, X_{50}, (mean of three replicates).

2.3.3 Bulk density analysis of bulk powder

For this study, the measured bulk densities were conducted at a specified level of compression by compacting into a 0.0136 cubic centimeter cavity tool using vacuum suction at a pressure of 81 kiloPascal. Excess powder was then doctored off. The resulting powder puck was expelled from the cavity with a burst of compressed air at 35 – 103 kPa, and the mass of powder determined on a Mettler Toledo AX206 balance (n = 10 replicates). The resulting bulk densities are lower than the corresponding particle densities, but the trends in values are expected to be similar, assuming similar cohesive forces, and packing factor across the powders.

2.3.4 Particle morphology by Scanning Electron Microscopy

Particle morphology was assessed by scanning electron microscopy. Powder samples were viewed under a Philips XL 30 Environmental Scanning Electron Microscope (ESEM; Philips Electron Optics, US). A thin layer of bulk powder was placed on a 1 cm x 1 cm silicon wafer disk (Omnisil, VWR IBSN3961559, US), and the sample was prepared for electron microscopy by sputter-coating a thin gold and palladium film (Denton, 21261 Cold Sputter/Etch and DTM-100, operated at <100 mTorr and 30 – 42 mA for 100 – 150 seconds). The coated samples were then loaded into the ESEM chamber and the filament current and accelerating voltage set to 1.6 A and 20 kV, respectively.

2.3.5 In vitro characterization of aerosol dose delivery performance

In vitro dose delivery performance was investigated using a capsule-based T-326 inhaler that is a low to medium resistance device (R ~ 0.08 cm $H_2O^{0.5}$/L/min). T-326 is a breath-activated unit dose inhaler relying on the mechanical motion associated with precession of the capsule to fluidize and disperse the bulk powder into a fine respirable aerosol (Geller, 2011; Maltz et al., 2011). Aerosol performance was evaluated using a standard square-wave flow profile generated with a timer-controlled vacuum source at pressure drops of 0.5, 1.3, and 2.3 kiloPascal (kPa) corresponding to flow-rates of 27, 45, and 60 L/min, respectively. Testing T-326 device at 4 kPa (corresponding to 80 L/min) for NGI was not possible due to of particle re-suspension in the stages, and therefore 2.3 kPa (or 60 L/min) was selected to enable NGI gravimetric analysis. Test attributes included the delivered dose (DD) and aerodynamic particle size distribution (aPSD).

The test fixture used for measurement of DD is shown schematically in **Figure 2.4**. When actuated with flow, the aerosolized dose leaving the inhaler mouthpiece is collected onto an 81 mm diameter filter (A/E type, Pall Corp., US). A customized filter holder was designed for engineered particles, which allow for gravimetric analyses with the T-326 inhaler. The larger 81 mm diameter filter was used to minimize filter pressure drop for the T-326 inhaler, which is a low-medium flow resistance, and therefore a higher airflow during testing. A 2 L sampling volume was maintained for each dose actuation for DD analyses. The results for DD are reported in terms of % of the nominal dose.

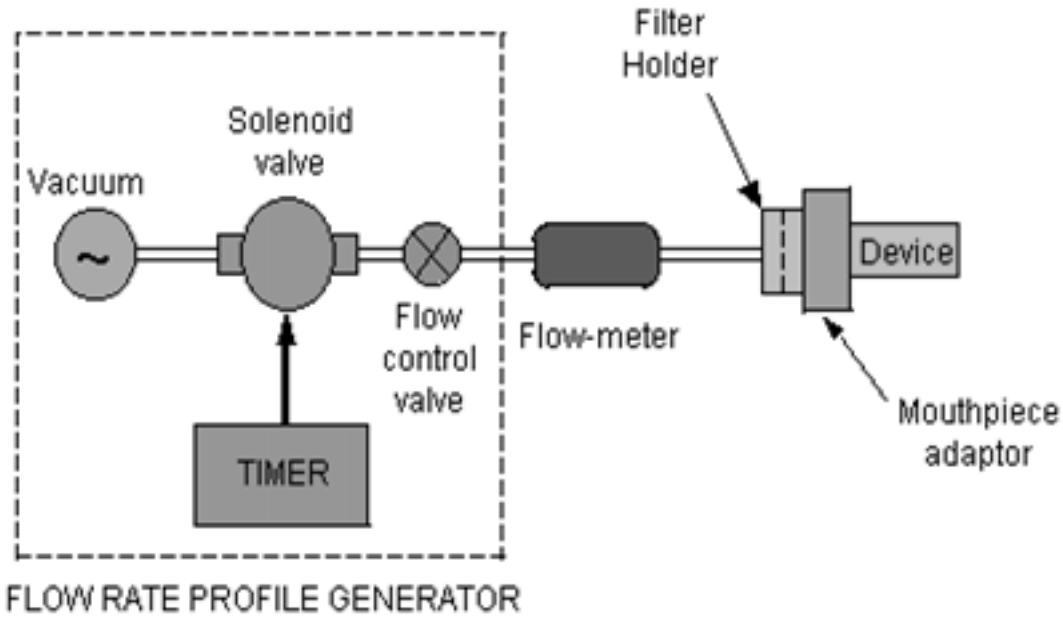

Figure 2.4 DD measurement set-up using customized filter holder designed for engineered particles.

For determining the aPSD, the NGI (Apparatus 5 in USP General Chapter <601>), was used with the Induction Port + NGI Body (**Figure 2.5**). To enable gravimetric analysis, the gravimetric NGI cups were fitted with 55 mm diameter glass fiber filters (A/E type, Pall

Corp, US). A 2 L sampling volume was maintained for each dose actuation for aPSD analyses.

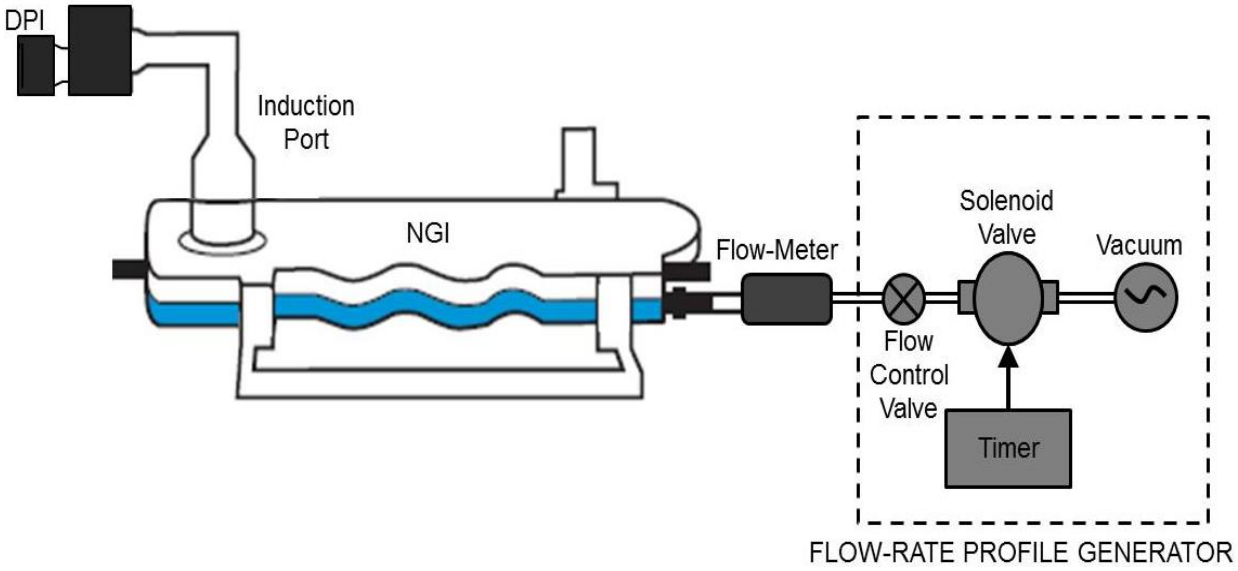

Figure 2.5 APSD measurement set-up.

2.3.6 NGI data analysis

Aerodynamic particle size distribution results for insulin formulation were expressed in the form of a fine particle mass (FPM, % of nominal), which represents the cumulative mass deposited on stages 3 to MOC (or filter) of the NGI and normalized to average capsule fill mass. The corresponding airflows and effective cut-off diameters (ECD) are summarized in **Table 2.3**.

Table 2.3 Stage cut-off diameters for NGI stage 3

Pressure Drop [kPa]	Flow-Rate [L/min]	NGI Stage 3[a] ECD [μm]
0.5	27	6.76
1.3	45	5.18
2.3	60	4.46

[a] Stage cut-off diameter-flow calculation for NGI stage 3 covering flow-rates from 27 - 60 L/min (Marple et al., 2003), $\boldsymbol{d_{50} = A\left(\sqrt{\frac{60}{Q}}\right)^{0.50}}$, where d_{50} represents new stage cut-off diameter-flow, Q, and A is stage cut-off at 60 L/min.

2.4 Results

2.4.1 Characterization of bulk powder physical properties

It is customary to seek correlations between the observed range of particle density and size with morphological characteristics of the powders. **Table 2.4** presents the bulk powder physical properties for 6 insulin formulations from spray drying runs where volume median diameters ranged from 1.23 – 1.51 μm, while bulk densities varied from 0.22 – 0.38 g/cm^3. There is no correlation observed between the co-solvent, bulk density, and particle size. EXP-1-01 (**Figure 2.6**) has no added solvent in the feedstock, bulk particles are mainly of corrugated raisin-like morphology that is consistent with other formulations of spray dried proteins (Balducci et al., 2015; White et al., 2005), while those with co-solvent spray dried formulations (with the exception of EXP-1-06, 1-butanol) showing a mixture of "wrinkled" and "balloon" particles, and having lower bulk density (**Table 2.4**). In addition, X_{50} numbers are slightly larger with solvent addition spray dried formulations (ranging from 1.47 – 1.51

μm) except 1-butanol (EXP-1-06) where particle size of 1.23 μm, which is even smaller than EXP-1-01 (1.35 μm) with no solvent addition in the feedstock.

Table 2.4 Spray dried powder physical properties, (mean, standard deviation shown in parenthesis, N = 3 – 10).

Lot No.	Organic Co-Solvent	X_{50} [μm]	Bulk Density [g/cm^3]
EXP-1-01	N/A	1.35 (0.02)	0.38 (0.01)
EXP-1-02	Ethanol	1.51 (0.03)	0.24 (0.01)
EXP-1-03	Methanol	1.51 (0.02)	0.27 (0.01)
EXP-1-04	Acetone	1.51 (0.03)	0.23 (0.01)
EXP-1-05	1-Propanol	1.47 (0.03)	0.22 (0.01)
EXP-1-06	1-Butanol	1.23 (0.02)	0.31 (0.01)

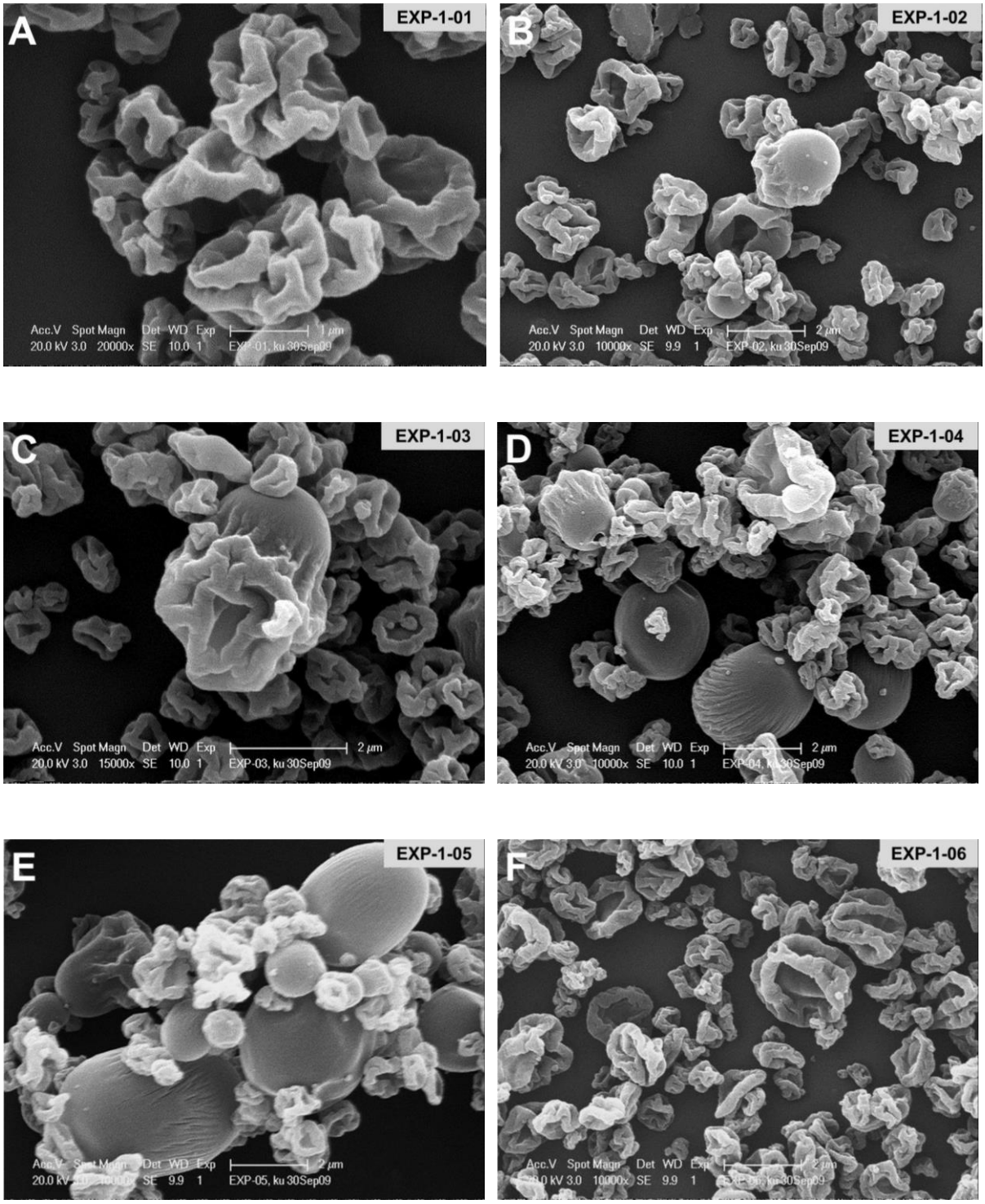

Figure 2.6 Scanning Electron Microscopy images of spray dried insulin particles for binary liquid mixtures of organic solvents; (A) water only- control, (B) ethanol, (C) methanol, (D) acetone, (E) 1-propanol, and (F) 1-butanol.

2.4.2 In vitro aerosol performance analysis

Having demonstrated the effect of solvent addition by spray drying insulin formulation on bulk powder properties, it is of interest to determine if these micromeritic properties can be correlated to aerosol dose delivery performance when delivering inhalation powders via dry powder inhaler. To answer this question, six spray dried insulin formulation powders covering a range of bulk densities and volume median diameters that varied from 0.22 – 0.38 g/cm^3 and 1.23 – 1.51 µm, respectively, were evaluated for *in vitro* aerosol performance. Aerosol performance testing was conducted with the T-326 inhaler at pressure drops of 0.5, 1.3, and 2.3 kPa, corresponding to flow-rates of 27, 45, and 60 L/min.

Table 2.5 and **Figure 2.7** present the delivered dose (DD) results tested over a range of flow-rates and correlate to bulk density. For 27 L/min flow-rate, it is seen as bulk density of the particles increases, the mean DD performance trends lower and variability higher. The DD performance is reasonably independent for flow-rate of 45 and 60 L/min. The drop in DD is accompanied by a corresponding increase in the amount of powder retained in the capsule.

Table 2.5 Summary of delivery dose (mean, standard deviation in parenthesis, N = 10).

	delivered dose (% of nominal)		
Lot No.	**27 L/min**	**45 L/min**	**60 L/min**
EXP-1-01	61 (9)	72 (5)	76 (2)
EXP-1-02	69 (5)	78 (3)	80 (2)
EXP-1-03	66 (6)	75 (4)	79 (3)
EXP-1-04	70 (6)	77 (3)	81 (2)
EXP-1-05	70 (3)	78 (3)	79 (2)
EXP-1-06	58 (8)	71 (5)	75 (5)

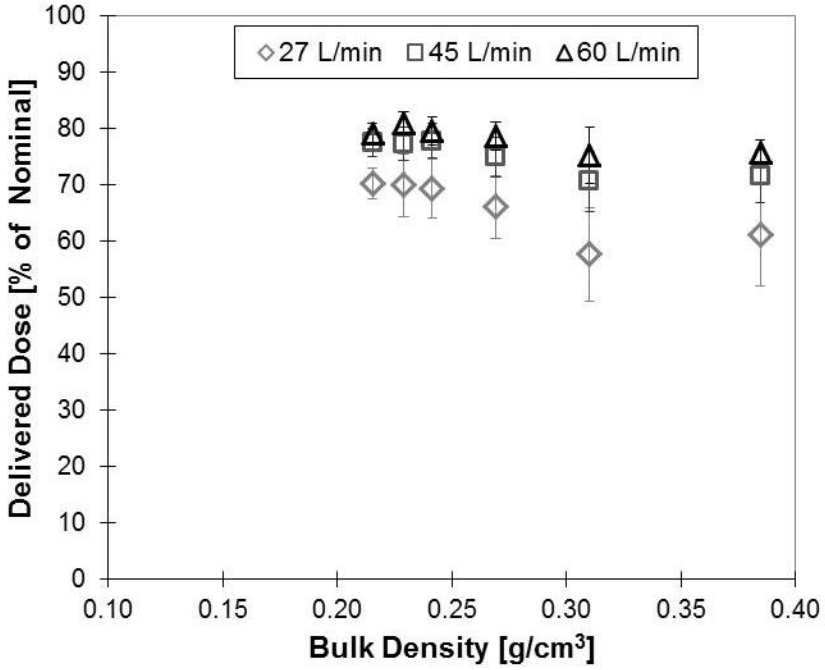

Figure 2.7 Delivered dose performance as function of bulk density.

A similar observation can also be seen for fine particle mass, where TLD trends lower and variability higher, as the bulk density increases. The results of flow-rate testing are presented in **Table 2.6** and **Figure 2.8**. **Table 2.6** summarizes the mean and standard deviation of fine particle mass (FPM) tested over a range of 27 – 60 L/min, while **Figure 2.8** presents the

same results graphically for the T-326 inhaler performance at 3 flow-rates. Despite the lower DD performance at 27 L/min as seen for all spray dried insulin powders, the FPM performance remains reasonably flow-rate independent over the range of flow-rate from 27 – 60 L/min and favors low bulk density powder ≤ 0.27 g/cm^3.

Table 2.6 Summary of fine particle mass (mean, standard deviation in parenthesis, N = 3).

	fine particle mass (% of nominal)		
Lot No.	**27 L/min**	**45 L/min**	**60 L/min**
EXP-1-01	45 (14)	59 (4)	62 (9)
EXP-1-02	60 (5)	67 (5)	68 (8)
EXP-1-03	59 (8)	65 (0)	64 (0)
EXP-1-04	66 (12)	65 (9)	64 (2)
EXP-1-05	66 (3)	64 (7)	65 (3)
EXP-1-06	41 (6)	56 (1)	67 (4)

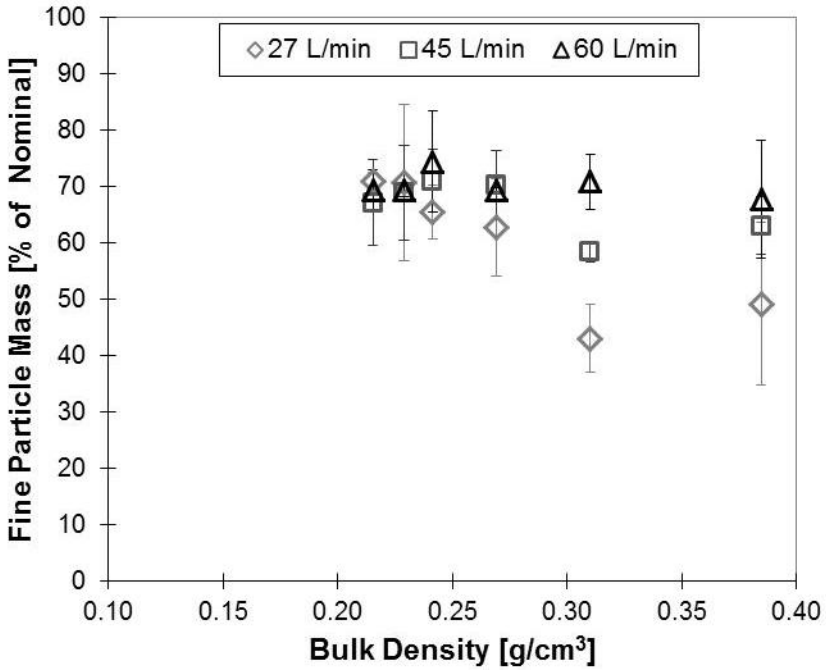

Figure 2.8 Fine particle mass performance as function of bulk density. Presented as the mean and standard deviation of five replicates.

2.5 Discussion

As presented in the introduction above for predicted saturated vapor pressures for binary liquid mixtures of selected organic solvents, an increase in vapor pressure will decrease the concentration X_1 value, indicating the importance of evaporation rate for a secondary solvent addition in the solution matrix. If the added solvent is volatile and likely to evaporate well before a solid shell has formed (e.g., acetone), the skin is expected to collapse creating small, wrinkled particles. In the event where the added solvent is less volatile and more likely to be trapped in the solid matrix (e.g., 1-butanol), it may act like a blowing agent and result in large and porous particles. However, based on experimental findings, the SEM images of the powders show all solvent additions produced a mix of morphologies with both corrugated and smooth oval shaped particles resulting in smaller bulk density powders than for EXP-1-

01, which represents a control powder produced by spray drying an aqueous feedstock with no added solvent. A high boiling point co-solvent such as 1-butanol (BP=117.7°C) would suggest that it would persist longer in the evaporating droplet, and therefore lead to porous and low density particles. However, that was not the case as SEM image (**Figure 2.6**, 1-butanol) shows mainly corrugated particles. Among the powders from the co-solvent runs, the 1-butanol run resulted in the highest bulk powder density and the smallest X_{50} with these properties being the closest to the control insulin powder (EXP-1-01). This suggests that controlling the morphology of the particles (i.e., size, density, and rugosity) should not be based solely on manipulation of the solution feedstock alone (i.e., total solids, co-solvent fraction), but must also consider process parameters; controlling the initial droplet size, drying kinetics and particle shell formation (Snyder et al., 2008; Vehring, 2007).

2.6 Conclusion

The experiments described above have produced outcomes different from that suggested by theory, indicating that further understanding is needed with regards to co-solvent evaporation during droplet drying, and interactions with insulin and other excipient compounds. However, it is clear that addition of a small amount of solvent to the feedstock solution for spray drying can greatly affect the micromeritic properties of the particles. The bulk density of the particles for the co-solvent systems was lower and X_{50} was mostly larger than those of the insulin powder that was spray dried with no added solvent in the aqueous solution. The *in vitro* aerosol performance using a T-326 inhaler was improved and favored lower bulk density insulin powders. Based on the results from this experiment and early research studies

by Edwards et al. (1997 & 1998), ethanol was selected for further investigation and will be discussed later in **Chapter 5**.

2.7 References

1. Balducci AG, Cagnani S, Sonvico F, Rossi A, Barata P, Colombo G, Colombo P, and Buttini F. Pure insulin highly respirable powders for inhalation. *Eur. J. Pharm. Sci*. 2015; **51**: 110 – 117.
2. Boraey MA, Hoe S, Sharif H, Miller DP, Lechuga-Ballesteros D, and Vehring R. Improvement of the dispersibility of spray-dried budesonide powders using leucine in an ethanol-water cosolvent system. *Powder Technol*. 2013; **236**: 171 – 178.
3. Dunbar C, Hickey A, and Holzner P. Dispersion and Characterization of Pharmaceutical Dry Powder Aerosols. *Kona Powder and Particle J*. 1998; **16**: 7 – 45.
4. Edwards AE, Hanes J, Caponetti G, Hrkach J, Ben-Jebria A, Eskew M L, Mintzes J, Deaver D, Lotan N, and Langer R. Large Porous Particles for Pulmonary Drug Delivery. *Sci*. 1997; **276**: 1868 – 1871.
5. Edwards AE, Ben-Jebria A, and Langer R. Recent Advances in Pulmonary Drug Delivery Using Large, Porous Inhaled Particles. *J. Appl. Physiol*. 1998; **85**: 379 – 385.
6. Geldart D. Types of Gas Fluidization. *Powder Technol*. 1973; **7**: 285 – 292.
7. Geller DE, Weers JG, and Heuerding S. Development of an inhaled dry-powder formulation of tobramycin using PulmoSphere™ technology. *J. Aerosol Med.* 2011; **24**: 175 – 182.
8. Green DW and Perry RH. Perry's Chemical Engineers' Handbook. 8th Edition. McGraw-Hill. 2008.
9. Maltz DS and Paboojian SJ. Device engineering insights into TOBI® Podhaler®: A development case study of high efficiency powder delivery to cystic fibrosis patients. *Proc. Respir. Drug Deliv.* 2011; **1**: 55 – 66.

10. Marple VA, Olson BA, Santhanakrishnan K, Mitchell JP, Murray SC, and Hudson-Curtis BL. Next Generation Pharmaceutical Impactor (A New Impactor for Pharmaceutical Inhaler Testing). Part II: Archival Calibration. *J. Aerosol Med*. 2003; **16**: 301-324.

11. Mao Z. Private Communication (2007).

12. Reid RC, Prausnitz B, and Polling E. The Properties of Gases and Liquids. 4th Edition. McGraw-Hill. 1988.

13. Rosenstock J, Muchmore D, Swanson D, and Schmitke J. AIR® Inhaled Insulin System: A Novel Insulin-Delivery System for Patients with Diabetes. *Expert Rev. Med. Devices*. 2007; **4**: 683 – 692.

14. Snyder HE and Lechuga-Ballesteros D. "Spray Drying: Theory and Pharmaceutical Applications." *Pharmaceutical Dosage Forms: Tablets*. *Informa Healthcare*. 2008; Third Edition Vol. **1**: 227 – 260.

15. Tanaka Y, Matsuda Y, Fujiwara H, Kubota H, and Makita T. Viscosity of (water + alcohol) mixtures under high pressure. *Int. J. Thermophysics*. 1987; **8**: 147 – 163.

16. Vanbever R, Ben-Jebria A, Mintzes JD, Langer R, and Edwards DA. Sustain release of insulin from insoluble inhaled particles. *Drug Dev. Res*. 1999; **48**: 178 – 185.

17. Vázquez G, Alvarez E, and Navaza JM. Surface tension of alcohol + water from 20 to 50 °C. *J. Chem. Eng. Data*. 1995; **40**: 611 – 614.

18. Vehring R. "Pharmaceutical Particle Engineering via Spray Drying." *Pharm. Res.* 2007; **25**: 999 – 1022.

19. Weers JG, Tarara TE, and Clark AR. Design of fine particles for pulmonary drug delivery. *Expert Opin. Drug Delivery*. 2007; **4**: 297 – 313.

20. White S, Bennett D, Cheu S, Conley PW, Guzek DB, Gray S, Howard J, Malcolmson R, Parker JM, Roberts P, Sadrzadeh N, Schumacher JD, Seshadri S, Sluggett GW, Stevenson CL, and Harper NJ. EXUBERA®: Pharmaceutical development of a novel product for pulmonary delivery of insulin. *Diabetes Technol. Ther.* 2005; **7**: 896 – 906.

Chapter 3

In vitro assessment of dose delivery performance of dry powders for inhalation

(Original article published in Aerosol Sci. & Tech., 2014)

3.1 Introduction

Particle deposition in the mouth and throat pose a great challenge to the dose delivery performance of inhaled medications. The geometry of the human airway is complex and variable (DeHaan et al., 2001), deposition is influenced not only by physiological differences in size, but also time-dependent changes associated with patient breathing maneuver, and factors related to the inhaler, such as the flow resistance, and mouthpiece geometry and position (McRobbie et al., 2003; McRobbie et al., 2005; Pritchard et al., 2004). Other factors including aerosol concentration and polydispersity, and environmental conditions such as humidity, can also affect the delivery of inhaled medication to the target airways (DeHaan et al., 2001). Understanding the effect of these factors on product performance and prediction of delivered lung doses, ahead of clinical trials, is of great utility to product designers and developers, and has therefore attracted considerable attention in the past decades.

Extrathoracic region deposition of inhaled aerosols has been studied in depth by Stahlhofen, and more recently by Finlay and others (DeHaan et al., 2001; Delvadia et al., 2012; Golshahi et al., 2013; Longest et al., 2008; Olsson et al., 2008; Stahlhofen et al., 1989). Stahlhofen et al. (1989) compiled data from multiple studies showing that extrathoracic region deposition

increases with increasing values of d^2Q, where d is the aerodynamic particle size and Q the volumetric flow-rate. This relationship indicates that inertial impaction is the dominant factor in determining extrathoracic region deposition. Finlay and coworkers further showed that a better correlation of extrathoracic region losses is achieved for pharmaceutical aerosols when the characteristic length scales of the inhaler mouthpiece (Finlay et al., 2002) as well as the mouth-throat geometry (Grgic et al., 2004) are considered, for example via a dimensionless parameter, the Stokes number. These studies provided justification for the use of predictive numerical models of mouth-throat losses based on semi-empirical correlations. Inputs to these models included inhalation airflow, inhaler mouthpiece geometry, airway geometry, as well as the aerodynamic particle size distribution of the delivered aerosol.

The aerodynamic particle size distributions (APSD) of inhalation aerosols are typically measured using an inertial impactor such as the Next Generation Pharmaceutical Impactor (NGI) with induction port and pre-separator per USP General Chapter <601>. Prediction of lung deposition based on stage groupings of APSD data, such as a fine particle dose fraction post induction port and pre-separator, is complicated and often poses a challenge, and while identifying a suitable fine particle mass (FPM) marker could be justified by correlation with *in vivo* lung deposition, such data is often not available. Moreover, the size distribution of the aerosol delivered from the inhaler is often incompletely characterized, due a significant un-sized fraction lost in the induction port. The incomplete size characterization of the delivered dose could potentially bias the estimation of *in vitro* lung dose. An alternative approach in estimating an *in vitro* lung dose would be to use a physical model of the idealized mouth-throat model. The benefits of this approach include (i) a simple and direct *in vitro* measurement of lung dose, that is expected to capture the physics of particle transport

and deposition in the human mouth-throat and (ii) the ability to measure aerosols generated under clinically relevant conditions, via the use of realistic patient flow profiles during actuation of an inhaler. Olsson et al. (2013) recently showed good *in vitro in vivo* correlation with the use of an anatomic throat model to assess nine different inhaler products.

To date, most publications on dry powder inhalers (DPI) have been focused on the delivery performance of blend formulations where small drug crystals (<2 μm) are attached to large lactose carrier particles with size >50 μm (Podczeck et al., 1998). There are relatively few published studies on engineered powders intended for inhalation. Such powders are typically characterized by low bulk-powder density (<0.2 g/cm^3) and primary particles having equivalent optical diameter ~2 μm, respectively (Weers et al., 2007). It is of interest to investigate the dose delivery performance of engineered powders, as exemplified by the low density porous particles produced using the PulmoSphere™ technology. Low density engineered powders have enabled the development of DPI products capable of delivering large lung doses via improvement in powder fluidization and dispersibility. Studies with PulmoSphere™ powder formulations have demonstrated that it is possible to achieve high lung deposition (>50% of dose) that is largely independent of inspiratory flow-rate (Duddu et al., 2002; Hirst et al., 2002; Newhouse et al., 2003).

The aim of this study was to use the idealized mouth-throat model to characterize the dose delivery performance of DPI products based on engineered powder and lactose-blend formulations. The idealized mouth-throat model provides an *in vitro* estimate of the lung dose, which is compared to *in vitro* markers based on semi-empirical models of extrathoracic region deposition.

3.2 Materials and Methods

3.2.1 Powder formulations and inhaler systems

Table 3.1 summarizes different devices and formulations investigated in this study. PulmoSphere™ placebo powder formulations were prepared by spray drying an emulsion of perflubron (PFOB; Allied, lot #101800, US) in water, stabilized by distearoylphosphatidylcholine (DSPC; Lipoid, lot #103605, Germany) and calcium chloride ($CaCl_2$; Sigma Alrich, lot #103936, US). The spray drying process eliminates water and PFOB, and produces porous particles of DSPC/$CaCl_2$, representing the key excipients in PulmoSphere™ formulations. The goal was to produce a panel of low-mass density porous particles having equivalent optical diameters in the range of 1.5 – 5.0 μm and tap densities of 0.03 – 0.15 $g \cdot cm^{-3}$. Particle sizes and densities were modulated by varying feedstock parameters such as the ratio of PFOB to water (0.04 – 0.87 w/w) and total solids (1.0 – 6.0% w/v); and process parameters such as air-to-liquid ratio (5 – 10 w/w) and drying kinetics (total gas flow 90 – 160 scfm; dryer outlet temperature maintained at 70°C). The rationale for study PulmoSphere™ placebo powders is that they are useful surrogates for studying a class of potent active formulations with low drug loading (<10% w/w). The incorporation of such small amounts of drug does not greatly affect the bulk powder properties, and consequently the aerosolization behavior. The PulmoSphere™ placebo powders were all filled into foil-foil blisters (fill mass of 2 mg), designed for actuation with the Simoon inhaler (Device A).

Table 3.1 DPIs and formulations used in the present study

DPI (Resistance) [cm $H_2O^{0.5}$/L/min]	Product Name (Treatment)	Drug Package	Label Claim [µg]	Formulation Platform	Composition Drug/Excipients	Tapped Density [g/cm^3]
Device A Simoon (0.20)	Placebo	Unit Dose Blister	N/A	Emulsion Spray dry	DSPC, $CaCl_2$	<0.2
Device B HandiHaler® (0.16)	Spiriva® (COPD)	Unit Dose Capsule	18[a]	Blend	TB/Lactose	>0.5
Device C Twisthaler® (0.14)	Asmanex® (Asthma)	Multi-dose Reservoir	220[a]	Spheronized	MF/Lactose	>0.5

[a] Label claim of marketed product; TB= Tiotropium Bromide; MF= Mometasone Furoate

Two marketed DPI products, Spiriva® and Asmanex®, were also evaluated in this study as products representative of lactose-based formulations. Asmanex® is an inhaled corticosteroid for asthma treatment, in which the micronized drug (mometasone furoate) is combined with micronized excipient (lactose) and formulated into large agglomerates to facilitate handling in the bulk state (Yang et al., 2001). The drug is delivered using a Twisthaler multi-dose reservoir device, and is available in two strengths, 220 μg and 110 μg of mometasone furoate (Patient's IFU). The therapeutic agent in Spiriva® is Tiotropium bromide, which is a long-acting (24-hour) muscarinic receptor antagonist also known as an anti-muscarinic or anti-cholinergic agent for treatment of reversible airways obstruction or chronic obstructive pulmonary disease (COPD). The inhalable formulation consists of tiotropium bromide blended with lactose monohydrate carrier particles (Patient's IFU; Chodosh et al., 2001). Each Spiriva® capsule contains 18 μg tiotropium (22.5 μg of inhalable tiotropium bromide monohydrate).

3.2.2 Determination of primary particle size of bulk powder

The optical equivalent diameter of the primary particle size distribution of PulmoSphere™ placebo powder was measured with a Sympatec HELOS Type BF Model Laser Light Diffraction Analyzer (Sympatec GmbH, Germany) with the RODOS-M (OASIS) dry disperser and the ASPIROS powder dosing unit. The instrument evaluation mode was set to high resolution laser diffraction (HRLD), which returns size distributions based on Fraunhofer diffraction theory. Powder samples of 5 – 15 mg of powder was placed into a 1 mL vial and loaded into the ASPIROS dosing unit set at a speed of 25 mm/s. The injector

length and primary pressure settings for the RODOS dry disperser were 4 mm and 4 bar, respectively. Measurements were performed using the R2 lens (particle size range of 0.45 – 87.5 μm). The RODOS settings were selected after verifying that they achieved essentially complete dispersion of the PulmoSphere™ powder down to the primary particles formed during the spray drying process. Results are reported here in terms of the mean volume median diameter, X_{50}. Repeatability tests of this method with representative powders (total 9 lots) have demonstrated relative standard deviation < 3% with triplicate samples.

3.2.3 Tapped density analysis of bulk powder

The tapped density of the PulmoSphere™ placebo formulations was measured by dispensing bulk powder into a 0.59 cm^3 cylindrical cavity, doctoring off excess powder, and manually tapping 3 – 5 times on a hard surface, while adding powder to compensate for powder settling. The cavity is placed onto a weighing pan for gravimetric analysis (Mettler Toledo AX206, US). Assessment of method precision was performed for low (0.04 g/cm^3), medium (0.07 g/cm^3), and high (0.12 g/cm^3) density powders with 6 replicates for each lot and the relative standard deviations were 2.8%, 6.7% and 4.5%, respectively. Other powder lots were based on duplicate samples. Results are reported as mean tapped density.

3.2.4 Scanning Electron Microscopy

Samples of the powder formulations were viewed under a scanning electron microscope using a Philips XL 30 Environmental Scanning Electron Microscope (ESEM; Philips

Electron Optics, US). A thin layer of powder was placed on a 1 cm x 1 cm of silicon wafer disk (Omnisil, VWR IBSN3961559, US) for engineered particles or on a 12 mm diameter carbon adhesive tape for lactose-based powders (Electron Microscopy Sciences, Cat. #77825-12, US), and the sample was prepared for electron microscopy by sputter-coating a thin gold and palladium film (Denton, 21261 Cold Sputter/Etch and DTM-100, operated at <100 mTorr and 30-42 mA for 100-150 seconds). Samples were then loaded into the ESEM chamber and the filament current and accelerating voltage set to 1.6 A and 20 kV, respectively.

3.2.5 In vitro mouth-throat model

The mouth-throat model was used for *in vitro* measurement of estimate total lung dose for devices and formulations listed in **Table 3.1**. The mouth-throat model used in this study was developed by Finlay and coworkers at the University of Alberta, Canada. They combined medical imaging technology, e.g. CT/MRI scans, and particle aerodynamics data to construct an idealized upper airway model whose aerosol deposition characteristics matched the average *in vivo* deposition data (DeHaan et al., 2001; Stapleton et al., 2000). In the present study, the anatomical throat model was fabricated out of aluminum using CAD geometry data provided by Professor Finlay. For ease of use, the model was fabricated in two parts, corresponding roughly to the "mouth" and "throat" sections of the airway. This two-staged construction of the throat allows some qualitative assessment of regional deposition in the upper airway. Suitable mouthpiece adapters were designed and customized for each inhaler

for attachment to the mouth-throat model, so that the inhalers were oriented approximately horizontally with respect to the mouth-throat model.

3.2.6 Semi-empirical correlations for estimating lung dose

Experimental data from the idealized mouth-throat model were compared to two proposed *in vitro* markers derived from cascade impactor measurements of aerosol size. The first proposed *in vitro* marker for lung deposition is based on a fine particle mass (FPM) corresponding to a selected cut-off value of the inertial impaction parameter, d^2Q, where d, is the aerodynamic diameter (μm) and Q, is volumetric airflow (L/min).

Thus, an *in vitro* estimate of lung dose can be obtained from standard cascade impactor measurements as $FPM_{d^2Q<C}$, where C is a suitable cut-off value. Note that this *in vitro* FPM marker factors in both particle size and inhaler flow-rate, and can be used to compare the performance of inhalers having different flow resistances (hence tested at different flow-rate), or of the same inhaler over a range of flow-rates. A cut-off value of C ~ 1450 μm^2 L/min corresponds to a mean extrathoracic region deposition of ~50% according to the model of Stahlhofen et al. (1989) and also represents ~50% deposition in the Alberta mouth-throat model for monodisperse aerosols introduced through a straight tube (DeHaan et al., 2001). For convenience, cut-off values in this study are selected based on NGI stage groupings, e.g. the mass fraction accumulated on stages 4 to multi-orifice collector (MOC) corresponding approximately to $FPM_{d^2Q<500}$, and mass on stages 3 to MOC, corresponding approximately to $FPM_{d^2Q<1300}$. Flow-rate effects on inhaler dose delivery performance are

thus assessed on the basis of fixed impactor stage groupings (essentially fixed d^2Q), rather than a fixed diameter cut-off alone as is customarily and incorrectly done (Clark and Hollingworth 1993).

A second measure of lung dose is derived from a semi-empirical correlation for estimating mouth-throat losses proposed by DeHaan and Finlay (2004). It is based on a Stokes number that incorporates the inhaler mouthpiece geometry as a length scale. The fraction of the delivered dose deposited in the mouth and throat is estimated from the following:

$$Mouth\ \&\ Throat\ Loss = \left[1 - \frac{1}{44.5St^{1.91} + 1}\right] + \left[\left(\frac{1}{44.5St^{1.91} + 1}\right) \cdot \left(1 - \frac{1}{3.5 \cdot 10^{-8}\,(d^2Q)^{1.7} + 1}\right)\right] \quad (1)$$

Where St is the Stokes number given by,

$$\mathrm{St} = \frac{\rho_p U_0 d_p^2}{18\mu d_m} \sim d^2\,\frac{Q}{d_m^3} \quad (2)$$

ρ_p is particle density, g/cm^3

U_0 is fluid velocity, cm/s

d_p is particle diameter, µm

µ is fluid dynamic/kinematic viscosity, kg/cm/s

d is aerodynamic diameter with the density of water, µm

Q is volumetric airflow, L/min

d_m is the inhaler mouthpiece diameter, cm

In equation (1), the first term represents losses in the mouth and is significant for inhalers having small mouthpiece diameters. The second term represents laryngeal losses according to Stahlhofen et al. (1989). The above semi-empirical correlation, equation 2, has been implemented in the form of an on-line calculator, ARLA Respiratory Deposition Calculator (Martin and Finlay 2008). Note that DeHaan and Finlay (DeHaan et al., 2001 & 2004; Finlay et al., 2002) developed their correlation using experimental data with the Alberta mouth-throat model, so it is reasonable to compare semi-empirical model predictions with results from the Alberta throat for the DPI products tested in this study.

The fraction of delivered dose deposited in the lung may be evaluated as the fraction penetrating through the mouth-throat:

$$Lung\ dose\ fraction = 1 - \ Mouth\ \&\ Throat\ loss\ fraction \qquad (3)$$

where the mouth-throat loss fraction is obtained from equation (1). Inputs to the ARLA calculator include the inhaler mouthpiece dimensions, the inhaler flow-rate, and the corresponding APSD of the delivered aerosol, which is modeled as having a log-normal distribution, and specified in terms of the mass median aerodynamic diameter (MMAD) and geometric standard deviation (GSD). For each of the inhalation products investigated, these APSD inputs were obtained by *in vitro* measurement of the delivered aerosol dose using the Next Generation Impactor (MSP Corp., US). Aerosol characterization methods are described below.

3.2.7 In vitro characterization of aerosol dose delivery performance

In vitro dose delivery performance was investigated over a range of pressure drops (1 – 6 kPa) considered representative of the range achievable by asthma and COPD patient populations (Al-Ahowair et al., 2007). Aerosol dose delivery tests were performed using a square-wave flow-rate profile generated using a timer-controlled vacuum source. A single inhalation actuation was conducted for each inhaler type. Test attributes included the (i) emitted powder mass (EPM), (ii) *in vitro* lung dose (LD), and (iii) aerodynamic particle size distribution (APSD) using the NGI cascade impactor. Note that tests (i) and (iii) are standard *in vitro* tests per USP General Chapter <601>. A 2-liter sampling volume was maintained for each dose actuation for EPM and LD analyses. However, for NGI analysis, a 4-liter volume was used to account for the large internal dead volume (2025 mL) of the NGI apparatus (Copley et al., 2005), including the induction port, pre-separator and NGI body.

The test fixture used for EPM measurement is shown schematically in **Figure 3.1**. When actuated with flow, the aerosolized dose leaving the inhaler mouthpiece was collected onto a 47 mm diameter filter (A/E type, Pall Corp., US). A custom filter holder designed for gravimetric analysis of engineered powder was used for testing Device A. Standard DUSA tubes were used for collecting doses from Device B and C. It should be noted that the gravimetric analysis approach is not commonly used in aerosol dose delivery testing for lactose blend formulations, but is entirely appropriate for engineered powder formulations. Engineered powders are reasonably homogeneous in composition, and the distribution of drug (when present) closely follows the distribution of powder mass. The results for EPM are reported in terms of % of label claim (devices B, C) or fill mass (device A).

For determination of *in vitro* lung dose fraction analysis, the test inhaler was coupled to the inlet of the idealized mouth-throat model, and the dose penetrating through the model was collected downstream on a 76 mm diameter filter (A/E type, Pall Corp., US), as shown in **Figure 3.2**. A polysorbate (EMD Chemicals, Cat. #8170072, US) wetting agent (equal parts of Tween 20 and methanol, v/v) was used for coating the interior walls of the cast model to prevent particle re-entrainment. The procedure for applying coating solution to the mouth-throat model was as follows; (a) ~15 mL of the coating solution was dispensed into the mouth-throat model, which was then capped at both ends (b) The solution was allowed to wet the internal walls of the mouth-throat model using a rocking or rotary motion to tilt the mouth-throat model from side to side; and (c) Excess solution was allowed to drain for 5 minutes before use. After five dose actuations, the mouth-throat model was rinsed with lukewarm water, air dried, and a fresh coating applied before the next use.

For determining the APSD, the NGI (Apparatus 5 in USP General Chapter <601>), was used with the Induction Port +Pre-Separator + NGI Body. As noted earlier, due to their homogeneous composition, the PulmoSphere™ placebo powders may be assayed using a gravimetric approach. To enable gravimetric analysis, the gravimetric NGI cups were fitted with 55 mm diameter glass fiber filters (A/E type, Pall Corp, US) and the pre-separator upper and lower compartments were coated 1 and 2 mL, respectively, with a polysorbate wetting agent (equal parts of Tween 20 and methanol, v/v).

For the lactose-based formulations, drug-specific HPLC assays were used to quantitate mometasone (with Device C) and tiotropium (with Device B). The collection substrates of the NGI along with the pre-separator were coated with polysorbate solution; 1 mL for small cups and 2 mL for pre-separator and large cups.

Mometasone content was determined using a Reverse Phase High Performance Liquid Chromatograph (RP-HPLC) method on a Dionex Ultimate 3000 system (Thermo Scientific Dionex, US) equipped with a photodiode array (PDA) detector set to 238 nm. Tiotropium content was determined on the same system using PDA detector set to 254 nm. Chromatographic separation was attained using an YMC-Pack ODS-AQ (50 x 4.6 mm, 3 µm) column at a flow-rate of 0.6 and 1.0 mL/min (50 and 30 µL injection volume) for tiotropium and mometasone, respectively. Mobile Phase A for tiotropium method was composed of 75% v/v water mixed with 25% acetonitrile and 0.1% phosphoric acid, and water with 0.1% trifluoroacetic acid for mometasone. The diluent used to dissolve drug samples before HPLC analysis for tiotropium and mometasone were 25% acetonitrile mixed with 75% water and 42% acetonitrile mixed with 58% water, respectively. Drug recoveries for both compounds were ≥97%.

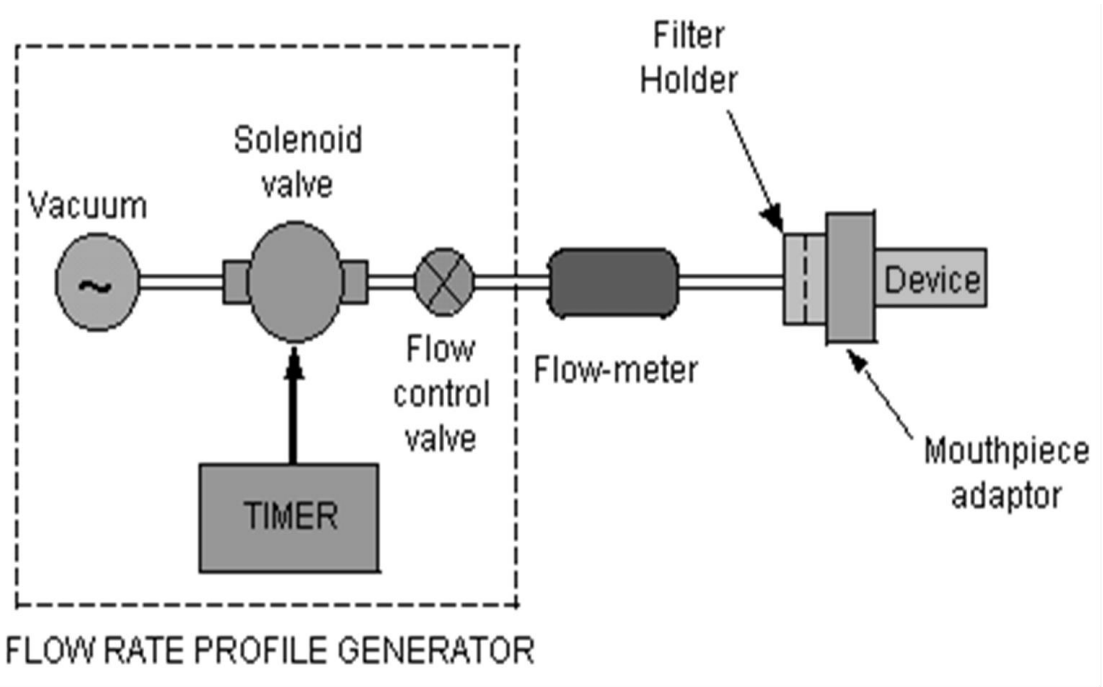

Figure 3.1 Emitted powder mass measurement set-up with a customized emitted dose powder collector for Device A and using DUSA tube for Devices B and C.

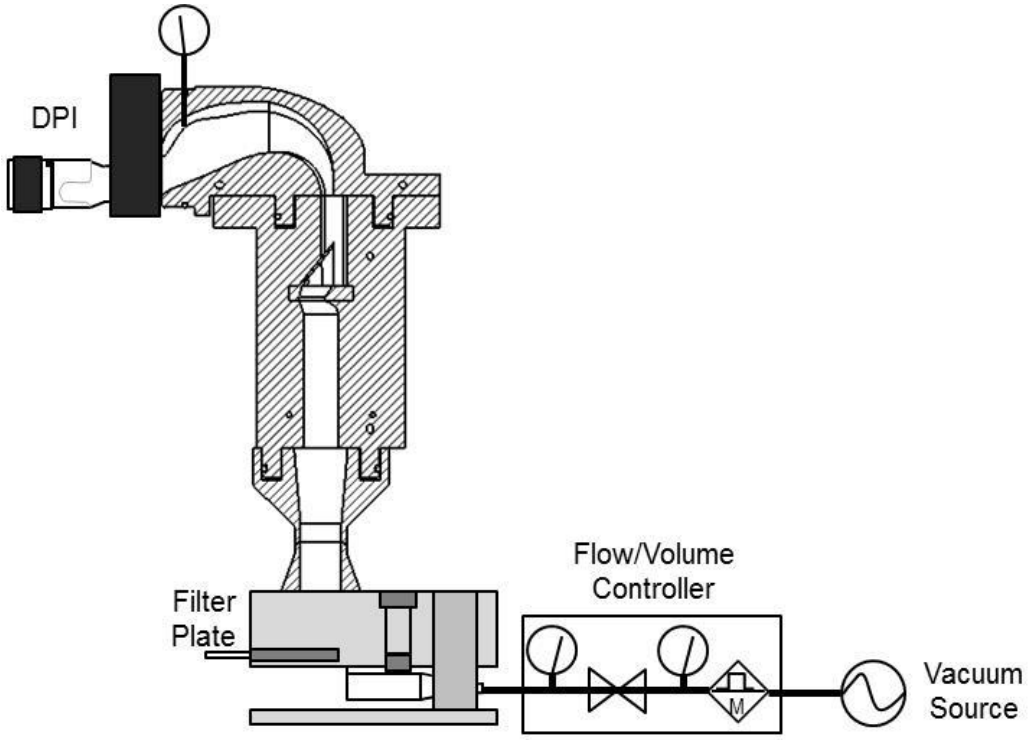

Figure 3.2 Cross-sectional view of the idealized mouth-throat model with an inhaler and filter housing attached upstream and downstream, respectively.

3.2.8 NGI data analysis

Aerodynamic particle size distribution results for all drug products were expressed in the form of a fine particle mass (FPM, % of label claim, or fill mass) with cut-off d^2Q<500 $\mu m^2 \cdot L/min$, which represents the cumulative mass deposited on stages 4 to MOC (or filter) of the NGI. The corresponding airflows and effective cut-off diameters (ECD) are summarized in **Table 3.2**. Note that APSD results were also used as inputs to the ARLA calculator for estimating total lung dose, as described later.

Table 3.2 Stage cut-off diameters for NGI stage 3 at test conditions

Inhaler	Flow Resistance [$cm \cdot H_2O^{0.5}/L/min$]	Pressure Drop [kPa]	Flow-Rate [L/min]	NGI Stage 3[a,b] ECD [μm]	$d^2 \cdot Q$ [$\mu m^2 \cdot L/min$]
Device A	0.20	1	16	5.39	465
		2	22	4.62	470
		4	32	3.87	484
		6	40	3.47	482
Device B	0.16	1	20	N/A [c]	N/A [c]
		2	28	4.13	478
		4	39	3.50	478
		6	47	3.18	475
Device C	0.14	1	23	N/A [c]	N/A [c]
		2	33	3.80	477
		4	47	3.19	478
		6	57	2.89	476

[a] Based on archival calibration for NGI at 15 L/min (Marple et al., 2004).

[b] Stage cut-off diameter-flow calculation for NGI stage 3 covering flow-rate from 30 - 100 L/min (Marple et al., 2003), $\boldsymbol{d_{50} = A\left(\sqrt{\frac{60}{Q}}\right)^{0.50}}$, where d_{50} represents new stage cut-off diameter-flow, Q, and A is stage cut-off diameter at 60 L/min.

[c] Not reported here as NGI data were not generated at 1 kPa for Device B and C due to steep drop in aerosol dose delivery.

3.3 Results and Discussion

3.3.1 In vitro aerosol data analysis

Table 3.3 presents the bulk powder properties of spray dried PulmoSphere™ powders. The results show the powder properties fall within the target values of 0.03 – 0.15 g/cm^3 for tapped density and 1.5 – 5.0 µm for primary particle size, thus allowing a range sufficiently wide to study the effects of these parameters. As noted earlier, the placebo powders (A – F) are useful surrogates for a class of potent active formulations with low drug loading, since incorporation of small amounts of drug (<10%) does not greatly affect the bulk powder properties or consequently the aerosolization behavior. An example of this is shown in **Table 3.3**, where active PulmoSphere™ formulations (G, H) with 2% and 6% Indacaterol (Novartis AG, Switzerland) had powder properties comparable to that of placebo formulations (A - C), which were processed within a similar range of conditions. It should be cautioned that the results for the Placebo powders studied here may not necessarily be representative of active formulations with significantly higher drug loading, or of performance in other inhalers.

Table 3.3 Bulk powder properties of spray dried PulmoSphere™ formulation

Powder Batch No.	Drug Loading [%]	Tapped Density [g/cm^3]	Primary Particle Size, Sympatec X_{50} [μm]
A	0	0.04	2.49
B	0	0.04	4.20
C	0	0.04	3.50
D	0	0.07	2.00
E	0	0.07	3.16
F	0	0.12	1.68
G*	2	0.04	3.05
H*	6	0.05	2.74

*PulmoSphere™ formulations of Indacaterol (Novartis AG, Switzerland).

Representative photomicrographs from SEM analyses are presented in **Figure 3.3** for the three formulation types investigated in this study. SEM images show three distinct particle morphologies for the formulation types. The PulmoSphere™ powder (A) has porous, roughly spherical particles, in the respirable size range (1 – 5 μm), whereas tiotropium formulation (B) with large angular feature and non-respirable particles >20 μm in size.

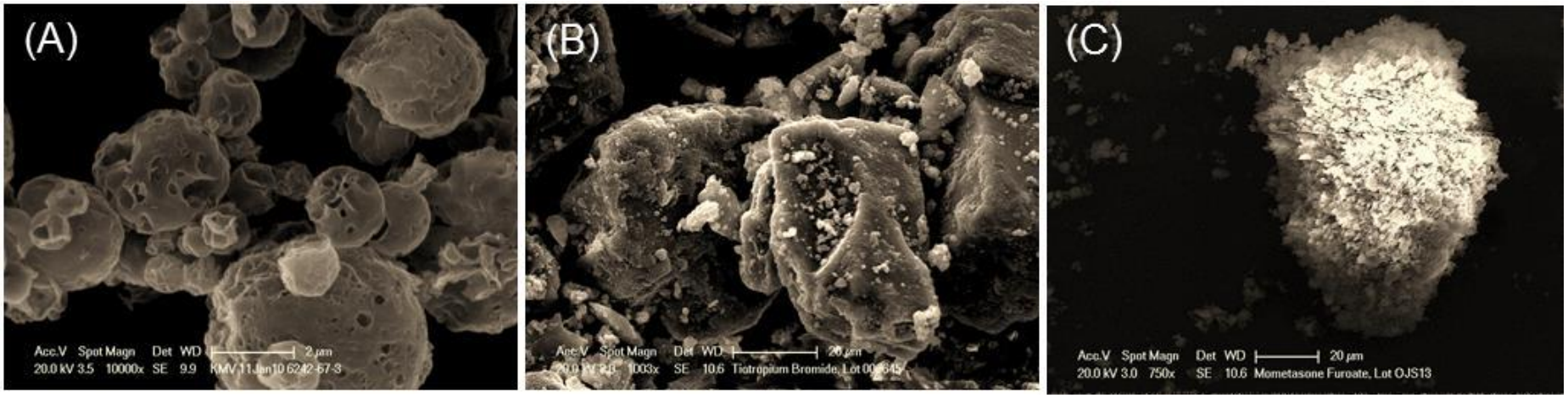

Figure 3.3 Three particle morphologies analyzed by Scanning Electron Microscopy; (A) spray dried PulmoSphere™ (Batch A), (B) traditional lactose-blend with tiotropium bromide and (C) spheronized mometasone furoate.

Figure 3.4 presents a correlation between bulk powder properties and *in vitro* aerosol performance from EPM and NGI data for the six PulmoSphere™ placebo powders (A – F) when tested with Device A at a pressure drop of 4 kPa. **Figure 3.4A** indicates a strong effect of tap density, with smaller tap density resulting in higher emitted powder mass fraction.

A one-way ANOVA of the 6 PulmoSphere™ powders showed a significant difference in EPM among the lots ($p < 0.0001$). A post-hoc means comparison test (Tukey-Kramer HSD) showed that the three low density powders (A, B, and C) were similar, but significantly different from the two medium density powders (D and E), and the high density (F) powder batch.

The effect of primary particle size on the FPM (% of mass recovered from cups) of the dispersed aerosol is shown in **Figure 3.4B**. The results show that the FPM initially increases with X_{50} and then appears to reach a plateau for $X_{50} \geq 2.5$ μm, suggesting greater cohesive forces with smaller particles. At first glance, it may appear counter-intuitive for the FPM to show an increasing trend with X_{50}. It should be kept in mind, however, that X_{50} represents a size metric for bulk powder, which is essentially completely dispersed to primary particles using compressed air at pressures up to 4 bar. The FPM, on the other hand is a measure of the incompletely de-agglomerated aerosol delivered by the Device A, where the powder is dispersed under relatively gentle conditions. The formation of aerosol agglomerates from the bulk powder is determined by the balance between "cohesive" inter-particle forces and the "dispersive" fluid hydrodynamic forces, both of which vary with primary particle size in a complex manner, resulting in the relationship plotted in **Figure 3.4B**.

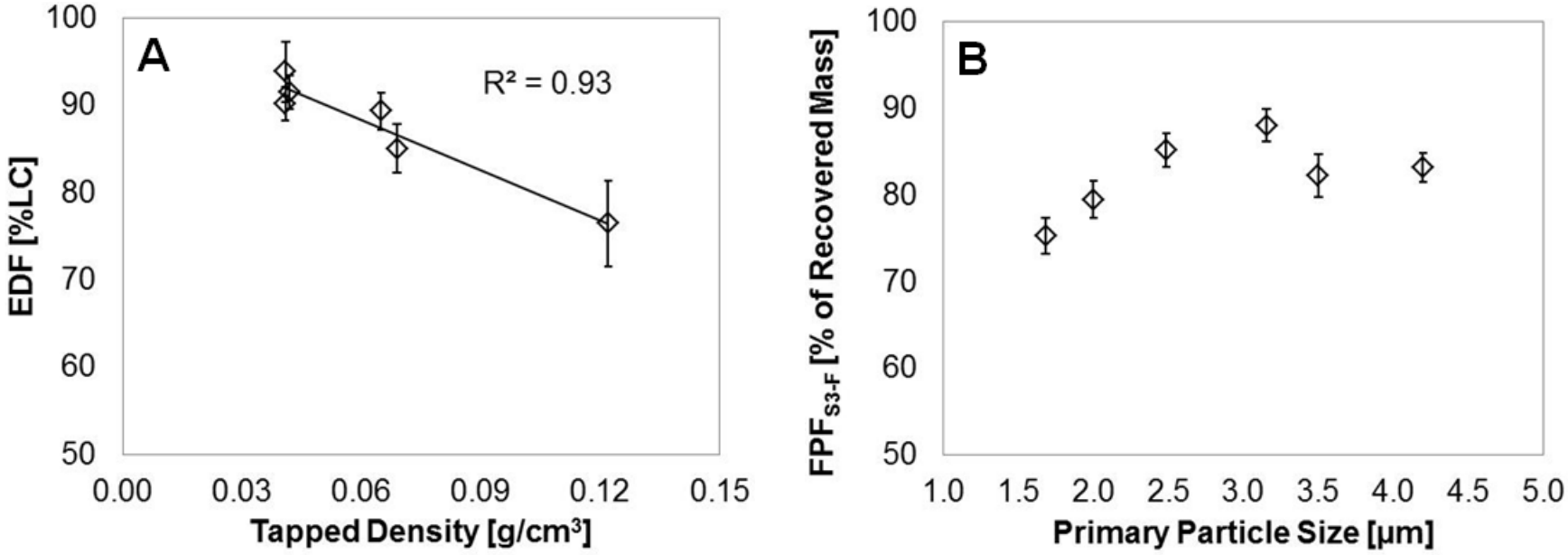

Figure 3.4 Effect of tapped density and primary particle size on *in vitro* aerosol performance; (A) tapped density as function of emitted powder mass (N= 10) and (B) primary particle size, X_{50}, as function of fine particle mass (N= 3) accumulated mass from stage 3 to MOC. Presented as the mean and standard deviation of five replicates.

Table 3.4 summarizes the mass median aerodynamic diameter (MMAD) and geometric standard deviation (GSD) derived from the NGI measurement for each inhalation product. The MMAD & GSD values were estimated based on the aerosol fraction deposited in the stages downstream of the throat and pre-separator. The drug masses distributed on the stages (often termed the impactor sized mass, ISM) were transformed to log probability coordinates, and best fit estimates of MMAD and GSD obtained, per USP General Chapter <601>. The MMAD and GSD values so obtained were used as inputs to the ARLA Respiratory Deposition Calculator, along with input parameters identified in **Table 3.5**. The output from the ARLA calculator represents the calculated lung dose, reported here as a fraction of the ISM, and also as a fraction of the label claim/fill mass.

In using these MMAD/GSD estimates to represent the aerosol delivery from the inhaler, it is implicitly assumed that the coarse aerosol fraction pre-filtered by the USP induction port + Pre-separator is deposited in the mouth-throat, and therefore does not contribute to lung dose. This assumption is justified based on experimental data on particle capture efficiency of mouth-throat model versus USP induction port, Zhou et al. (2011), and has been verified in a sensitivity analysis (not reported here).

In addition to the aerosol size distribution, the ARLA calculator also requires the diameter of the inhaler mouthpiece to be specified as an input. As seen in **Figure 3.5**, the inhaler mouthpiece exits have a complex shape, and based on the internal geometry, an "effective" diameter was estimated for each inhaler and used as an input to the ARLA on-line calculator. For example, the effective diameter of Device A was based on the diameter of the internal flow passage issuing into the mouthpiece.

Table 3.4 NGI analysis data and mean of triplicates

Inhaler	Formulation Platform	MP Air Inlet Dimension	1 kPa		2 kPa		4 kPa		6 kPa	
			MMAD [µm]	GSD [c]	MMAD [µm]	GSD [c]	MMAD [µm]	GSD [c]	MMAD [µm]	GSD [c]
Device A	Emulsion Spray dry [a]	0.48 [b]	4.3	2.1	3.9	1.8	3.5	1.8	3.2	1.9
Device B	Blend	0.53 [b]	Not Tested [d]	Not Tested [d]	4.0	1.8	3.9	2.1	3.7	1.9
Device C	Spheronized	0.53 [b]	Not Tested [d]	Not Tested [d]	2.9	1.9	2.6	1.9	2.4	1.9

[a] Representative PulmoSphere™ powder batch A (X_{50} of 2.49 µm and tapped density 0.04 g/cm^3) was used for comparison.

[b] Approximate inhaler mouthpiece exit diameter in cm.

[c] $= \sqrt{\frac{d_{84}}{d_{16}}}$, where d_{84} and d_{16} represent the diameters of the aerosol mass at 84 and 16%, respectively.

[d] NGI data were not generated at 1 kPa for Device B and C due to steep drop in aerosol dose delivery.

Table 3.5 ARLA calculator selection and input parameters. All others set to default mode.

Parameters	Input 1	Input 2	Input 3	Input 4
Particle Properties	Particle density= 1 $g \cdot cm^{-3}$	Log-normal distribution	MMAD (Table 3.4)	GSD (Table 3.4)
Gas Properties	Default	--	--	--
Age	Adult	--	--	--
Delivery Route	Oral	--	--	--
Breathing Conditions	Single inhalation through mouthpiece	Inhalation flow (Table 3.2)	--	--
Respiratory Tract Geometry	Diameter of MP inhaler (Table 3.4)	--	--	--
Gravity	Default	--	--	--

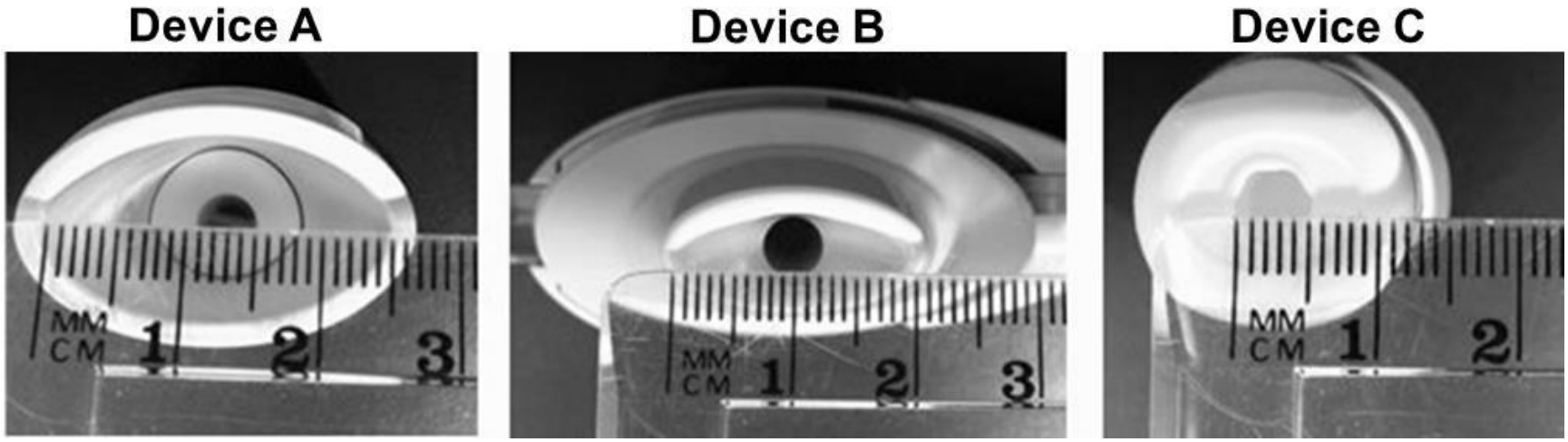

Figure 3.5 Photographs of DPI mouthpiece showing internal geometry of aerosol flow path.

3.3.2 Idealized mouth-throat model data analysis

The *in vitro* lung dose fraction was measured experimentally using the idealized mouth-throat model at pressure drops ranging from 1 – 6 kPa. **Figure 3.6** presents the measured *in vitro* lung dose fraction as a function of inhaler pressure drop for the six PulmoSphere™ placebo powder formulations tested using Device A. For volume median primary particle size ≥2.5 μm, the data show consistently a low extrathoracic region deposition (hence higher lung deposition) that is independent of primary particle size and flow-rate. However, for particle sizes <2.5 μm, lung deposition is significantly decreased, with greater variability and flow-rate dependence of primary particle size. These results suggest that the optimal equivalent optical diameter size range for PulmoSphere™ placebo powders delivered using Device A is ≥2.5 μm. Below this size, inter-particle attractive forces are greater than drag and lift forces generated in the inhaler. This negatively impacts powder fluidization and dispersion. The data in **Figure 3.6** represents the same device with 6 different variants of the PulmoSphere™ placebo powder. The data clearly demonstrate that the properties of the PulmoSphere™ powder can be tailored to achieve significant improvements in dose delivery for a given device.

Figure 3.7 summarizes *in vitro* aerosol performance data from the idealized mouth-throat model for the three inhalation powder types studied. One of the six PulmoSphere™ powders (primary particle size of 2.49 μm and tapped density 0.04 g/cm^3) was used to generate results with Device A. The results show that the *in vitro* lung dose for this PulmoSphere™ powder when delivered with Device A was greater than that of the other two products. The PulmoSphere™ data presented in **Figure 3.6** & **3.7** are consistent with recent studies that

suggest that a drug/device combination comprising of PulmoSphere™ powder and blister-based inhaler enable consistent and high delivery efficiency performance over a range of patient inspiratory flow-rates (Weers et al., 2012 & 2013).

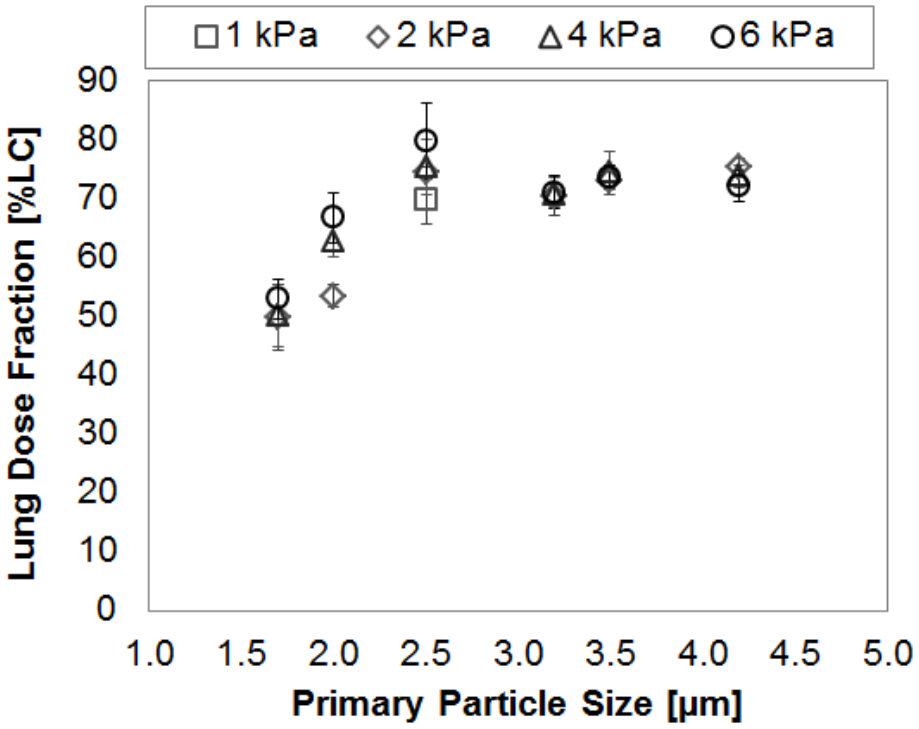

Figure 3.6 ***In vitro*** **lung dose performances as measured from the mouth-throat model for PulmoSphere™ delivered by Device A as a function of mean primary particle size, tested at 1 – 6 kPa inhaler pressure drops. Presented as the mean and standard deviation of five replicates.**

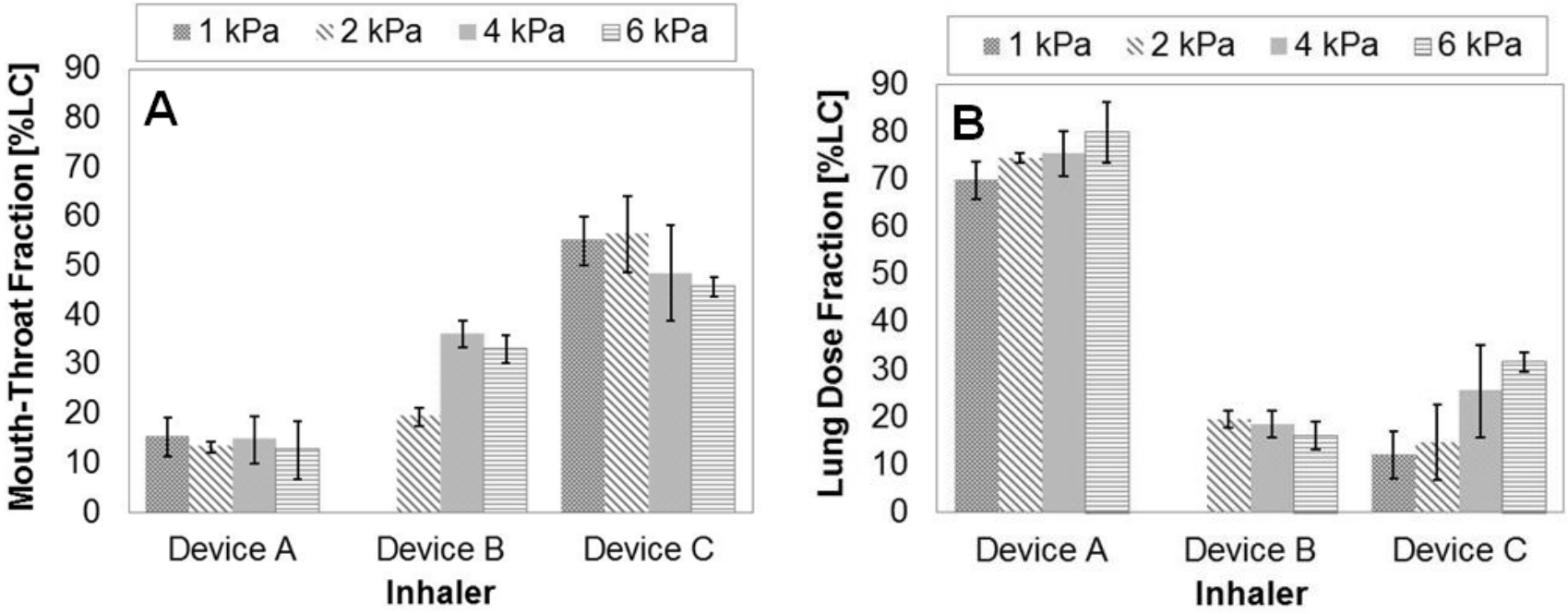

Figure 3.7 Mouth-throat model *in vitro* aerosol data comparing three different powder technology platforms; (A) mouth-throat deposition and (B) lung dose fraction. Presented as the mean and standard deviation of five replicates.

3.3.4 Comparing extrathoracic region deposition from physical mouth-throat model and semi-empirical models

Table 3.6 is a summary of *in vitro* markers of lung dose from the idealized mouth-throat model and semi-empirical models of mouth-throat deposition accounting for inertial impaction due to the effects of airflow (Q), aerodynamic particle size of the dispersed powder, and inhaler mouthpiece dimension. Data are presented as estimated *in vitro* aerosol delivered dose as percent of label claim or fill mass, along with airflows and corresponding pressure drops for each formulation and inhaler platform. The PulmoSphere™ powder shows a slight increase in lung dose with increasing airflow, but equation 3 predicts a small drop in lung dose across the range of airflow tested. In contrast, Device B shows strong flow-rate dependence across the range of airflows tested. Measured lung doses using the mouth-throat model are significantly higher than the values predicted from the semi-empirical model. It should be noted that the internal flow path geometry within the mouthpiece of many inhalers and assumptions regarding the "effective" exit diameter of the inhaler mouthpiece could bias prediction of inhaler exit flow velocities and the associated mouth-throat deposition (Cardwell et al., 2014). Despite this, the *in vitro* mouth-throat model and extrathoracic region numerical model predict a similar trend and performance ranking for the different aerosol delivery platforms. The experimentally measured *in vitro* lung dose (using the idealized mouth-throat model) also correlates with the values predicted using the inertial impaction parameter, d^2Q (**Figure 3.8**). Interestingly, the correlation is better using the prediction at d^2Q<1300 μm^2·L/min (i.e., NGI stages 3 to MOC) than d^2Q<500 μm^2·L/min (i.e., NGI stages 4 to MOC). This observation is consistent with the cut-off value of ~1450

$\mu m^2 \cdot L/min$ reported for the mouth-throat model for monodisperse aerosols (DeHaan and Finlay, 2001).

Table 3.6 Mean and standard deviation shown in parenthesis of *in vitro* aerosol delivered dose for different formulation platforms.

Compound Name (Inhaler)	Powder Platform (Lot)	ΔP / Q [kPa / mL/s]	EPM [%LC]	MT [a] IVLD [%LC]	$FPM_{d^2Q<500}$ [%LC]	$FPM_{d^2Q<1300}$ [%LC]	Equation 3 LDF [% of ISM]	Equation 3 LDF [% of LC]
Placebo (Device A)	Spray Dried PulmoSphere™ (0.04 g/cm^3, 2.49 µm)	1 / 265	85 (3)	70 (4)	44 (3)	58 (3)	52 (2)	34 (1)
		2 / 373	88 (2)	74 (1)	45 (2)	63 (2)	48 (1)	35 (0)
		4 / 530	90 (2)	75 (5)	41(3)	61 (3)	44 (2)	31 (1)
		6 / 660	92 (2)	80 (6)	42 (8)	64 (9)	43 (3)	33 (2)
Tiotropium Bromide (Device B)	Blend (002383B)	1 / 333	No Data [b]	No Data [b]	No Data [b]	No Data [b]	No Data [b]	No Data [b]
		2 / 467	39 (17)	20 (20)	5 (0)	8 (1)	45 (2)	4 (0)
		4 / 650	55 (8)	19 (3)	11 (1)	20 (2)	39 (1)	10 (0)
		6 / 788	49 (6)	16 (3)	9 (3)	17 (5)	36 (2)	8 (0)
Mometasone Furoate (Device C)	Spheronized (OJS5)	1 / 383	67 (3)	12 (5)	No Data [b]	No Data [b]	No Data [b]	No Data [b]
		2 / 550	71 (5)	15 (8)	8 (1)	11 (10	56 (1)	7 (0)
		4 / 783	74 (4)	26 (10)	13 (2)	18 (2)	54 (1)	11 (0)
		6 / 950	77 (6)	32 (2)	15 (1)	21 (1)	52 (1)	13 (0)

[a] MT- Mouth-throat model

[b] No data generated due to poor aerosol performance

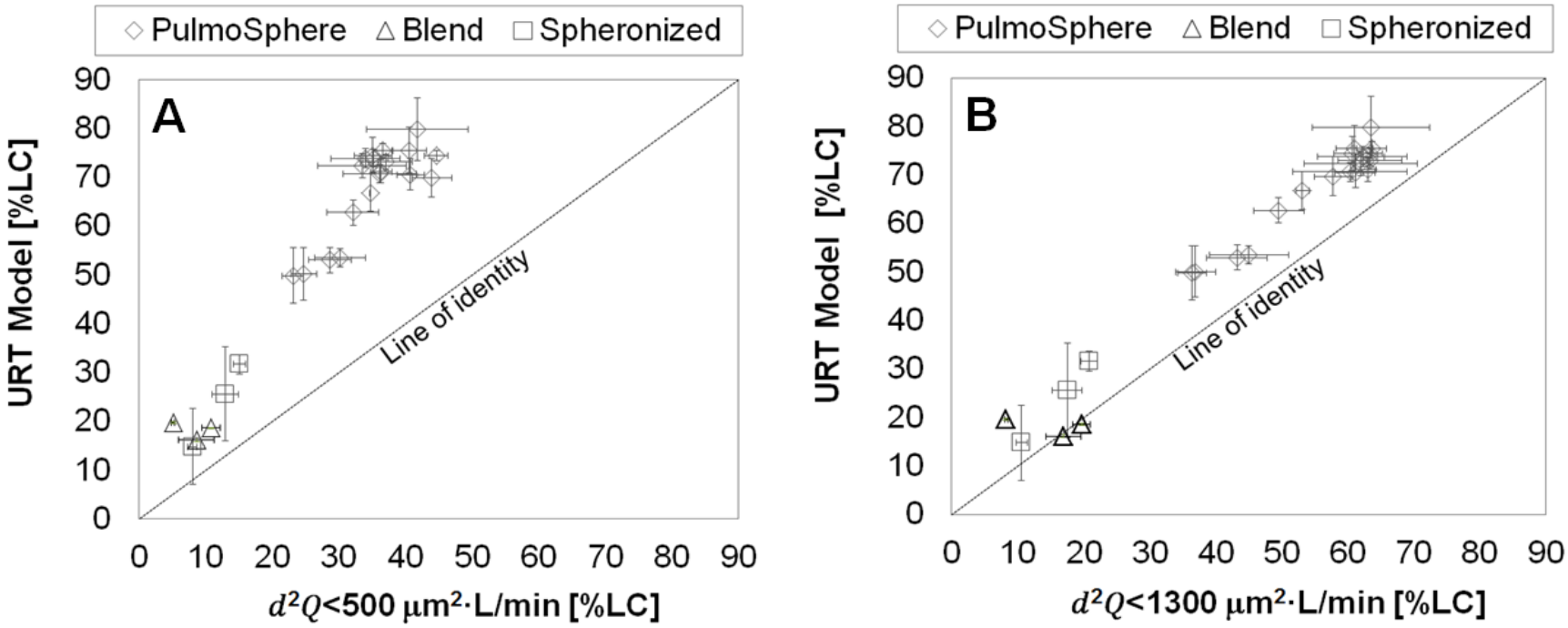

Figure 3.8 Comparison of results from the mouth-throat model, *in vitro* lung dose (experimental data), and inertial impaction parameter model where (A) d^2Q<500 and (B) d^2Q<1300 μm²·L/min. Presented as the mean and standard deviation of five replicates.

3.4 Conclusion

The idealized mouth-throat model is an effective tool for assessing the design space for engineered particles and can be used to tailor engineered powders for a specific DPI system. In this study, application of this tool showed that for porous PulmoSphere™ powders delivered with Device A, enhanced delivery to the lung is favored by low particle density and large particle size. In addition, the idealized mouth-throat model provides a simple and direct method to compare the dose delivery performance among different types of inhalation products, covering a broad range of device and powder technologies, and operating over a range of inhalation flow-rates. In this study, the idealized mouth-throat model was used to compare the performance of engineered powders with that of lactose-based formulations over a clinically relevant range of inhaler pressure drops (1 – 6 kPa). The results showed that the engineered powders ranked higher in *in vitro* measures of lung dose compared to the lactose-based products. These findings are consistent with predictions based on cascade impactor data for the same products. Although the *in vitro* lung dose derived from the idealized mouth-throat model are higher than that predicted from the semi-empirical correlations, the results from all the approaches rank-order the products in a similar manner. Potential advantages of the idealized mouth-throat model over standard cascade impactor sizing tools (e.g., NGI, ACI) are; (i) direct measurement of *in vitro* lung dose, (ii) less analytical burden, and (iii) allowing the use of realistic breath profiles, which have not been considered in this study.

3.5 References

1. Al-Ahowair RAM, Tarsin WY, Assi KH, Pearson SB, and Chrystyn H. Can all Patients with COPD use the Correct Inhalation Flow with all Inhalers and does Training Help? *Resp. Med*. 2007; **101**: 2395 – 2401.

2. Asmanex® Twisthaler®, Patient's Instruction for Use.

3. Cardwell ND, Zee J, Kadrichu NP, Rao NP, and Clark AR. Flow Field Characterization of Three Dry Powder Inhalers. *Respiratory Drug Delivery*. 2014; pp. 501 – 505.

4. Chodosh S, Flanders JS, Kesten S, Serby CW, Hochrainer D, and Witek TJ. Effective Delivery of Particles with the HandiHaler Dry Powder Inhalation System over a Range of Chronic Obstructive Pulmonary Disease Severity. *J. Aerosol Med.* 2001; **14**: 309 – 315.

5. Clark AR and Hollingworth AM. The Relationship between Powder Inhaler Resistance and Peak Inspiratory Conditions in Healthy Volunteers – Implications for In Vitro Testing. *J. Aerosol Med.* 1993; **6**: 99 – 110.

6. Copley M, Smurthwaite M, Roberts DL, and Mitchell JP. Revised Internal Volumes of Cascade Impactors for Those Provided by Mitchell and Nagel. *J. Aerosol Med*. 2005; **18**: 364 – 366.

7. DeHaan WH and Finlay WH. In Vitro Monodisperse Aerosol Deposition in a Mouth and Throat with Six Different Inhalation Devices. *J. Aerosol Med.* 2001; **14:** 361-367.

8. DeHaan WH and Finlay WH. "Predicting Extrathoracic Deposition from Dry Powder Inhalers." *Aerosol Sci*. 2004; **35**: 309 – 331.

9. Delvadia RR, Longest PW, and Byron PR. In Vitro Tests for Aerosol Deposition. I: Scaling a Physical Model of the Upper Airways to Predict Drug Deposition Validation in Normal Humans. *J. Aerosol Med.* 2012; **25**: 32 – 40.

10. Duddu SP, Sisk SA, Walter YH, Tarara TE, Trimble KR, Clark AR, Eldon MA, Elton RC, Pickford M, Hirst PH, Newman SP, and Weers JG. Improved Lung Delivery from a Passive Dry Powder Inhaler Using an Engineered PulmoSphere® Powder. *Pharm. Res.* 2002; **19**: 689 – 695.

11. Finlay WH, DeHaan W, Grgic B, Heenan A, Matida EA, Hoskinson M, Pollard A, and Lange CF. Fluid Mechanicals and Particle Deposition in the Oropharynx: The Factors that Really Matter. *Respiratory Drug Delivery VIII*. 2002; pp. 171 – 177.

12. Golshahi L, Noga ML, Vehring R, and Finlay WH. An In Vitro Study on the Deposition of Micrometer-Sized Particles in the Extrathoracic Airways of Adults during Tidal Oral Breathing. *Annals of Biomed Eng.* 2013; **41**: 979 – 989.

13. Grgic B, Finlay WH, and Heenan AF. Regional Aerosol Deposition and Flow Measurements in an Idealized Mouth and Throat. *J. Aerosol Sci.* 2004; **35**: 21 – 32.

14. Hirst PH, Pitcairn G R, Weers JG, Tarara TE, Clark AR, Dellamary LA, Hall G, Shorr J, and Newman SP. In Vitro Lung Deposition of Hollow Porous Particles from a Pressurized Metered Dose Inhaler. *Pharm. Res.* 2002; **19**: 258 – 264.

15. Longest, P. W., Hindle, M., Choudhuri, S. D., and Xi, J. Comparison of Ambient and Spray Aerosol Deposition in a Standard Induction Port and More Realistic Mouth–Throat geometry. *J. Aerosol Sci.* 2008; **39**: 572 – 591.

16. Marple VA, Olson BA, Santhanakrishnan K, Mitchell JP, Murray SC, and Hudson-Curtis BL. Next Generation Pharmaceutical Impactor (A New Impactor for Pharmaceutical Inhaler Testing). Part II: Archival Calibration. *J. Aerosol Med*. 2003; **16**: 301 – 324.

17. Marple VA, Olson BA, Santhanakrishnan K, Roberts DL, Mitchell JP, and Hudson-Curtis BL. Next Generation Pharmaceutical Impactor: A New Impactor for Pharmaceutical Inhaler Testing. Part III. Extension of Archival Calibration to 15 L/min. *J. Aerosol Med*. 2004; **17**: 335 – 343.

18. Martin AR and Warran FH. An Online Calculator for Predicting Respiratory Deposition of Inhaled Aerosols. *Respiratory Drug Delivery*, Book 2. 2008; pp. 801 – 805. *www.mece.ualberta.ca/arla/aerosoldepositioncalculator_adult.html*

19. McRobbie DW, Pritchard S, and Quest RA. Studies of Human Oropharyngeal Airspaces Using Magnetic Resonance Imaging. I. Validation of a Three-Dimensional MRI Method for Producing *Ex Vivo* Virtual and Physical Casts of the Oropharyngeal Airways During Inspiration. *J. Aerosol Med.* 2003; **16**: 401 – 415.

20. McRobbie DWand Pritchard S. Studies of Human Oropharyngeal Airspaces using Magnetic Resonance Imaging. II. The Effects of Device Resistance with Forced Maneuver and Tidal Breathing on Upper Airway Geometry. *J. Aerosol Med.* 2005; **18**: 325 – 336.

21. Newhouse MT, Hirst PH, Duddu SP, Walter YH, Tarara TE, Clark AR, and Weers JG. Inhalation of a Dry Powder Tobramycin PulmoSphere Formulation in Healthy Volunteers. *Chest*. 2003; **124**: 360 – 366.

22. Olsson B, Borgstrom L, Svensson M, and Lundback H. Modeling Oropharyngeal Cast Deposition to Predict Lung Delivery from Powder Inhalers. *Respiratory Drug Delivery*. 2008; pp. 197 – 205.

23. Olsson B, Borgström L, Lundbäck H, and Svensson M. Validation of a General *In Vitro* Approach for Prediction of Total Lung Deposition in Healthy Adults for Pharmaceutical Inhalation Products. *J. Aerosol Med.* 2013; **26**: 1 – 15.

24. Podczeck F. The Relationship between Physical Properties of Lactose Monohydrate and the Aerodynamic Behavior of Adhered Drug Particles. *Int. J. Pharm.* 1998; **160**: 119 – 130.

25. Pritchard S and McRobbie DW. Studies of Human Oropharyngeal Airspaces using Magnetic Resonance Imaging. II. The Use of Three-Dimensional Gated MRI to Determine the Influence of Mouthpiece Diameter and Resistance of Inhalation Devices on the Oropharyngeal Airways Geometry. *J. Aerosol Med.* 2004; **17**: 310 – 324.

26. Spiriva® HandiHaler®, Patient's Instruction for Use.

27. Stahlhofen W, Rudof G, and James AC. Intercomparison of Experimental Regional Aerosol Deposition Data. *J. Aerosol Med.* 1989; **2**: 285 – 308.

28. Stapleton KW, Guentsch E, Hoskinson MK, and Finlay WH. On The Suitability of k-e Turbulence Modeling for Aerosol Deposition in the Mouth and Throat: A Comparison with Experiment. *J. Aerosol Sci.* 2000; **31**: 739 – 749.

29. Weers JG. Dispersible Powders for Inhalation Applications. *Innovation in Pharm. Technol*. pp. 111 – 116.

30. Weers JG, Maltz DS, Ung K, Chan L, Glusker M, Ament B, Le J, Rao N, and Axford G. Minimizing Human Factors Effects through Inhaler Design. *Respiratory Drug Delivery*. 2012; pp. 217 – 226.

31. Weers JG, Tarara TE, and Clark AR. Design of Fine Particles for Pulmonary Drug Delivery. *Expert Opin. Drug Delivery.* 2007; **4**: 297 – 313.

32. Weers JG, Ung K, Le J, Rao N, Ament B, Axford G, Maltz D, and Chan L. Dose Emission Characteristics of Placebo PulmoSphere® Particles Are Unaffected by a Subject's Inhalation Maneuver. *J. Aerosol Med.* 2013; **26**: 56 – 68.

33. Yang TT, Li S, Wyka B, and Kenyon D. "Drug Delivery Performance of the Mometasone Furoate Dry Powder Inhaler." *J. Aerosol Med.* 2001; **14**: 487 – 494.

34. Zhou Y, Sun J, and Cheng Y. Comparison of Deposition in the USP and Physical Mouth-Throat Models with Solid and Liquid Particles. *J. Aerosol Med.* 2011; **24**: 277 – 284.

Chapter 4

Effects of ramp-up of inspired airflow on in vitro aerosol dose delivery performance for certain dry powder inhalers

(Original article published in Eur. J. Pharm. Sci., 2016)

4.1 Introduction

There are many inhalation drug products currently available on the market that deliver an aerosolized medicine to the lung for treatment of respiratory diseases (e.g., Asthma, COPD, and Cystic Fibrosis). Many of these are passive, breath-actuated dry powder inhalers (DPIs) relying on the patient's inspiratory breathing effort to deliver the drug dose for local or systemic effect. The total dose delivered to the lungs depends on product related factors such as the inhaler design and particle formulation characteristics, as well as patient related factors such as the airway geometry, and inspiratory flow characteristics (i.e., peak inspiratory flow-rate, PIF; ramp-up rate of inspired airflow, and inhalation volume) that vary from patient to patient.

DPIs of different designs rely on a variety of working principles to fluidize and disperse bulk powder into respirable aerosol agglomerates. There have been several studies aimed to understanding the dose delivery performance of different inhalers as a function of patient inspiratory flow parameters. Most prior studies on this subject have focused on the effect of patient PIF on dose delivery performance (Auty et al., 1987; Parry-Billings et al., 2008;

Pedersen et al., 1990; Ramsgaard et al., 1989). There have been comparatively fewer studies on the effect of the ramp-up of flow-rate (Beron et al., 2008; Chavan et al., 2000; De Boer et al., 1997; Everard et al., 1997). These studies have shown that for some passive DPIs, the ramp-up of airflow can adversely influence powder emptying and the respirable dose fraction delivered, especially if the aerosolization event duration is short and occurs within the ramp-up period. For some DPIs, such unfavorable airflow conditions could lead to high deposition in the mouth-throat, resulting in unwanted oral absorption for some drugs, and in some instances may increases in both local and systemic side-effects (Byron, 1986; Grim et al., 2001; Newman et al., 1983).

There have been recent attempts by DPI designers to address and mitigate the flow ramp-up effect on inhalation drug delivery. One approach has been to provide the inhaler with a breath-actuated-trigger to delay aerosol generation until a threshold flow-rate (or pressure drop) is achieved (Kohler, 2004). An alternative approach is to slow down the aerosol emission kinetics, such that the bulk of the aerosol emission occurs when the flow-rate is fully developed (Ung et al., 2012). Indeed, Coates et al. (2006) found that significant dispersion reductions may occur when a large amount of powder is released from the device before both the turbulence levels and particle impaction velocities were fully developed.

These recent innovations have stimulated an investigation of flow ramp effects in commonly available DPIs. This study investigates several different marketed oral inhalation products to assess sensitivity to flow ramp-up (or flow acceleration), and its impact on *in vitro* aerosol delivery performance. Experiments focused on testing inhaler dose delivery performance

under two flow-ramp conditions (i.e., slow and fast ramp), using airflow profiles generated by a custom-designed breath-simulator. Measurements were focused on three dose delivery attributes; aerosol emission kinetics as measured by a custom-designed laser photometer, delivered dose (DD), and total lung dose (TLD) as measured by an anatomical mouth and throat model (the Alberta Idealized Throat model; DeHaan and Finlay, 2001). Results from the laser photometry, DD, and *in vitro* TLD tests will be used to assess the sensitivity of the inhalers to ramp-up of inspired airflow.

4.2 Materials and Methods

4.2.1 Dry powder inhalers and formulations

Table 4.1 summarizes the DPIs and formulations investigated in this study. Except for the first, all of the products listed in the table are commercially marketed and will not be described in detail here. The selection of the marketed dry powder inhalers is intended to cover different powder dispersion mechanisms, powder formulation technologies (e.g., spray dried powders versus micronized blends), drug package types (e.g., capsule, blister, or reservoir) and inhaler flow resistances, see **Tables 4.1** and **4.2**. The Simoon is a unit-dose, blister-based inhaler being developed by Novartis (Maltz et al., 2008; Ung et al., 2012). The development prototype used in this study has a high resistance (R ~ 0.19 $cm \cdot H_2O^{0.5}/L/min$), and relies on inspiratory airflow to fluidize and de-agglomerate the powder (Ung et al., 2012; Weers et al., 2013). In this study, the Simoon device is paired with a dry powder formulation of Indacaterol Maleate, prepared using the PulmoSphere™ technology (Weers and Tarara,

2014). PulmoSphere™ powder formulations were prepared by spray drying a feedstock comprising the drug, either in solution or suspension, along with a perflubron (PFOB) in water emulsion, stabilized by distearoylphosphatidylcholine (DSPC) and calcium chloride ($CaCl_2$). The spray drying process eliminated water and PFOB, and produced low density porous particles containing drug, DSPC, and $CaCl_2$. The Indacaterol PulmoSphere™ formulation used in this study contained 8% Indacaterol maleate (QAB149), 86% DSPC, 6% $CaCl_2$ and was filled into a foil-foil blisters (fill mass of 2 mg) designed for use with the Simoon inhaler.

Table 4.1 DPIs and formulations used in the present study.

DPI	Product Name (Indication)	Composition API/Excipients	Label Claim [µg]	Formulation Platform	Drug Package	Source
Simoon (Prototype)	N/A*	Indacaterol Maleate/DSPC, CaCl2	40	Spray Dried	Unit Dose Blister	Novartis
Podhaler®	Tobi® (CF)	Tobramycin Sulfate/DSPC, CaCl2	27500	Spray Dried	Unit Dose Capsule	Novartis
Breezhaler®	OnBrez® (COPD)	Indacaterol Maleate/ Lactose	150	Lactose Carrier Blend	Unit Dose Capsule	Novartis
Diskus®	Advair® (Asthma/ COPD)	Fluticasone Propionate/ Salmeterol/ Lactose	250/50	Lactose Carrier Blend	Multi-Dose Blister Strip	GSK
Handihaler®	Spiriva® (COPD)	Tiotropium Bromide/Lactose	18	Lactose Carrier Blend	Unit Dose Capsule	BI/Pfizer
Flexhaler®	Pulmicort® (Asthma)	Budesonide	180	Soft Agglomerates	Multi-dose Reservoir	Astra Zeneca
Twisthaler®	Asmanex® (Asthma)	Mometasone Furoate/ Lactose	220	Soft Agglomerates	Multi-dose Reservoir	Merck

*Not marketed product.

4.2.2 Inhalation flow profile simulator

Inhalers were tested using idealized inhalation flow profiles having two different flow ramp-up rates, representing "slow" and "fast" ramp-up. The flow profiles were generated using a custom-built inhalation profile simulator (IPS-2, Novartis Corp., US). The IPS-2 uses computer-controlled, proportional solenoid valve connected to a vacuum source to generate target flow profiles. The "slow" ramp profile targeted a ramp-up time of 1 second, while the "fast" ramp profile represents the fastest ramp time that was practical for the test system. **Figure 4.1** presents example flow profiles representing slow and fast ramp-ups for the Breezhaler device. The peak inspiratory flow-rate (PIF) for both profiles is the same (104 L/min), and corresponds to a pressure drop of 4 kPa across the inhaler. The test condition of 4 kPa is used in compendial aerosol test methods and is within the range of inhalation efforts that can be achieved by both Asthma and COPD patients (Al-Ahowair et al., 2007). Note that the PIF and pressure drop are related as shown in equation 1 (Clark et al., 1992),

$$R = \frac{\sqrt{\Delta P}}{Q} \qquad (1)$$

where R is the inhaler flow resistance ($cm \cdot H_2O^{0.5}$/L/min), Q is the volumetric flow-rate (L/min), and ΔP is the inhaler pressure drop (centimeter of water). Q and ΔP are obtained through measurements. **Table 4.2** summarizes the inhalation flow profile characteristics (peak flow-rate and ramp-up time) for each of the inhalers tested in this study. The flow ramp-up time is specified in terms of T_{90}, which is the total time taken by the IPS-2 breath simulator to reach 90% of the PIF.

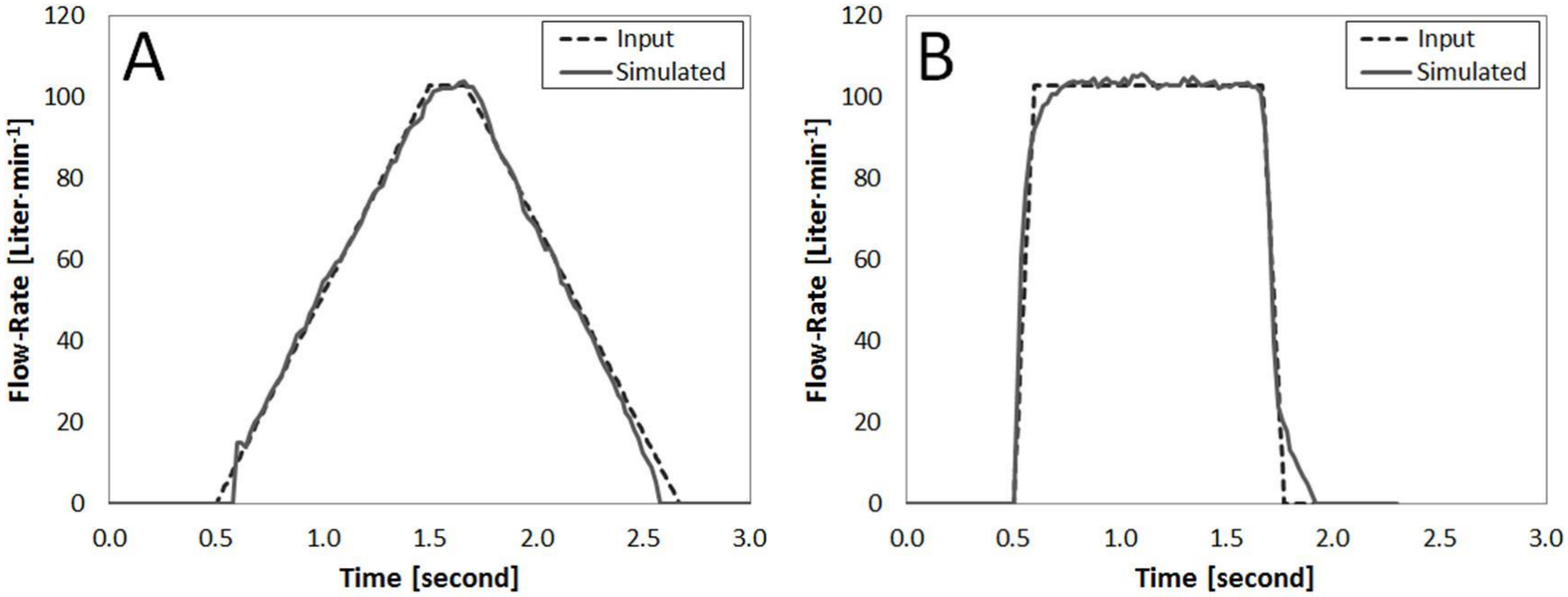

Figure 4.1 Simulated inhalation flow-rate profile for Breezhaler device (A) slow and (B) fast ramp-up.

Table 4.2 Flow resistance, flow-rate, and ramp-up time at 4 kPa pressure drop for each inhaler. Presented as the mean and standard deviation shown in parenthesis of three replicates.

DPI	Flow Resistance [cm·$H_20^{0.5}$/L/min]	Flow-Rate [L/min]	T_{90} Slow Ramp-up [second]	T_{90} Fast Ramp-up [second]
Simoon	0.19	33	0.84 (0.00)	0.34 (0.00)
Podhaler®	0.08	76	0.85 (0.01)	0.39 (0.22)
Breezhaler®	0.06	103	0.91 (0.01)	0.30 (0.02)
Diskus®	0.08	81	0.84 (0.00)	0.20 (0.00)
Handihaler®	0.16	39	0.95 (0.06)	0.39 (0.12)
Flexhaler®	0.11	58	0.79 (0.01)	0.26 (0.00)
Twisthaler®	0.14	45	0.86 (0.00)	0.27 (0.01)

4.2.3 Laser photometry

The kinetics of powder emptying from each DPI was characterized using a custom designed laser photometer based on a commercially available laser sensor head (Keyence Corp., model LX2-13W, US). **Figure 4.2** presents a laser photometer set-up for measuring the aerosol pulse exiting the DPI mouthpiece (MP). The laser photometer comprises an aerosol flow cell with a cross-sectional area illuminated by a laser sheet. The presence of aerosol causes obscuration of the sheet laser and is detected by a photo-detector. The photo-detector's

response is linear with obscuration (i.e., laser intensity). Beer's law was then used to convert the photo-detector response to an aerosol concentration.

BEER'S LAW

$$C_v \propto -ln\left(\frac{V}{V_0}\right) \quad (2)$$

C_v is the aerosol concentration, V is the baseline corrected photo-detector response in the presence of the aerosol, and V_0 is the corresponding photo-detector response in the absence of aerosol pulse. Suitable mouthpiece adapters were developed for each DPI for attachment to the laser photometer inlet port. The IPS-2 breath simulator was used to simulate slow and fast ramp-up flow profiles for each DPI. The laser photometer is also provided with a filter to collect the emitted dose downstream of the photo-detector. Before each measurement, the data acquisition software performs a background scan to update the baseline response of the system, which shifts gradually over time due to powder residue buildup on the flow-cell windows.

For the tests performed with the laser photometer, the aerosol emission event is observed as a pulse (**Figure 4.2**). Past characterization with engineered powders at Novartis (unpublished research) has shown that the area under the curve (AUC) may be correlated to the emitted mass of powder using a suitable calibration procedure. However, in the case of products generating a very high aerosol concentration, (e.g., Tobi® Podhaler® with ~48 mg powder fill mass), the transmission of laser light falls to undetectable levels and the detector output is considered saturated. Under these conditions, it is generally observed that the aerosol emission pulse "width" is still sharply defined, though the pulse "height" may not always be

well defined due to detector saturation at the high powder payloads being delivered. Therefore, the steep drop-off of the photo-detector signal at the end of the aerosol emission event provides a reliable estimate of the aerosol pulse duration (e.g., aerosol emptying time), and largely independent of the pulse height.

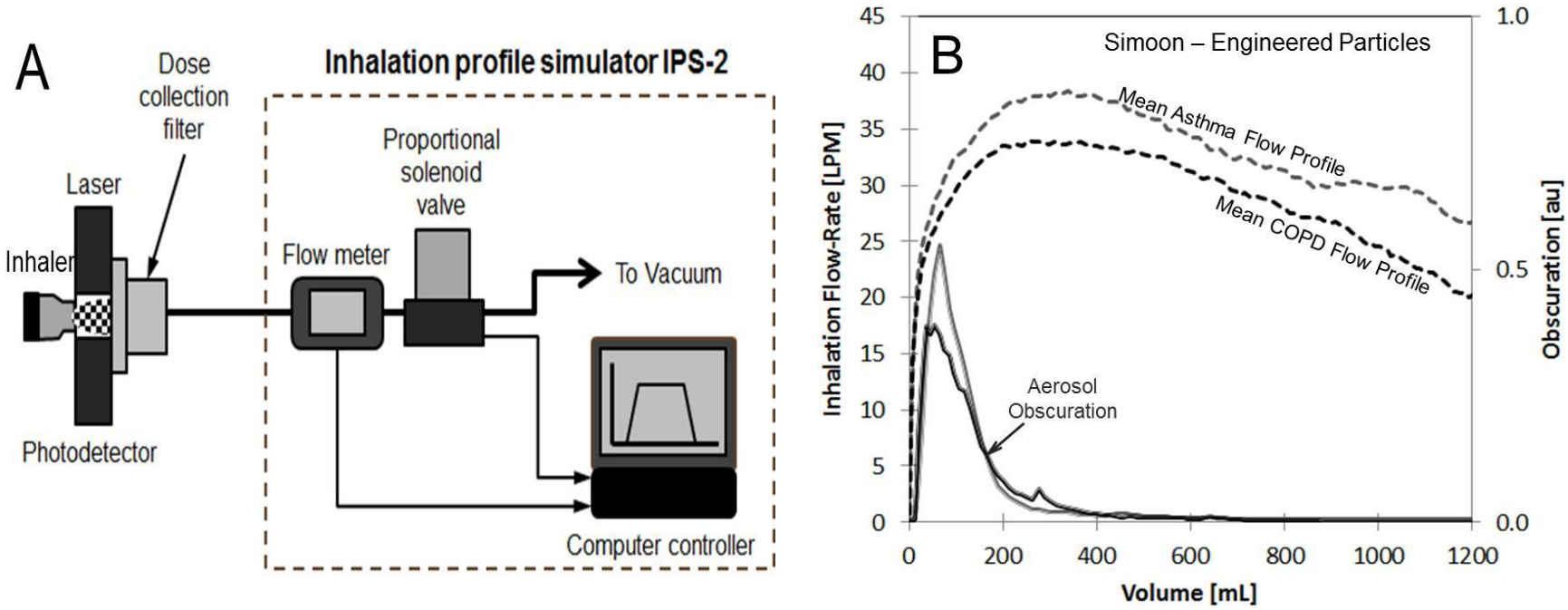

Figure 4.2 (A) Schematic diagram of test set-up used for assessing the aerosol emission kinetics from a DPI, comprising a laser photometer coupled to the inhalation flow profile generator (IPS-2). (B) Example plot of results showing traces of the flow profile and associated aerosol emission. Average inspiratory flow profiles were obtained from published studies (Ament *et al*, 2012 for COPD patients and unpublished study from Novartis for asthma patients).

Two methods of determining aerosol pulse duration or aerosol emptying volume were used. Under normal conditions, the volume of air (V_{90}) needed to clear 90% of the emitted aerosol mass (i.e., AUC) was taken as the estimate of aerosol emptying volume. This analysis is not strictly justified when detector saturation occurs (as in the case for Tobi® Podhaler® with ~48 mg delivered mass). Under these circumstances, an alternative approach for estimating of aerosol clearance volume was used, that being the volume of air at which the tail of the aerosol concentration pulse falls below a pre-specified threshold value (i.e., 2). For each DPI, N= 3 replicate runs were performed to determine aerosol emission characteristics, with each inhaler being actuated only once per replicate run.

4.2.4 In vitro characterization of aerosol dose delivery performance

In vitro aerosol dose measurement was performed at 4 kPa for two ramp-up flows (slow and fast) and used the IPS-2 for simulating the two ramp profiles. Each dose measurement represents one inhaler actuation with a constant sampled volume of 2 liters. Testing attributes included measurements of *in vitro* delivered dose (DD) and total lung dose (TLD), the latter measured using an idealized throat model, the Alberta idealized throat (AIT).

The Alberta idealized throat has been developed to mimic the aerosol deposition characteristics of the human mouth and throat, and incorporates essential geometric features of the upper respiratory tract and their average dimensions from imaging studies (Finlay et al., 2010). This geometry has been well characterized in a series of published studies (DeHaan and Finlay 2001; Finlay et al., 2002; Grgic et al., 2004), which demonstrate that it

accurately mimics the mean *in vivo* deposition in humans. The AIT enables a direct and simple *in vitro* assessment of the total lung dose delivered by a test inhaler, measured as the aerosol drug mass collected downstream of the mouth-throat model. **Figure 4.3A** shows the AIT model used in this study. It is based on CAD design data from the University of Alberta, and has been fabricated as a two-stage assembly, enabling drug deposition in the mouth and throat sections to be assayed separately if needed. **Figure 4.3B** shows the test set-up used in the study.

The AIT approach provides some advantages over the cascade impactor method often used as the *in vitro* basis for estimating the lung dose for inhalation drug products. In comparison to the USP induction port used in cascade impactor tests, the Alberta idealized throat is expected to more realistically simulate the physics of aerosol transport and deposition in the human mouth and throat (Zhang et al., 2007; Zhou et al., 2011). The cascade impactor approach relies on fixed flow-rates and *in vitro* markers such as fine particle mass (FPM) cuts or stage groupings, and the selection of these may not be readily apparent, especially when comparing or interpreting data across different types of inhalers, each with its own characteristic flow resistance and associated range of inspiratory flow-rates during use. In contrast, the Alberta idealized throat allows for a relatively straightforward comparison and interpretation of lung dose data across different inhalers and flow-rate regimes. Furthermore, while cascade impactors are designed to operate at constant flow-rates, the Alberta idealized throat allows for more realistic simulation of human use scenarios during testing, e.g., by accommodating the use of realistic, time-varying inspiratory flow profiles that may influence the performance of some inhalation drug products. It is reasonable to expect some degree of correlation between AIT and cascade impactor data when fixed flow regimes are employed

during testing (Ung et al., 2014). The approach of using a mouth and throat model to estimate lung deposition has been shown to be effective for a wide variety of inhalation drug products (Delvadia et al., 2013; Olsson et al., 2013; Weers et al., 2014).

For the delivered dose (DD) tests, the aerosol emitted from the inhaler mouthpiece was collected by a standard dose uniformity sampling apparatus (DUSA, Westech Scientific Inc., USA) having a diameter of 47 mm filter (A/E type, Pall Corp. US). For the Tobi® Podhaler®, a larger 81 mm diameter filter (Durapore, EMD Millipore, US) housed in a custom filter holder was used to collect the large dose (~48 mg powder) without overloading. For each DPI N= 5 replicate determinations were performed, with each inhaler being actuation only once per DD determination. The DD results are presented as a mean value, normalized to the nominal dose.

For the TLD measurements, test DPIs were coupled to the inlet of the AIT model, and the dose penetrating through the model was collected downstream on a filter (76 mm diameter, A/E type, Pall Corp., US; Durapore, EMD Millipore, US), as shown in **Figure 4.3B**. A polysorbate (EMD Chemicals, Cat. #8170072, US) wetting agent (equal parts of Tween 20 and methanol, v/v) was used for coating the interior walls of the AIT model to prevent particle re-entrainment. The procedure for applying coating solution to the AIT was as follows; (i) ~15 mL of the coating solution was dispensed into the AIT, which was then capped at both ends, (ii) the solution was allowed to wet the internal walls of the AIT using a rocking or rotary motion to tilt the AIT from side to side, and (iii) excess solution was allowed to drain for 5 minutes before use. After five dose actuations, the AIT was rinsed with lukewarm water, air dried, and a fresh coating applied before the next use. Note, that

for the Tobi® Podhaler®, cleaning and re-coating were performed after each dose actuation because of high powder mass loading. The TLD results are reported in terms of percent of the nominal dose.

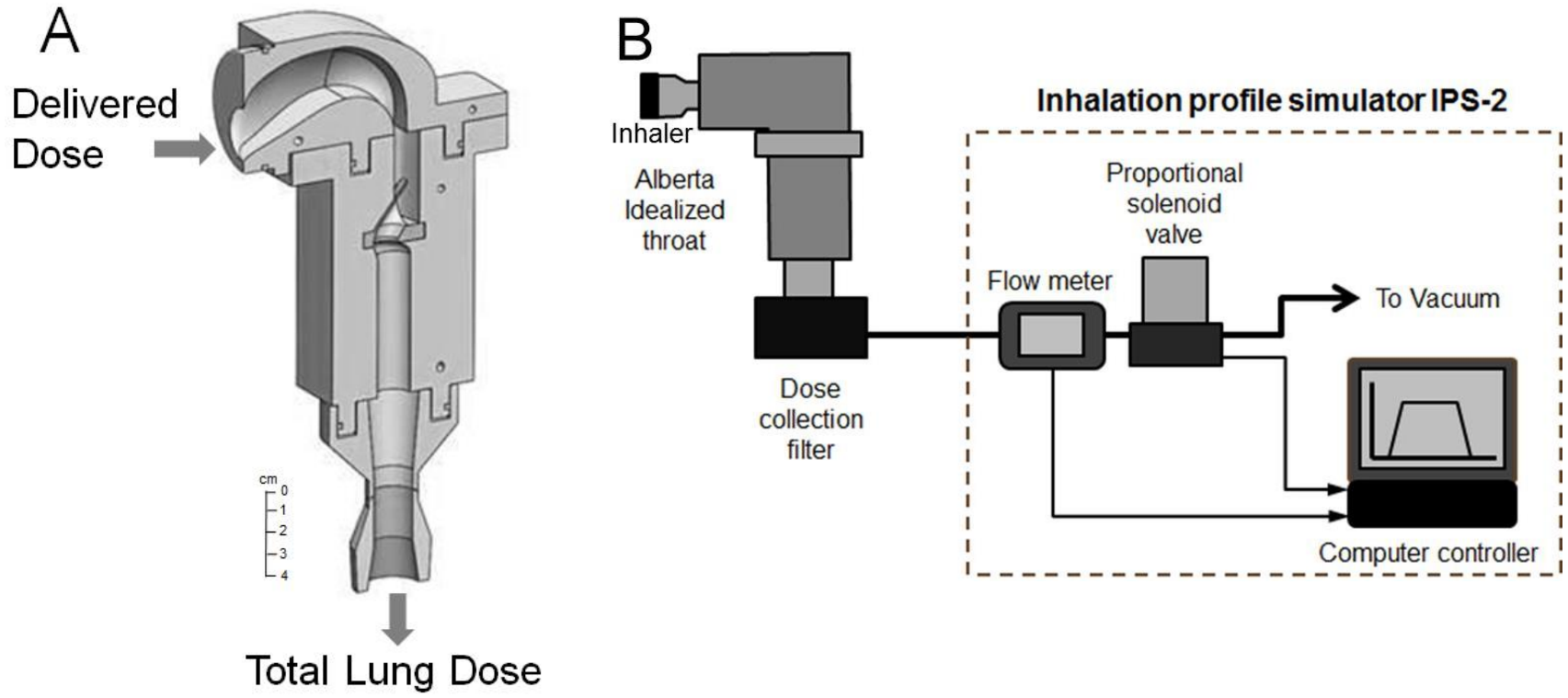

Figure 4.3 (A) Drawing of Alberta idealized throat and (B) experimental arrangement for measuring the *in vitro* TLD using an AIT.

4.2.5 High performance liquid chromatography (HPLC) analysis

Table 4.3 presents the HPLC methods used in the study for drug-specific assay of the collected dose of each drug compound. Known volumes of solvents were used for dissolving the drug deposits on the various parts of the experimental set-ups. For Indacaterol and Tobramycin PulmoSphere™ formulations, an additional sample preparation step was employed by using a centrifuge (Eppendorf AG, Centrifuge 5424, US) to separate un-dissolved DSPC from dissolved drug in solvent solution before injection into the HPLC column. This process ensures the durability of the HPLC column.

Table 4.3 Chromatography methods

Compound	Column	Flow [mL/min]	Injection Volume [µL]	Detector and Wavelength [nm]	Mobile Phase	Solvent	Recovery
Indacaterol	YMC-Pack ODS-AQ [a]	1.5	50	Diode array, 254	H_2O/0.1% TFA; ACN/0.1% TFA	50% H_2O, 50% MeOH	> 98%
Indacaterol	YMC-Pack ODS- AQ [a]	1.0	50	Diode array, 260	H_2O/0.1% TFA; ACN/0.1% TFA	0.5M Acetic Acid/H_2O	> 98%
Tobramycin	Supelcosil LC-18-DB [b]	1.0	20	365	74% TRIS, 2% SO_4, 24% ACN	H_2O	> 98%
Fluticasone /Salmeterol	Zorbax XDB C-18 [a]	1.0	20	225	50% Na_2HPO_4 (0.05M), 35% ACN, 15% MeOH	50% Na_2HPO_4 (0.05M), 35% ACN, 15% MeOH	> 97%
Budesonide	Waters Symmetry C-18 [c]	1.5	20	240	Phosphate Buffer Solution, ACN	70% Phosphate Buffer Solution, 30% ACN	> 97%
Tiotropium	YMC-Pack ODS- AQ [a]	0.6	50	Diode array, 238	75% H_2O, 25% ACN, 0.1% H_3PO_4	75% H_2O, 25% ACN	> 97%
Mometasone	YMC-Pack ODS- AQ [a]	1.0	30	Diode array, 254	H_2O, 0.1% TFA	58% H_2O, 42% ACN	> 97%

H_2O- water; MeOH- methanol; TFA- trifluoroacetic acid; ACN- acetonitrile; Na_2HPO_4- sodium phosphate dibasic; H_3PO_4- phosphoric acid; SO_4- sulfate

[a] 3µm size and 4.6 x 50 mm

[b] 5µm size and 4 x 150 mm

[c] 3µm size and 4.6 x 75 mm

4.3 Results and Discussion

4.3.1 Aerosol powder emission kinetics by laser photometry

Figure 4.4 presents the applied flow-rate and resulting aerosol emission profiles as a function of flow-volume for each DPI for slow and fast ramp-up flows. In general, PulmoSphere™ formulations (i.e., Simoon – placebo & Tobi® Podhaler®) generated a higher aerosol signal obscuration than micronized lactose-based carrier formulations (e.g., OnBrez Breezhaler of 25 mg capsule fill mass) due to their low density (bulk powder density <0.2 g/cm^3), which translates to a larger aerosol volume concentration (i.e., total particle volume per unit volume of air), and increased light extinction. It should also be noted that for micronized lactose-based carrier formulations, the measured aerosol emission intensities are predominately of lactose carriers as the API fraction in the blend is typically small and unlikely to be selectively detected by the photo-detector. For Tobi® Podhaler®, the AUC is considered unreliable because the high aerosol concentration caused the photo-detector to saturate; however the clearance time required to emptying a dose could still be measured.

Overall, the aerosol clearance for fast ramp-up flow is quicker, showing consistent and uniform aerosol emission profiles, and resulted in higher AUC numbers compared to the slow ramp-up flow. In addition, the drug products at the higher end of the fill mass range, i.e., Tobi® Podhaler® (48 mg) and OnBrez Breezhaler (25 mg) required larger volumes of air (~1500 mL) for aerosol clearance, compared to products with lower fill masses (**Figures 4.4 & 4.5)**. As will be discussed in Section 3.2, the delivered dose for these products is not sensitive to ramp effect, although more variation is seen for the total lung dose.

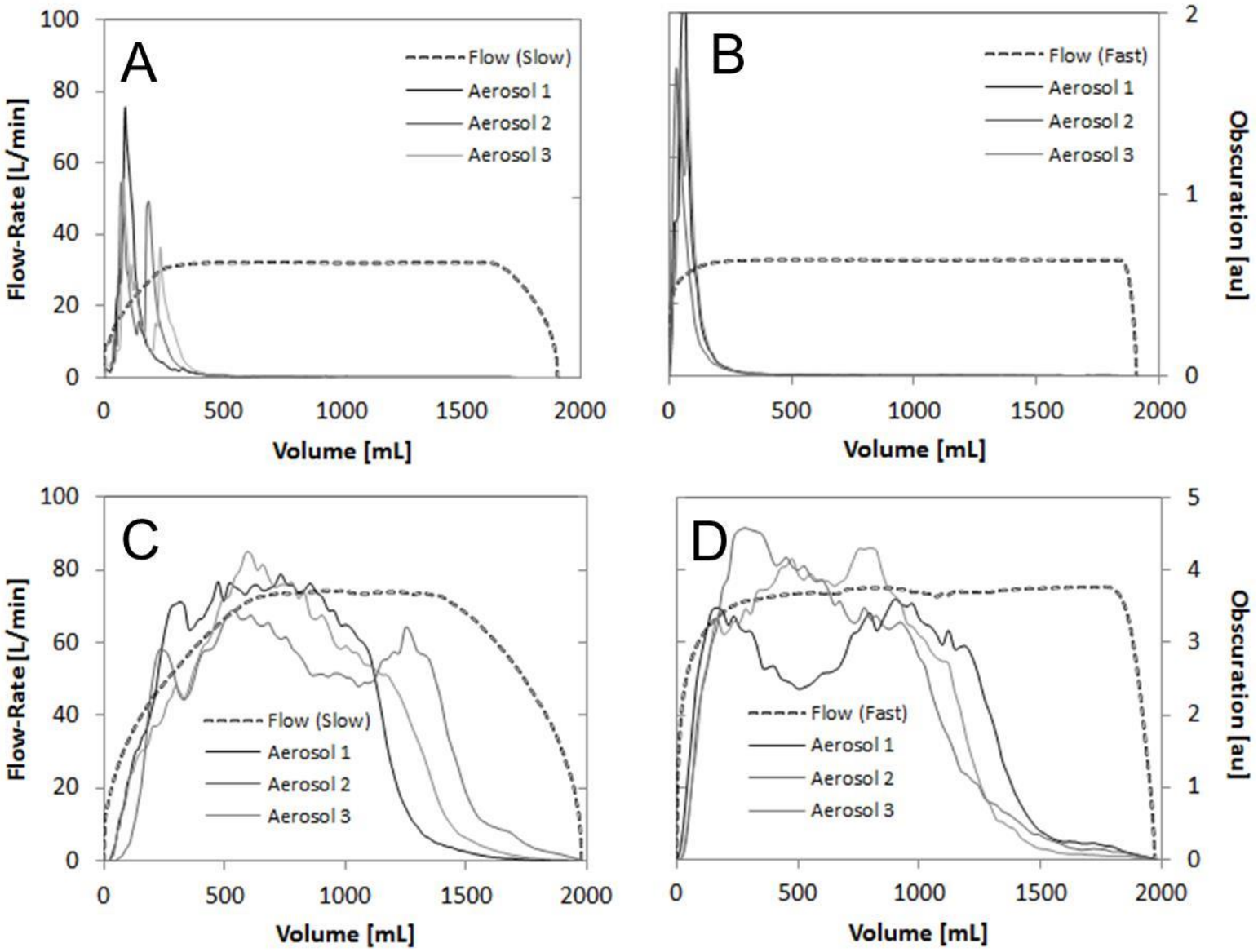
A
Flow (Slow)
Aerosol 1
Aerosol 2
Aerosol 3
Flow-Rate [L/min]
Volume [mL]
B
Flow (Fast)
Aerosol 1
Aerosol 2
Aerosol 3
Obscuration [au]
Volume [mL]
C
Flow (Slow)
Aerosol 1
Aerosol 2
Aerosol 3
Flow-Rate [L/min]
Volume [mL]
D
Flow (Fast)
Aerosol 1
Aerosol 2
Aerosol 3
Obscuration [au]
Volume [mL]

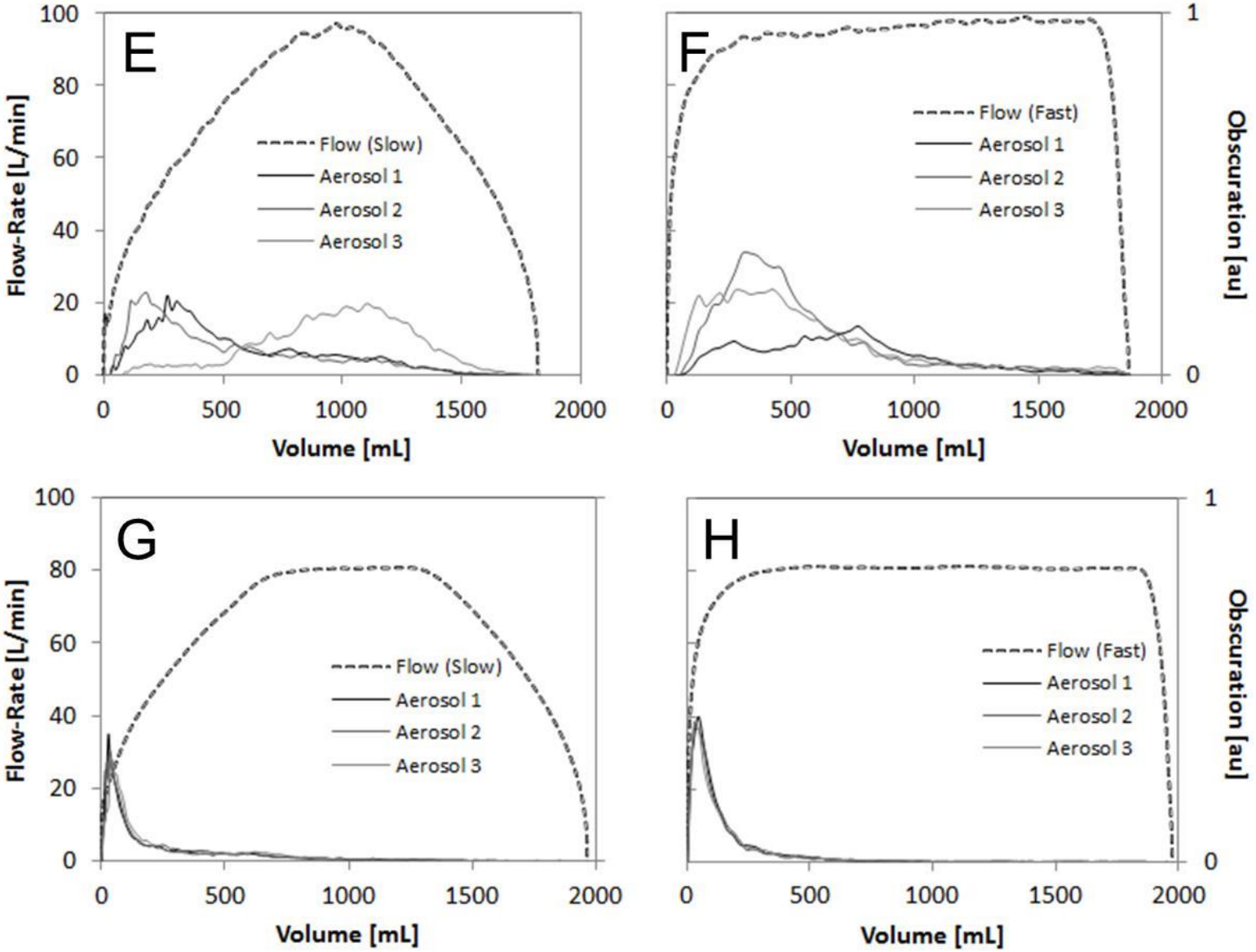
E
Flow-Rate [L/min]
Volume [mL]
Flow (Slow)
Aerosol 1
Aerosol 2
Aerosol 3
F
Obscuration [au]
Flow (Fast)
G
H

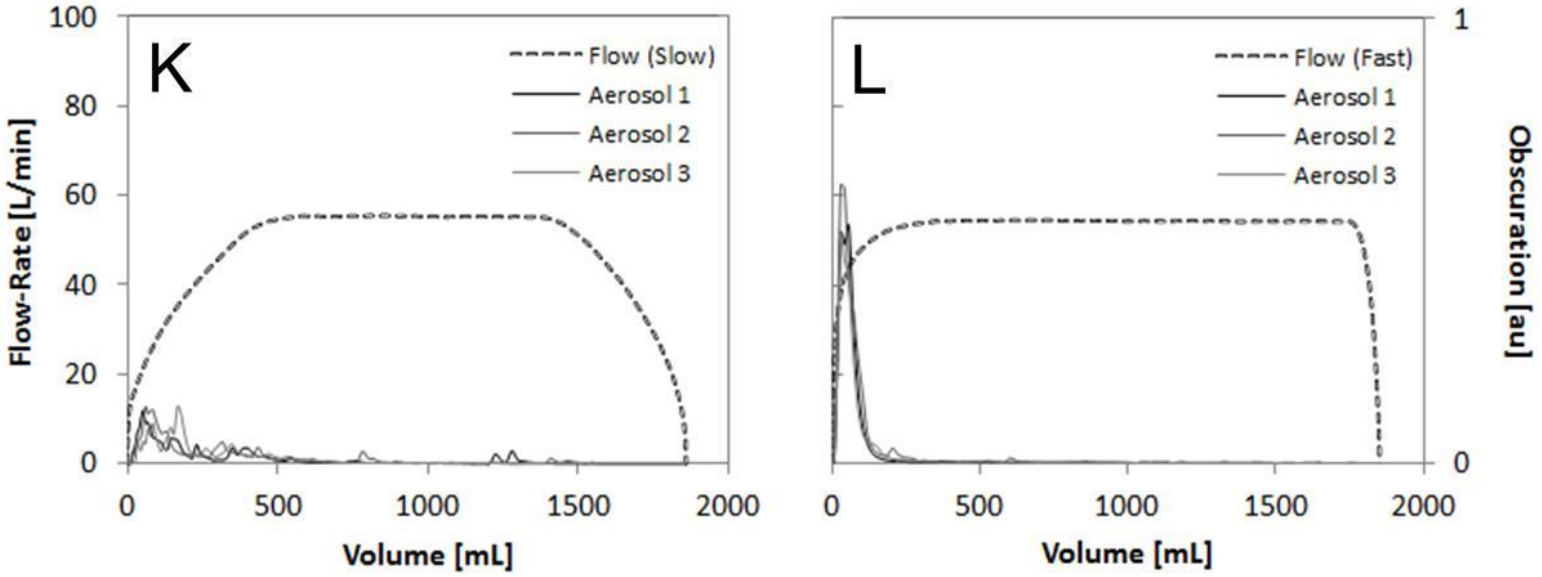

Figure 4.4 Aerosol release kinetics measured at the inhaler mouthpiece by laser photometry for slow and fast ramp-up flows; (A-B) Simoon, (C-D) Podhaler®, (E-F) Breezhaler®, (G-H) Diskus®, (I-J) Handihaler®, (K-L) Flexhaler®, and (M-N) Twisthaler®.

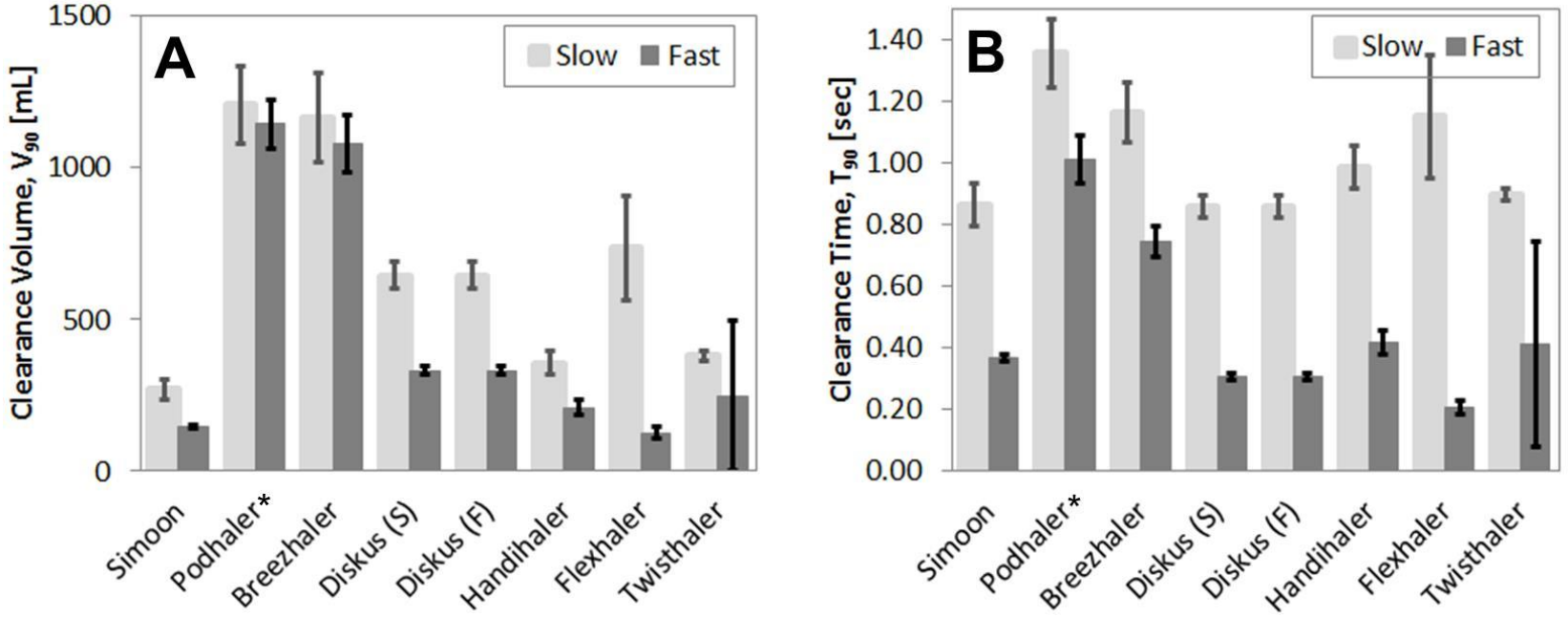

*Laser photometer detector saturated due to high powder loading of 48 mg fill mass.

Figure 4.5 Aerosol clearance (A) volume and (B) time to empty ninety percent of the total delivered dose from the inhaler. Presented as the mean and standard deviation of three replicates.

4.3.2 In vitro aerosol performance analysis

Figure 4.6 summarizes the dose delivery performance for the seven DPIs tested at two ramp-up flows. The results show that the mean DD is relatively insensitive to flow ramp effects, i.e., the mean delivered dose for all DPIs are similar for slow and fast ramp-up flows

(**Figure 4.6**). The mean delivered dose is >80% of nominal dose for all DPIs, except the Spiriva® Handihaler®, which has a lower value of ~ 60% consistent with previously published results (Chodosh et al., 2001)

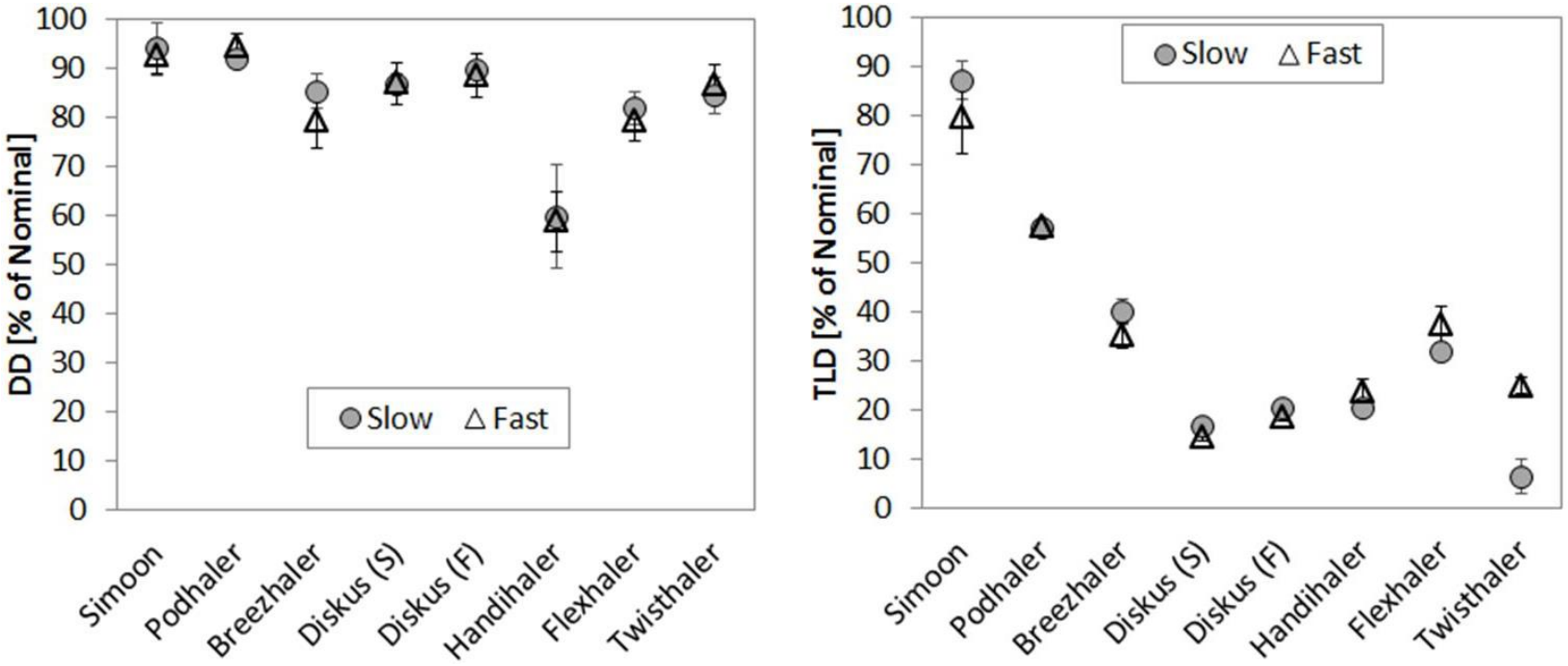

Figure 4.6 Results from *in vitro* testing: (A) Delivered dose and (B) total lung dose for the DPIs tested where Diskus® (S) and (F) represent Salmeterol and Fluticasone Propionate, respectively. Presented as the mean and standard deviation of five replicates.

In contrast, the TLD shows more variation with flow ramp as well as DPI type. The DPI with PulmoSphere™ formulations had TLD ranging from 57 – 87% of nominal dose, significantly higher than that for the other formulations, which had TLD ranging from 7 – 40% of nominal dose. The effect of flow ramp on TLD was relatively small for all DPIs, except the Asmanex® Twisthaler®. This is seen more clear in **Figure 4.7,** which presents the ratio of DD and TLD for slow and fast ramp-up flows, for each drug product. The DD ratio is close to unity for all DPIs (to within ± 0.06), indicating that the DD is relatively insensitive to the flow ramp-up. In contrast, the TLD data show more variation, with all DPIs (except the Asmanex® Twisthaler®) having TLD ratios within the interval 1 ± 0.2. The TLD ratio for Asmanex® Twisthaler® is ~0.28, significantly lower than unity and the TLD ratio values for all other DPIs. Note that the TLD ratio ≅1 for the Tobi® Podhaler®, >1 for the Simoon, OnBrez® Breezhaler® and Advair® Diskus®, and <1 for the remaining DPIs.

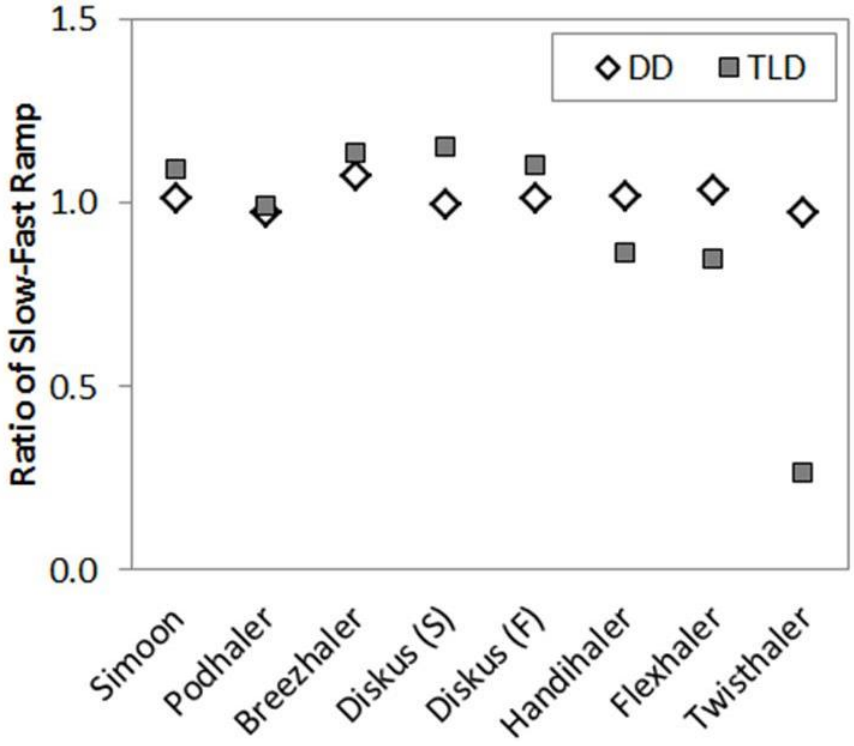

Figure 4.7 Ratio of slow to fast ramp-up for DD and TLD, where Diskus® (S) and (F) represent Salmeterol and Fluticasone Propionate, respectively.

The TLD ratios reflect the sensitivity of dose delivery performance to variation in flow-rate during aerosolization, and can be considered a measure of flow-rate independence. The slow and fast ramp flow profiles subject dry powder inhalers to different flow-rates during aerosolization, with a slow ramp resulting in a lower "effective" flow-rate compared to the targeted peak inspiratory flow-rate. DPIs exhibiting a significant flow-rate effect on TLD would therefore be expected to have TLD ratio deviating from 1. If the TLD increases relatively steeply with increasing flow-rate, a TLD ratio <1 would be expected, while a flat or decreasing TLD trend with flow-rate would result in TLD ratios >1. Note that longer aerosol emission times help to counter the ramp effect by weighting the flow-rate during aerosolization towards higher values, closer to the peak value. This is seen for the case of the

OnBrez Breezhaler, which has an aerosol emission time that is relatively long, coupled with a decreasing trend in TLD *versus* flow-rate (**Figure 4.8**). This should result in a TLD ratio being close to 1 and the observed value of 1.14 is thus consistent with expectation. The Tobi® Podhaler® also has relatively long aerosol event times, and a previous study (Haynes et al., 2014) has shown that the *in vitro* TLD is essentially invariant with flow-rate. The observed TLD ratio ~1 for the Podhaler® is also consistent with expectation.

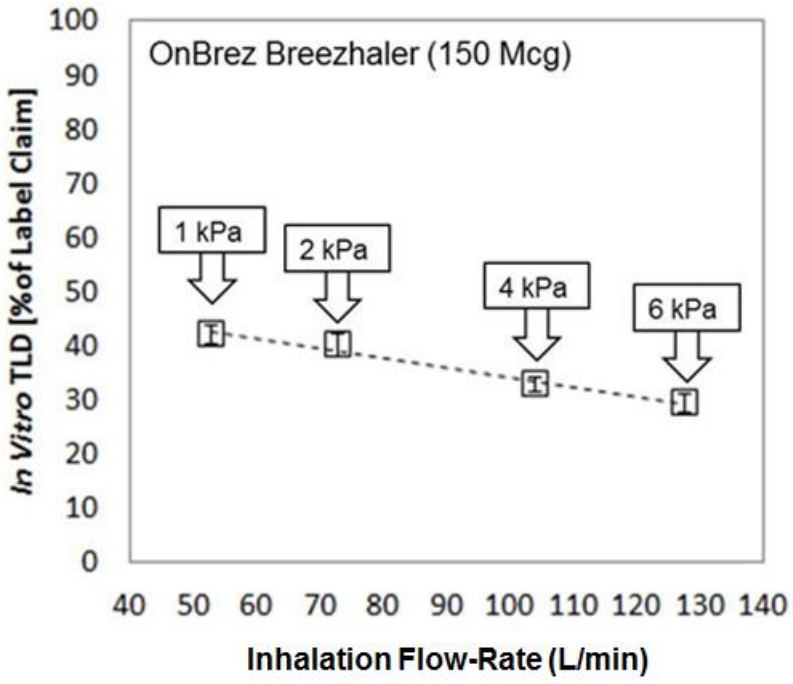

Figure 4.8 Total lung dose as a function of DPI flow-rate for indacaterol maleate (QAB149) lactose blend delivered via Breezhaler®. These data were all generated under fast ramp conditions. Presented as the mean and standard deviation of five replicates.

In contrast, the TLD ratio <<1 for the Asmanex® Twisthaler® indicates a strong flow ramp effect. Since TLD data at different flow-rates are not available for this inhaler, an alternate

metric (i.e., fine particle mass, FPM, measured by cascade impaction) could be considered when examining the observed TLD ratio. Next Generation Impactor (NGI) tests reported in a previous study (Ung et al., 2014) has shown that the particle size distribution of the aerosol emitted by the Asmanex® Twisthaler® is strongly influenced by flow-rate, with the FPM increasing sharply by a factor ~2 when the flow-rate was increased from 33 to 47 L/min (i.e., pressure drop increasing from 2 kPa to 4 kPa, respectively). The observed TLD ratio <<1 is therefore consistent with this flow-rate behavior.

The Pulmicort Flexhaler also exhibits a positive FPM trend with flow-rate, with the FPM increasing by 40-50% when the flow rate is increased from 30 L/min to 60 L/min (Label for Pulmicort Flexhaler TM 180 mcg), and the TLD ratio <1 could again be attributed to this behavior. Published *in vitro* data for the Advair® Diskus® (Demoly et al., 2014) indicate that the fine particle mass is relatively flat over a broad range of flow-rates, which could explain the TLD ratio >1 observed for this inhaler product. Results from this study are consistent with early published data for Pulmicort Turbuhaler (Chavan et al., 2000; De Boer et al., 1997; Everard et al., 1997).

Implications for *in vitro* testing of DPIs: Standard *in vitro* tests of dose delivery performance are conducted using test set-ups that control volumetric flow-rate, but not the ramp-up time. In practice, the flow ramp-up times associated with the test equipment vary greatly depending on target flow-rate, and the internal "dead volume" of the dose collection apparatus used in the tests (Greguletz et al., 2013). Also actual patient inspiratory flow profiles can exhibit a wide range of ramp-up times. The potential for flow ramp effects should be taken into account when interpreting *in vitro* product performance data, whether for quality control purposes, or for assessing performance during actual use by patients.

4.5 Conclusion

The results show that the effect of flow ramp on delivered dose (DD) is relatively small for all DPIs tested in the study. However, greater variation was observed in the TLD, with the Asmanex® Twisthaler® showing the greatest variation as a function of flow ramp. The flow ramp effect on TLD essentially reflect an underlying flow-rate dependence effect, since different ramp conditions lead to differences in the "effective" flow-rate during the aerosolization event. Historically, attention has been focused on peak inspiratory flow-rate as the flow parameter influencing dose delivery performance. The results from the present study indicate that the ramp-up of flow should also be considered as a factor contributing to variation in dose delivery, during *in vitro* testing, as well as during clinical use of DPIs.

4.6 References

1. Al-Ahowair RAM, Tarsin WY, Assi KH, Pearson SB, and Chrystyn H. Can all Patients with COPD use the Correct Inhalation Flow with all Inhalers and does Training Help? *Resp. Med*. 2007; **101**: 2395 – 2401.

2. Ament BJ, Weers JG, Maltz DS, and Chan L. Analysis of Inhalation Profiles from Elderly COPD Subjects. *Resp. Drug Delivery*. 2012; 613 – 616.

3. Auty RM, Brown K, Neale M, and Snashall PD. Respiratory tract deposition of sodium cromoglycate is highly dependent upon technique of inhalation using the Spinhaler. *Br. J. Dis. Chest*. 1987; **81**: 371 – 380.

4. Beron K, Grabek CE, Jung JA, and Shelton CM. Flow rate ramp profile effects on the emitted dose from dry powder inhalers. In: Drug delivery to the lungs, 19. Edinburgh: *The Aerosol Society*. 2008; pp. 61 – 74.

5. Parry-Billings M, Birrell C, Oldham L, and O'Callaghan C. Inspiratory Flow Rate through a Dry Powder Inhaler (Clickhaler1) in Children with Asthma. *Pediatric Pulmonology*. 2003; **35**: 220 – 226.

6. Byron PR. Prediction of drug residence times in regions of the human respiratory tract following aerosol inhalation. *J. Pharm. Sci*. 1986; **75**: 433 – 438.

7. Chavan V and Dalby R. "Effect of rise in simulated inspiratory flow rate and carrier particle size on powder emptying from dry powder inhalers." *AAPS Pharm Sci.* 2000; **2**: 1 – 7.

8. Chodosh S, Flanders J, and Serby CW. Effective use of Handihaler dry powder inhalation system over a range of COPD severity. *J. Aerosol Med*. 2001; **14**: 309 – 15.

9. Clark AR and Hollingworth AM. The Relationship between Powder Inhaler Resistance and Peak Inspiratory Conditions in Healthy Volunteers – Implications for In Vitro Testing. *J. Aerosol Med.* 1993; **6**: 99 – 110.

10. Coates M, Chan H-K, Fletcher D, and Raper JA. Effect of Design on the Performance of a Dry Powder Inhaler Using Computational Fluid Dynamics. Part 2: Air Inlet Size. *J. Pharm. Sci*. 2006; **95**: 1382 – 1392.

11. De Boer AH, Bolhuis GK, Gjaltema D, and Hagedoon P. "Inhalation characteristics and their effects on *in vitro* drug delivery from dry powder inhalers. Part 3: The effect

of flow increase rate (FIR) on the *in vitro* drug release from the Pulmicort 200 Turbuhaler." *Int. J. Pharm.* 1997; **153**: 67 – 77.

12. DeHaan WH and Finlay WH. In Vitro Monodisperse Aerosol Deposition in a Mouth and Throat with Six Different Inhalation Devices. *J. Aerosol Med.* 2001; **14**: 361 – 367.

13. Delvadia RR, Hindle MP, Longest PW, and Byron PR. *In vitro* tests for aerosol peposition II: IVIVCs for different dry powder inhalers in normal adults. *J. Aerosol Med.* 2013; **26**: 138 – 144.

14. Demoly P, Hagedoorn P, de Boer AH, and Frijlink HW. The clinical relevance of dry powder inhaler performance for drug delivery. *Resp. Med*. 2014; **108**: 1195 – 1203.

15. Everard ML, Devadason SG, and Le Souëf PN. "Flow early in the inspiratory manoeuvre effects the aerosol particle size distribution from a Turbuhaler". *Respr. Med*. 1997; **91**: 624 – 628.

16. Finlay WH, Golshahi L, Noga M, and Flores-Mir C. Choosing 3-D Mouth-Throat Dimensions: A Rational Merging of Medical Imaging and Aerodynamics. *Resp. Drug Delivery*. 2010; 185 – 193.

17. Greguletz R, Andersson P, Arp J, Blatchford C, Daniels G, Glaab V, Hamilton M, Hammond M, Mitchell J, Roberts D, Shelton C, and Watkins A. "Collaborative Study by the European Pharmaceutical Aerosol Group (EPAG) to Assess the Flow-Time Profile of Test Equipment Typically Used for pMDI/DPI testing – Part 2: Flow-Time

Profile testing". Proceedings Drug delivery to the lungs 24. Edinburgh: *The Aerosol Society*. 2014.

18. Grim C, Pierre LN, and Daley-Yates PT. A review of the pharmacology and pharmacokinetics of inhaled fluticasone propionate and mometasone furoate. *Clinical Therapeutics*. 2001; **23**: 1331 – 1354.

19. Haynes A, Ament B, Heng C, Le J, Ung K, Rao R, Malcolmson R, Weers J, Pavkov R, Heuerding S, and Geller DE. "In-vitro Aerosol Delivery Performance of Tobramycin Powder for Inhalation (TOBI® Podhaler®) Using Inspiratory Flow Profiles from Cystic Fibrosis Patients" *Poster presented at the North American Cystic Fibrosis Conference*. Salt Lake City, Utah, USA, October 17 – 19 (2013).

20. Kohler D. The Novolizer: Overcoming inherent problems of dry powder inhalers. *Resp. Med*. Supplement A. 2004; S17 – S20.

21. Maltz DS, Glusker M, Axford G, Postich M, Rao N, and Ung K. A novel passive dry powder inhaler for unit dose delivery to the deep lung. *Proc. Respir. Drug Deliv.* 2008; **3**: 669 – 674.

22. Newman SP and Clarke SW. Therapeutic aerosols l-physical and practical considerations. *Thorax*. 1983; **38**: 881 – 886.

23. Olsson B, Borgström L, Lundbäck H, and Svensson M. Validation of a general *in vitro* approach for prediction of total lung deposition in healthy adults for pharmaceutical inhalation products. *J. Aerosol Med.* 2013; **26**: 1 – 15.

24. Pedersen S, Hansen OR, and Fuglsang G. Influence of inspiratory flow rate upon the effect of Turbuhaler. *Arch. Dis. Child*. 1990; **65**: 308 – 319.

25. PULMICORT FLEXHALER™ 180 mcg label: www.accessdata.fda.gov/drugsatfda_docs/label/2008/021949s004lbl.pdf

26. Ramsgaard, Hansen O, and Pedersen S. Optimal inhalation technique with terbutaline Turbuhaler. *Eur. J. Respir. Dis*. 1989; **2**: 637 – 639.

27. Ung TK, Axford G, Chan L, Glusker M, Le J, Maltz D, Rao N, and Weers JG. Effect of powder release kinetics on the performance of a dry powder inhaler. *Proc. Respir. Drug Deliv*. 2012; **3**: 627 – 630.

28. Ung TK, Rao N, Weers JG, Clark AR, and Chan H-K. *In vitro* assessment of dose delivery performance of engineered dry powders for inhalation. *Aerosol Sci. & Tech*. 2014; **48**: 1099 – 1110.

29. Weers JG, Ung K, Le J, Rao N, Ament B, Axford G, Maltz D, and Chan L. Dose emission characteristics of placebo PulmoSphere® particles are unaffected by a subject's inhalation maneuver. *J. Aerosol Med.* 2013; **26**: 56 – 68.

30. Weers JG, Clark AR, Rao N, Ung K, Haynes A, Khindri SK, Sheryl A, Perry SA, Machineni S, and Colthorpe P. *In vitro–in vivo* correlations observed with indacaterol-based formulations delivered with the Breezhaler®. *J. Aerosol Med*. 2014; **28**: 1 – 13.

31. Weers J and Tarara T. The PulmoSphere™ platform for pulmonary drug delivery. *Ther. Deliv*. 2014; **5**: 277 – 295.

32. Zhang Y, Gilbertson K, and Finlay WH. *In vivo-in vitro* comparison of deposition in three mouth-throat models with QVAR® and Turbuhaler® inhalers. *J. Aerosol Med*. 2007; **20**: 227 – 235.

33. Zhou Y, Sun J, and Cheng Y, 2011. Comparison of Deposition in the USP and Physical Mouth-Throat Models with Solid and Liquid Particles. *J. Aerosol Med.* 2011; **24**: 277 – 284.

Chapter 5

Design of spray dried insulin microparticles to bypass deposition in the extrathoracic region and maximize total lung dose

(Accepted for publication by Int. J. Pharm., 2016)

5.1 Introduction

For medications administered via oral inhalation, improved lung targeting may be achieved, in part, by minimizing deposition in the extrathoracic region (i.e., mouth and throat). Unwanted deposition in the mouth-throat can lead to an increase in systemic exposure for drugs that are orally bioavailable, and in some instances increases in local and systemic side effects (e.g., for inhaled corticosteroids). In addition, higher nominal doses might be required to compensate for the off-target deposition, which could further exacerbate the problem. Deposition in the extrathoracic region is primarily governed by inertial impaction, with deposition proportional to the inertial parameter ($d_a^2 Q$), where d_a is the aerodynamic diameter and Q is the volumetric flow-rate (Stahlhofen et al., 1989). The aerodynamic diameter depends both on the geometric diameter (d_g) and density (ρ_p) of the particles, viz:

$$d_a = d_g \sqrt{\frac{\rho_p}{\rho_0 \chi}} \qquad (1)$$

where $\frac{\rho_p}{\rho_0}$ represents the specific gravity of the particle, and χ is the dynamic shape factor (Shekunov et al., 2006). For a single particle, deposition in the extrathoracic region will be reduced with decreases in d_a, d_g and ρ_p. For spray-dried powder formulations, the story is more complex as in the bulk state they exist as agglomerates of non-spherical particles that need to be dispersed to primary particles, or smaller respirable agglomerates to enable efficient delivery to the lungs. It should also be noted that equation 1 represents a simplification for spray dried powder composed of non-spherical, low density particles, and a volume equivalent diameter may be used in place of geometric diameter. Furthermore, the Cunningham slip correction should not be neglected when dealing with engineered particles having small size and low density.

Delivery of dry powder aerosols to the lungs depends on interplay between the powder formulation and inhaler device. The ability to effectively fluidize and disperse dry powder agglomerates is dependent on the ratio of inter-particle cohesive forces present in the powder, to the hydrodynamic forces (e.g., drag and lift forces) generated in the dry powder inhaler. At a low relative humidity environment, inter-particle cohesive forces are dominated by van der Waals interactions. For perfectly smooth spheres, van der Waals forces (F_{vdw}) are directly proportional to d_g and the Hamaker constant (A), and inversely proportional to the square of the separation distance (r), viz:

$$F_{vdw} = \frac{Ad_g}{24r^2} \text{ (Rigid spheres)} \qquad (2)$$

In contrast, drag and lift forces scale with d_g^2 (Finlay, 2001). As d_g decreases into sizes required for efficient delivery into the lungs (e.g., aerodynamic diameter ranging from 1 – 5 μm), cohesive forces typically are larger than the hydrodynamic forces resulting in powders that are poorly dispersed and total lung deposition of 10 – 30% of the nominal dose. Note that in the case of insulin particles comprised of rugose surfaces (e.g., collapsed hollow or wrinkled particles) modified cohesion models, such as that by Rumpf (1990) and Rabinovich et al (2000) should be considered.

Particle engineering may be utilized to minimize inter-particle cohesive forces via control of the surface composition and morphology of particles. In this regard, spray drying is a bottom-up manufacturing process that enables production of micron-sized particles, with control of the surface composition and micromeritic properties of the particles (e.g., size, density, and rugosity). Spray dried proteins, such as insulin, may adopt a corrugated (i.e., raisin-like) particle morphology provided they are dried rapidly (Balducci et al., 2015; White et al., 2005). The protuberances, called asperities, typically have a small radius of curvature (<0.1 μm) (Dunbar, 2006). The mean van der Waals force depends strongly on the surface structure of the particles, i.e., the size distribution of the asperities and their surface density. To calculate the van der Waals force for corrugated particles, it has been proposed to not use d_g in Eq. 2, but instead to use an effective diameter (d_{eff}), as defined by the effective interaction area (Dunbar, 2006; Rietema, 1991). For corrugated particles with high surface asperity densities, d_{eff} approaches the diameter of the asperities. Under these conditions, the van der Waal's forces can be several orders of magnitude lower than is observed for micron-sized solid spheres (Weiler et al., 2010). Indeed, Chew and Chan (Chew et al., 2001) have demonstrated significant improvements in respirable fraction (d_a < 5μm) for bovine serum

albumin particles, as the morphology is altered to increase surface roughness or corrugation. The goal in this paper is to design neat insulin particles that bypass deposition in the extrathoracic region and increase delivery efficiency to the lungs. This is accomplished by adjustment of the feedstock composition and spray drying parameters to achieve particles with a low bulk density and small size.

Respirable particles of biologics like insulin have previously been prepared by spray drying using an ethanol-water co-solvent based feedstock (Edwards et al., 1997 & 1998; Vanbever et al., 1999). Ethanol-water co-solvent feedstocks have also been used to tailor particle morphology by spray drying for small molecules like budesonide (Boraey et al., 2013). In these previous studies, feedstocks with relatively large volume fractions of ethanol have been used (>70%). In contrast, this paper explores a co-solvent spray drying approach where relatively small amounts of organic solvents added to water can be used to modulate particle morphology. This approach has been used to prepare engineered dry powder formulations of insulin (as a model compound) for use in dry powder inhalers.

5.2 Materials and Methods

5.2.1 Feedstock preparation and spray drying

Recombinant human insulin was obtained from Diabel GmbH & Co KG (Frankfurt, Germany). Feedstock solutions for spray drying were prepared by dissolving insulin powder in water or water-ethanol mixtures while mixing gently on a magnetic stir plate. The pH was lowered with hydrochloric acid (pH 3.0 – 3.25) to facilitate rapid dissolution of the drug

substance, and then adjusted with sodium hydroxide to bring the final solution feedstock back to pH 7.5 – 7.9.

This investigation used a Novartis Spray Dryer (NSD, Novartis Pharmaceuticals Corp, San Carlos, CA) a custom-built bench-scale spray drier, that is similar in scale to a commercially available Büchi 191 mini spray dryer (BÜCHI Labortechnik, AG). The air-assisted atomizer nozzle is a modified version of Büchi 191 atomizer, designed to produce sprays with smaller and more uniform droplet size. The NSD dryer body and high efficiency cyclone collector are made from stainless steel. The dryer body is insulated to improve temperature and relative humidity control within the process train.

In order to produce engineered particles with varying micromeritic properties (e.g., particle density and size), two spray-drying campaigns were conducted to cover the particle design space. The experimental matrix for campaign-1 is summarized in **Table 1**, where particle properties were modulated by varying feedstock composition (i.e. the total solids, and ethanol-to-water ratio of the solution feedstock), while holding the spray drying parameters constant.

Table 5.1 Test matrix for spray drying campaign-1, where feedstock composition was varied. Spray drying process parameters were kept constant; atomizer gas flow = 26 L/min, drying gas flow= 560 L/min, liquid feed rate= 2.6 mL/min, inlet temperature = 103°C.

Lot No.	Solids Content [% w/w]	Ethanol Fraction [% w/w]
EXP-C1-01	0.75	0
EXP-C1-02	0.75	5
EXP-C1-03	1.50	5
EXP-C1-04	3.00	5
EXP-C1-05	1.50	10
EXP-C1-06	3.00	10

Due to the decreased solubility of insulin in the presence of ethanol in aqueous solutions, it was expected that particle shell formation and the resulting particle density would be modulated by varying the ethanol-to-water ratio in the feedstock. In the experiments listed in **Table 5.1**, the ethanol-to-water ratio in the feedstock was varied over the range (0 – 10% w/w) to vary particle density.

The experiments in **Table 5.1** also aimed to vary the primary particle diameter by varying the total solids content in the feedstock, with the expectation that higher total solids would lead to larger particles. Thus, total solids content was varied from 0.75 – 3.0% w/w.

Campaign-2 included the study of the effects of droplet size and drying kinetics on particle densities and sizes, by varying additional spray-drying parameters. Droplet size was varied by changing the air-to-liquid ratio (ALR) from 2.3×10^3 to 13.9×10^3 g/g, and the total solids

from 0.75 to 5.0% w/w. Inlet temperatures were varied between 103 – 115 °C, and drying gas flow-rates from 500 – 700 L/min (**Table 5.2**). As a rule of thumb, increases in total solids, decreases in ALR, and more rapid drying (increased inlet temperature, greater drying gas flow-rates) would result in larger sized particles.

Samples of the spray dried powders listed in **Tables 5.1** and **5.2** were characterized for bulk powder properties (primary particle size, bulk density, and morphology). Although, residual water content of the spray dried powders was not measured, based on past experience, it is not expected to affect the physical properties of the particles. These powders were also filled into hypromellose size 2 capsules (Qualicaps, US) and aluminum foil-foil unit-dose blisters for *in vitro* testing with capsule and blister-based inhalers, as described in a later section. The nominal fill mass for capsules and blisters are 5 and 2 mg, respectively. The powder and aerosol characterization methods are described below.

Table 5.2 Test matrix for spray drying campaign-2

Lot No.	Ethanol Fraction [% w/w]	Atomizer Gas Flow [L/min]	Liquid Feed Rate [mL/min]	ALR [g/g]	Inlet Temp [°C]	Drying Gas Flow [L/min]	Solids Content [% w/w]
EXP-C2-01	5	15	8.0	2.3×10^3	115	700	5.0
EXP- C2-02	5	15	4.0	4.6×10^3	110	500	5.0
EXP- C2-03	0	26	2.3	13.9×10^3	103	560	0.75
EXP- C2-04	5	26	2.3	13.9×10^3	103	560	0.75
EXP- C2-05	5	15	8.0	2.3×10^3	115	700	0.75
EXP- C2-06	5	26	2.3	13.9×10^3	103	560	1.5
EXP- C2-07	10	26	2.3	13.9×10^3	103	560	3.0

5.2.2 Determination of primary particle size of bulk powder

The primary particle size distribution of inhaled insulin powder was measured with a Sympatec HELOS Type BF Model Laser Light Diffraction Analyzer (Sympatec GmbH, Germany), the RODOS-M (OASIS) dry powder disperser, and the ASPIROS powder dosing unit. The instrument evaluation mode was set to high resolution laser diffraction (HRLD), which measured size distributions is based on Fraunhofer diffraction theory. Powder sample (5 – 15 mg) was placed into a 1 mL vial and loaded into the ASPIROS dosing unit set at a speed of 25 mm/sec. The injector distance and primary pressure settings for the RODOS dry disperser were 4 mm and 4 bar, respectively. The RODOS settings were selected to achieve complete dispersion of the bulk powder to primary particles formed during the spray-drying process. Measurements were performed using the R1 lens (R1: 0.1/0.18 – 35 μm). Three replicate measurements were performed for each powder formulation. Results are reported here in terms of the volume weighted median diameter, X_{50} (mean of three replicates).

5.2.3 Bulk density analysis of spray dried powder

No direct measurement of particle densities exists. In this study, we chose to measure bulk densities at a specified level of compression using a custom-designed powder dosing wand, intended for manual filling of powder doses into capsules or blisters. The dosing wand is provided with a cylindrical cavity of known volume (0.0136 cm^3) at its tip. The bottom end of the cavity is lined with a filter, and can be connected to a vacuum or compressed air line via pneumatic actuated valves. During density measurement, the wand was positioned over a bulk powder bed, and vacuum applied at a specified pressure of 81 kPa (25” Hg) to aspirate and consolidate bulk powder into the cavity. Excess powder was then doctored off. The

resulting powder puck was expelled from the cavity with a burst of compressed air at 35 – 103 kPa, and the mass of powder was determined on a Mettler Toledo AX206 balance (n = 3 – 5 replicates). The resulting bulk densities are lower than the corresponding particle densities, but the trends are expected to be similar. This assumes similar cohesive forces of the particle agglomerates. The bulk density determined with this method is relevant to powder filling on drum fillers used at Novartis, and is sometimes referred to as the "puck density".

5.2.4 Particle morphology by Scanning Electron Microscopy

Particle morphology was assessed by scanning electron microscopy. Powder samples from campaign-2 were viewed under a Philips XL 30 Environmental Scanning Electron Microscope (ESEM; Philips Electron Optics, US). A thin layer of bulk powder was placed on a 1 cm x 1 cm silicon wafer disk (Omnisil, VWR IBSN3961559, US), and the sample was prepared for electron microscopy by sputter-coating a thin gold and palladium film of 32 – 37 nm thickness (Denton, 21261 Cold Sputter/Etch and DTM-100, operated at <100 mTorr and 30 – 42 mA for 100 – 150 seconds). The coated samples were then loaded into the ESEM chamber and the filament current and accelerating voltage set to 1.6 A and 20 kV, respectively.

5.2.5 In vitro characterization of aerosol dose delivery performance

In vitro dose delivery performance was investigated using two different DPIs that fluidize and disperse powder using different principles. The blister-based Simoon inhaler (Novartis Pharmaceuticals Corp, USA) is a high resistance device (R ~ 0.19 cm $H_2O^{0.5}$/L/min) that utilizes airflow to fluidize and de-agglomerate the powder (Maltz et al., 2008; Ung et al.,

2012; Weers et al., 2013). In contrast, the capsule-based T-326 inhaler (Novartis Pharmaceuticals Corp, USA) is a low-medium resistance device (R ~ 0.08 cm $H_2O^{0.5}$/L/min), which relies on the mechanical motion associated with precession of the capsule to fluidize and disperse the bulk powder into a fine, respirable aerosol (Geller, 2011; Maltz et al., 2011).

In vitro test attributes included the delivered dose (DD), which represents the total aerosol dose discharged from the inhaler; and the total lung dose (TLD), which represents the respirable dose, and is measured as the aerosol dose fraction that bypass deposition in an idealized anatomical throat model, i.e. the Alberta idealized throat (AIT) model, and deposits on a filter downstream. The traditional *in vitro* approach of estimating the aerosol performance is based on using a cascade impactor to measure the aerodynamic size distribution of the emitted aerosol, and designating a fine particle fraction less than 5 μm as a marker for the respirable fraction expected to deposit in the lungs. Anatomical throat models provides a rapid and simplified *in-vitro* approach to estimating TLD, which correlates well with estimates from cascade impactor measurements (Ung et al., 2014). Moreover, recent studies have demonstrated good *in vitro-in vivo* correlations (IVIVC) in total lung deposition for anatomical throats (Zhang et al., 2007; Delvadia et al., 2013; Olsson et al., 2013; Weers et al., 2015).

Aerosol performance was evaluated using a standard square-wave flow profile generated with a timer-controlled vacuum source at pressure drops of 2, 4, and 6 kPa. This pressure drop range represents the range of inspiratory efforts achievable by most subjects, including healthy volunteers and patients with obstructive lung disease (Al-Ahowair et al., 2007). Clark et al. (1993) derived an Eq. for determining the inhaler flow resistance, $R = \sqrt{\Delta P}/Q$ where

ΔP is the inhaler pressure drop (centimeter of water) and Q is the corresponding volumetric flow-rate (L/min), which is obtained from measurements.

Test attributes included the delivered dose (DD) measured gravimetrically for the neat insulin powders, and an *in vitro* measure of total lung dose (TLD) determined with an idealized anatomical throat model. The traditional *in vitro* approach of estimating the aerosol performance is based on using a cascade impactor to measure the aerodynamic particle size distribution of the emitted aerosol, and designating a fine particle fraction as a marker for the respirable fraction expected to deposit in the lungs. The anatomical throat models provide a rapid and simplified *in vitro* approach to estimating TLD, which correlates well with estimates from cascade impactor measurements (Ung et al., 2014). Moreover, recent studies have demonstrated good *in vitro in vivo* correlations (IVIVC) in total lung deposition for anatomical throats (Delvadia et al., 2013; Olsson et al., 2013; Weers et al., 2015; Zhang et al., 2007).

The test fixture used for measurement of DD is shown schematically in **Figure 5.1**. When actuated with flow, the aerosolized dose leaving the inhaler mouthpiece is deposited onto a filter (type A/E, Pall Corp, US), having a diameter of 47 mm (Simoon) or 81 mm (T-326). Customized filter holders were designed for engineered particles, which allow for gravimetric analyses with both inhaler devices. The larger 81 mm diameter filter was used to minimize filter pressure drop for the T-326 device, which has a low flow resistance, and therefore a higher airflow during testing. A 2 L sampling volume was maintained for each dose actuation for DD and TLD analyses. The results for DD and TLD are reported in terms of % of the nominal dose.

In vitro estimates of TLD were obtained using an anatomical throat model, i.e., the Alberta Idealized Throat (AIT), which represents the mouth/throat airway of an average human adult. The AIT was developed and characterized by Finlay and coworkers at the University of Alberta, Canada (DeHaan et al., 2001; Stapleton et al., 2000). The Alberta throat test setup used for determination of *in vitro* TLD is shown in **Figure. 5.2**. The test inhaler was coupled to the inlet of the AIT model using a molded mouthpiece adaptor, and the downstream end of the throat was mounted upon the filter housing stage of the Fast Screening Impactor (MSP Corporation, USA). For determination of *in vitro* TLD, the test inhaler was coupled to the inlet of the AIT model, and the dose penetrating through the model was collected downstream on a 76 mm diameter filter (A/E type, Pall Corp., US), as shown in **Figure 5.2**. A polysorbate (EMD Chemicals, Cat. #8170072, US) wetting agent (equal parts of Tween 20 and methanol, v/v) was used for coating the interior walls of the AIT model to prevent particle re-entrainment. The procedure for applying coating solution to the AIT was as follows; (i) ~15 mL of the coating solution was dispensed into the AIT, which was then capped at both ends (ii) The solution was allowed to wet the internal walls of the AIT using a rocking or rotary motion to tilt the AIT from side to side; and (iii) Excess solution was allowed to drain for 5 minutes before use. After five dose actuations, the AIT was rinsed with lukewarm water, air dried, and a fresh coating applied prior to the next use.

The powder dose collected on filters for both DD and TLD tests were measured by gravimetric analysis and reported in terms of % of the nominal dose. It should be noted that the gravimetric analysis of aerosol dose is not commonly used in aerosol performance testing of dry powder inhalers. This is because many DPI formulations e.g. lactose carrier-based formulations are inhomogeneous mixtures composed of micronized drug particles and carrier

particles, for which drug-specific assays are needed. However the gravimetric approach is entirely appropriate for engineered powder formulations prepared by spray drying from a solution based feedstock, as the resulting powders are homogeneous in composition to the individual particle level, and thus where the distribution of drug closely follows the distribution of powder mass (Harper et al., 2007; Ung et al., 2014). To minimize environmental effects on gravimetric measurement, all performance testing was conducted in a laboratory with controlled temperature (T) and relative humidity (RH) (T= 20 – 25°C; RH= 40 ± 5%). DD and TLD measurements were performed by weighing of filters before and after device actuation, using a Mettler Toledo AX26 balance (or Mettler Toledo AT20), which has a readability of 0.01 mg, and repeatability of 0.006 mg at full load (21 g). When the test procedure was simulated with empty capsules (i.e., no powder deposited on filters), the gravimetric analysis of filters was experimentally verified to have a repeatability of 0.03 mg, which is sufficient measurement precision for this study, considering that most of the DD and TLD doses were in the range 1.2 mg or greater.

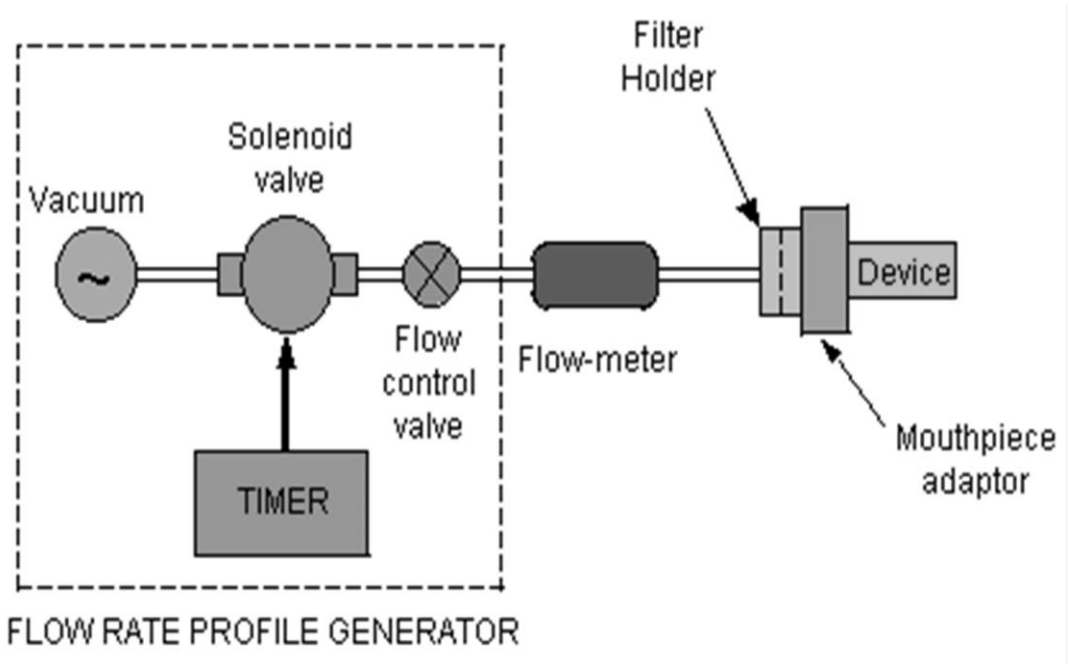

Figure 5.1 Delivered dose measurement set-up with customized filter holders designed for engineered particles.

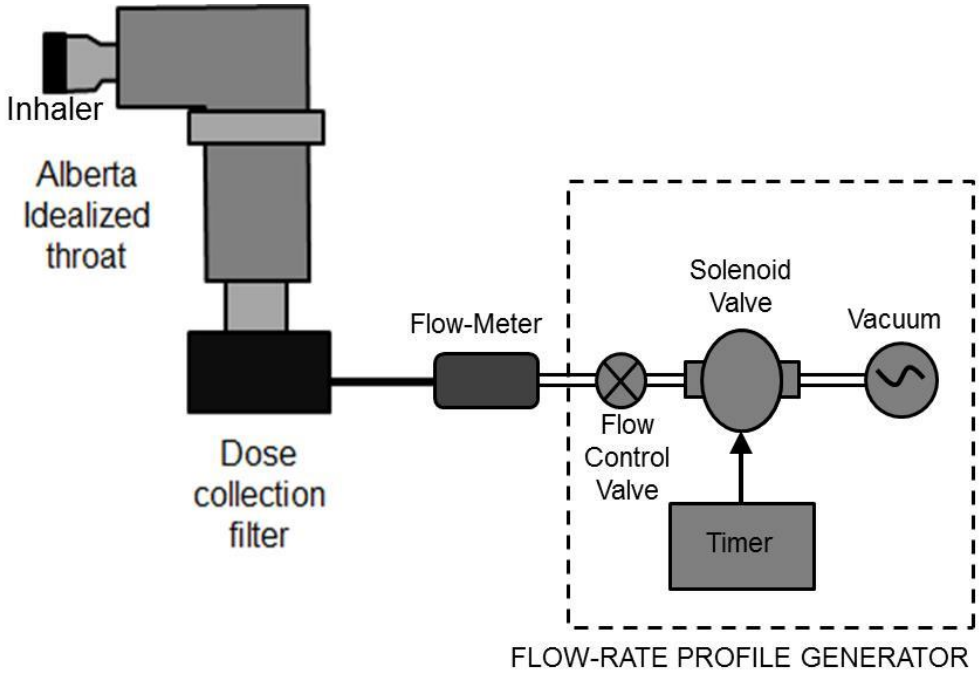

Figure 5.2 Test set-up for measurement of total lung dose measurement using the AIT, with an inhaler mounted at the inlet, and a filter collector mounted at the outlet.

5.2.6 Measurement of aerodynamic diameter

In vitro measurements of the mass median aerodynamic diameter were conducted for Simoon device and selected powder formulations with a Next Generation Impactor (NGI; Apparatus 5 in USP General Chapter <601>). The NGI was assembled with the induction port/pre-separator stage and operated at a pressure drop of 4 kPa (i.e., 33 L/min) with a sampled volume of 4 L. Drug quantitation was performed gravimetrically. To enable gravimetric analysis, the gravimetric NGI cups were fitted with 55-mm diameter glass fiber filters (A/E type, Pall Corp, USA) and the pre-separator upper and lower compartments were coated with 1 mL and 2 mL, respectively, with a polysorbate wetting agent (equal parts of Tween 20 and methanol, v/v). For the T-326 device, gravimetric determination of the aerodynamic particle size distribution was not possible due to significant particle bounce/re-suspension observed in the NGI stages at the test condition of 4 kPa (and corresponding flow-rate of 78 L/min).

5.3 Results

5.3.1 Characterization of bulk powder physical properties

The two spray drying campaigns produced 13 batches of neat insulin inhalation powders with a broad range of bulk densities and primary particle sizes (**Table 5.3**). Volume weighted median diameters (X_{50}) varied from 1.36 to 2.58 µm, while bulk densities varied from 0.15 to 0.31 g/cm^3.

Table 5.3 Spray dried powder physical properties, (mean, standard deviation shown in parenthesis, N = 3 – 5).

Lot No.	Volume Weighted Median Diameter, X_{50} [μm]	GSD* [μm]	Bulk Density [g/cm^3]
EXP-C1-01	1.36 (0.03)	1.69 (0.01)	0.31 (0.02)
EXP-C1-02	1.52 (0.01)	1.88 (0.02)	0.21 (0.01)
EXP-C1-03	1.89 (0.02)	2.20 (0.02)	0.19 (0.00)
EXP-C1-04	1.84 (0.04)	1.96 (0.02)	0.26 (0.01)
EXP-C1-05	1.77 (0.02)	2.02 (0.02)	0.20 (0.01)
EXP-C1-06	1.89 (0.04)	2.05 (0.04)	0.25 (0.01)
EXP-C2-01	2.46 (0.03)	2.24 (0.01)	0.30 (0.00)
EXP-C2-02	2.58 (0.04)	2.14 (0.04)	0.30 (0.00)
EXP-C2-03	1.36 (0.01)	1.65 (0.01)	0.26 (0.02)
EXP-C2-04	1.40 (0.01)	1.71 (0.01)	0.17 (0.01)
EXP-C2-05	1.76 (0.05)	2.02 (0.02)	0.15 (0.01)
EXP-C2-06	1.70 (0.01)	1.88 (0.01)	0.21 (0.00)
EXP-C2-07	1.74 (0.06)	1.85 (0.01)	0.24 (0.01)

*Geometric Standard Deviation (GSD) = $\sqrt{\frac{X_{84}}{X_{16}}}$, where X_{84} and X_{16} represent the diameters corresponding to 84% and 16%, of the cumulative volume, respectively, under the distribution.

Representative SEM images for the powders produced in campaign-2 are presented in **Figures 5.3** to **5.8**. EXP-C2-03 represents a control powder produced by spray drying an aqueous feedstock with no added ethanol. The particles show a corrugated raisin-like morphology that is consistent with other formulations of spray dried proteins, e.g., Exubera®, Pfizer (White et al., 2005). The particles exhibit a relatively high bulk density (0.26 g/cm^3) and a small primary particle size (1.36 μm). An attempt was made with EXP-C2-01 to create

a lower bulk density powder with the same volume-weighted median diameter as EXP-C2-02 by lowering the ALR and increasing the total dry gas flow (**Table 5.2**). However, the outcome failed to achieve the target, and the powder had physical properties similar to EXP-C2-02 (**Table 5.3**). As such, SEM analysis was not performed for EXP-C2-01. Formulation EXP-C2-04 was manufactured with the same total solids, ALR, and drying conditions to the control powder, differing only in the composition of the liquid phase with 5% w/w ethanol in feedstock. The SEM image shows particle morphologies that are similar to those achieved for the control powder. Despite the lack of significant morphological changes, the bulk density of the EXP-C2-04 powder is significantly lower (bulk density = 0.17 g/cm^3, X_{50} = 1.40 μm).

Formulation EXP-C2-02 was manufactured at a low ALR (4.6 x 10^3) and high total solids loading (5.0%). The low ALR produces relatively large droplets, and the high total solids content lead to precipitation of the particles earlier in the drying process. This results in larger-sized particles with a higher bulk density (bulk density = 0.30 g/cm^3, X_{50} = 2.58 μm). A mix of morphologies is observed with both corrugated particles and smooth oval shaped particles. Spray drying with a low ALR, low total solids (0.75%), and fast drying rates (Formulation EXP-C2-05) results in a complex mixture of particle morphologies. Interestingly, this formulation exhibits the lowest bulk density of the formulations prepared (bulk density = 0.15 g/cm^3, X_{50} = 1.76 μm). Compared to the control, the EXP-C2-05 formulation has an X_{50} that is 0.4 μm larger.

Formulations EXP-C2-06 and EXP-C2-07 were prepared at intermediate total solids contents and exhibit physical properties intermediate to those discussed previously. For example, formulations EXP-C2-04 and EXP-C2-06 differ only in the total solids content, which

increase from 0.75% to 1.5%. This leads to an increase in X_{50} from 1.40 – 1.70 μm and an increase in bulk density from 0.17 – 0.21 g/cm^3.

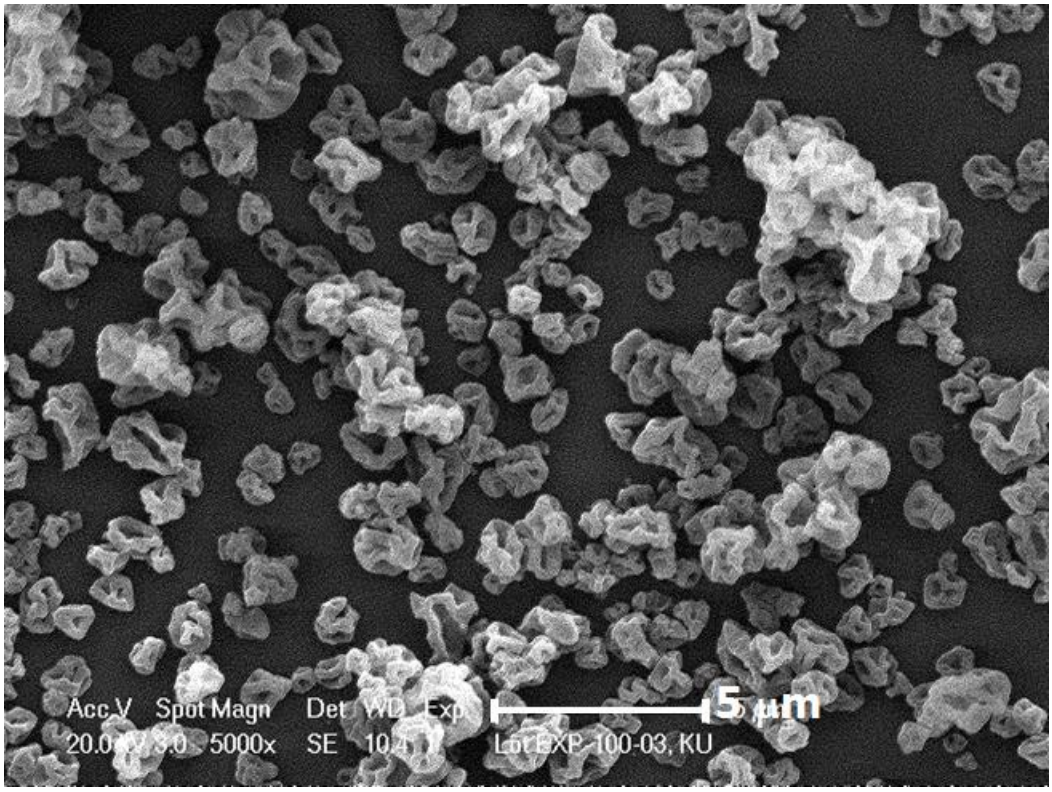

Figure 5.3 Scanning electron microscopy image of spray dried insulin particles from campaign-2 for powder lot EXP-C2-03; ethanol= 0%, solids= 0.75%, and ALR= 13.9 x 10^3.

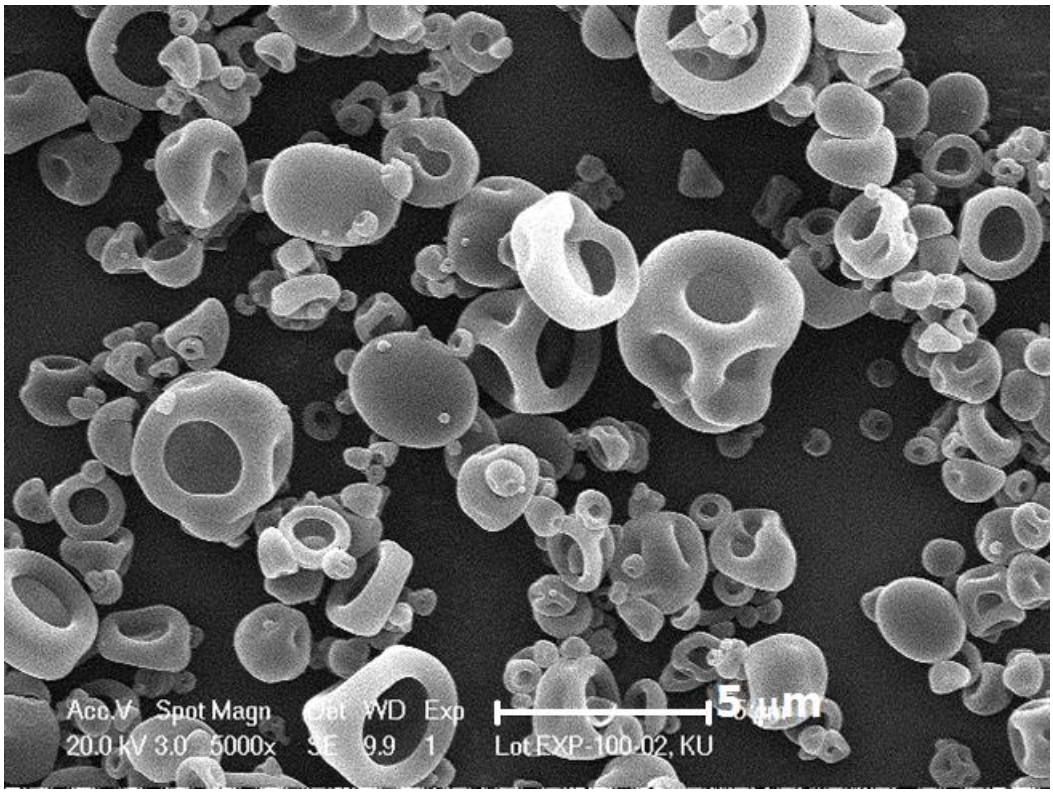

Figure 5.4 Scanning electron microscopy image of spray dried insulin particles from campaign-2 for powder lot EXP-C2-02; ethanol= 5%, solids= 5%, and ALR= 4.6 x 10^3.

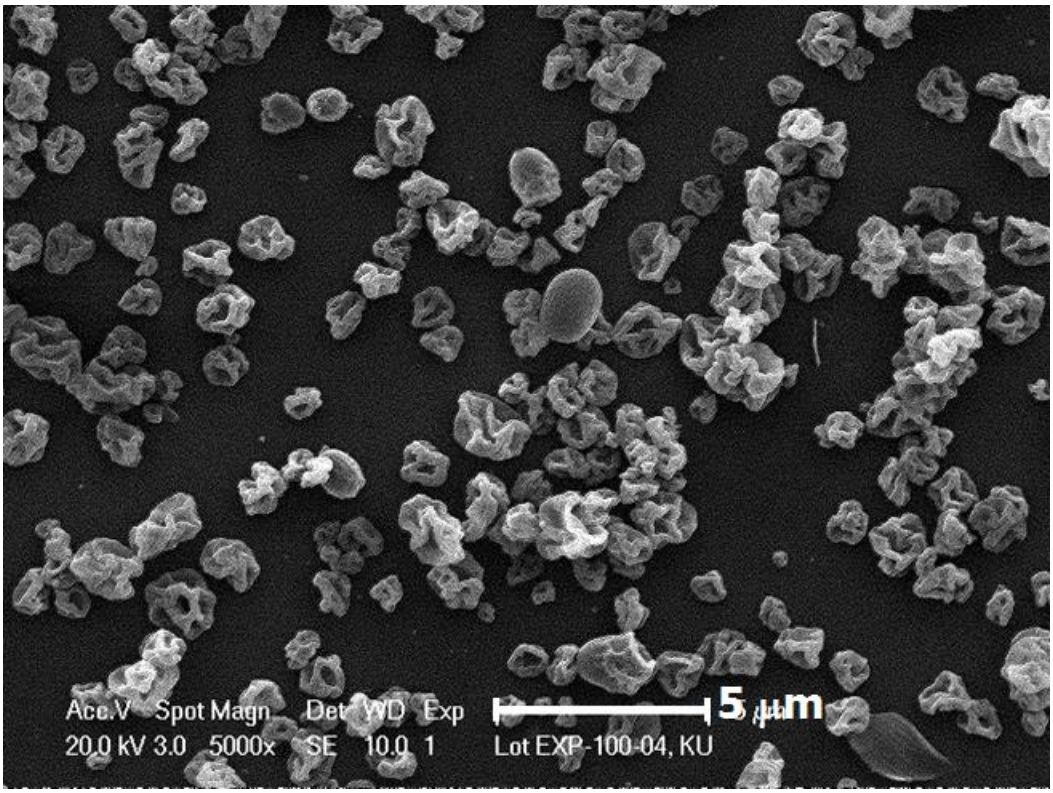

Figure 5.5 Scanning electron microscopy image of spray dried insulin particles from campaign-2 for powder lot EXP-C2-04; ethanol= 5%, solids= 0.75%, and ALR= 13.9 x 10^3.

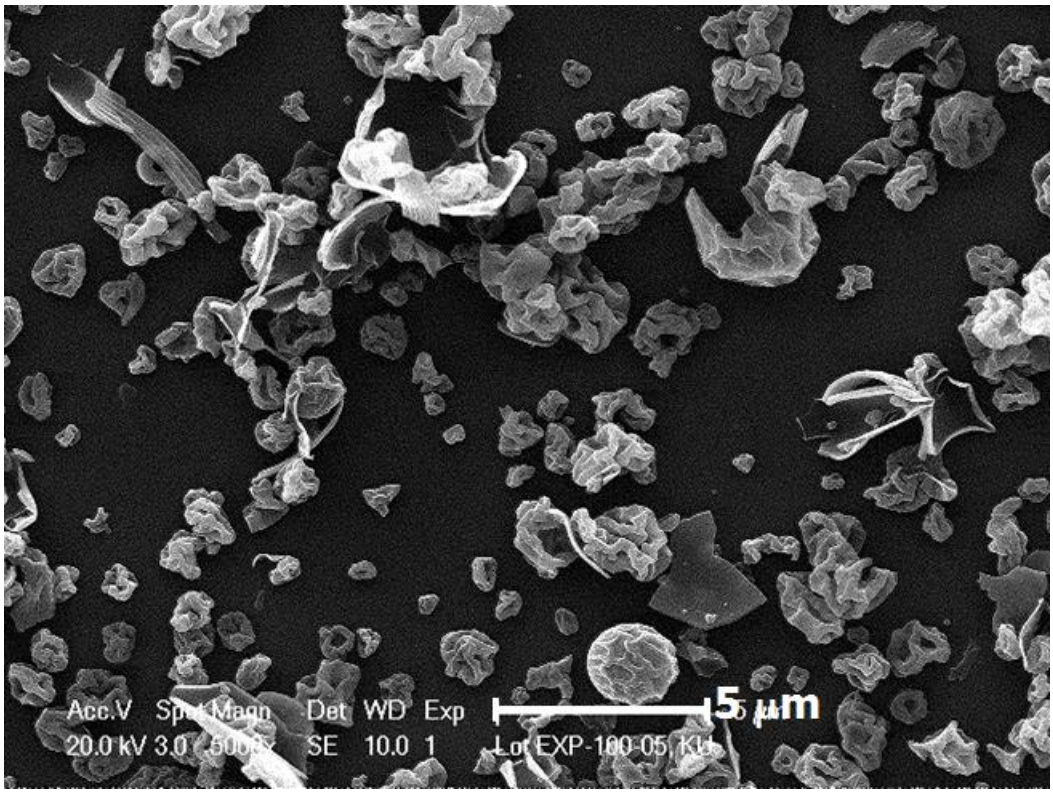

Figure 5.6 Scanning electron microscopy image of spray dried insulin particles from campaign-2 for powder lot EXP-C2-05; ethanol= 5%, solids= 0.75%, and ALR= 2.3 x 10^3.

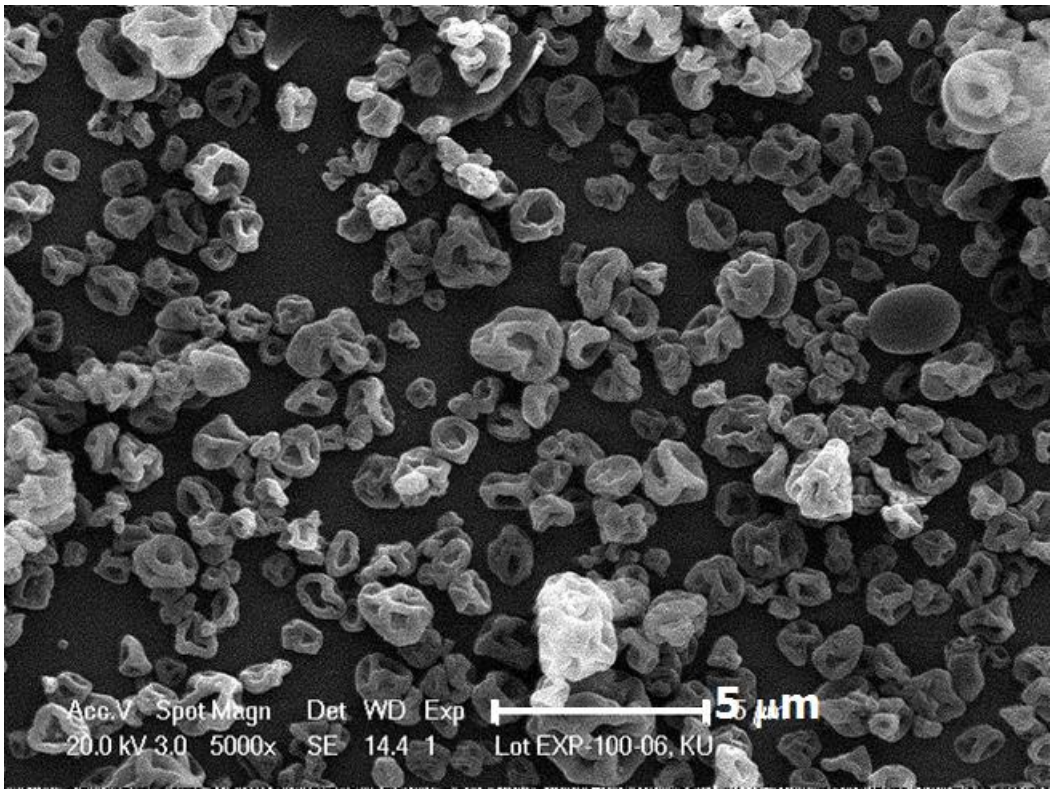

Figure 5.7 Scanning electron microscopy image of spray dried insulin particles from campaign-2 for powder lot EXP-C2-06; ethanol= 5%, solids= 1.5%, and ALR= 13.9 x 10^3.

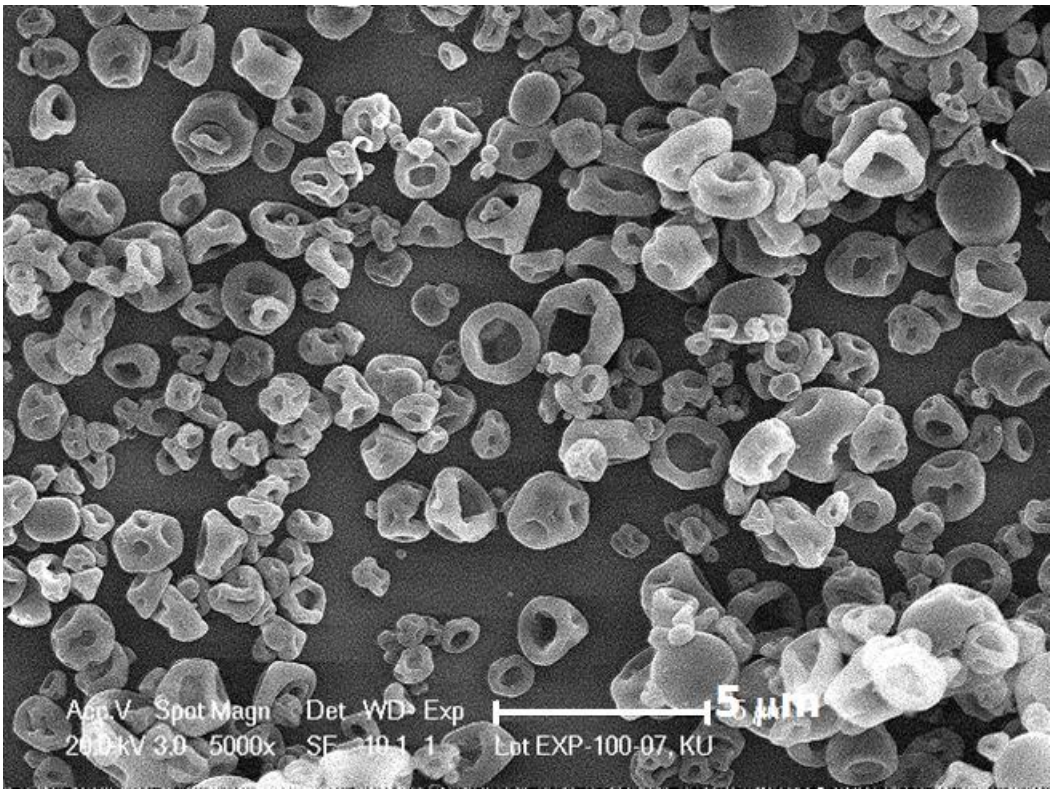

Figure 5.8 Scanning electron microscopy image of spray dried insulin particles from campaign-2 for powder lot EXP-C2-07; ethanol= 10%, solids= 3%, and ALR= 13.9 x 10^3.

5.3.2 In vitro aerosol performance analysis

Having demonstrated a control of powder properties such as particle size and density, it is of interest to determine if these properties can be modulated and optimized for aerosol performance in terms of dose delivery via dry powder inhalers. To answer this question, six spray dried insulin powders covering a wide range of bulk densities (0.15 – 0.30 g/cm^3) and X_{50} (1.36 – 2.58 µm) from campaign-2 were selected for *in vitro* aerosol performance analysis. Aerosol performance testing was conducted for these powders across a range of pressure drops; 2, 4, and, 6 kPa. All of the six selected powders were tested with the Simoon inhaler, and a subset of four was further tested with the T-326 inhaler.

Figures 5.9 to **5.11** summarize results from aerosol performance testing at 4 kPa pressure drop. **Figure 5.9** plots the delivered dose (DD) as a function of bulk density for the six selected powder batches. **Figure 5.9** shows that the DD trends lower with increasing powder bulk density, with the Simoon inhaler showing markedly greater sensitivity to powder bulk density than the T-326 inhaler. The observed decreasing trend in DD with density is accompanied by a corresponding increase in the amount retained in the blister or capsule. The lower variability in fluidization observed for the T-326 inhaler in comparison to the Simoon is attributed to the different mechanisms of powder emptying. The T-326 relies on capsule spinning and agitation, whereas in the Simoon inhaler, powder fluidization is accomplished by a relatively minor airflow passing through the stationary blister, the major fraction of the airflow bypasses the blister (Maltz et al., 2008; Ung et al., 2012). A lower density powder is expected to fill the blister volume more completely, and thus enables the small airflow to be more effective in clearing the powder out of the blister.

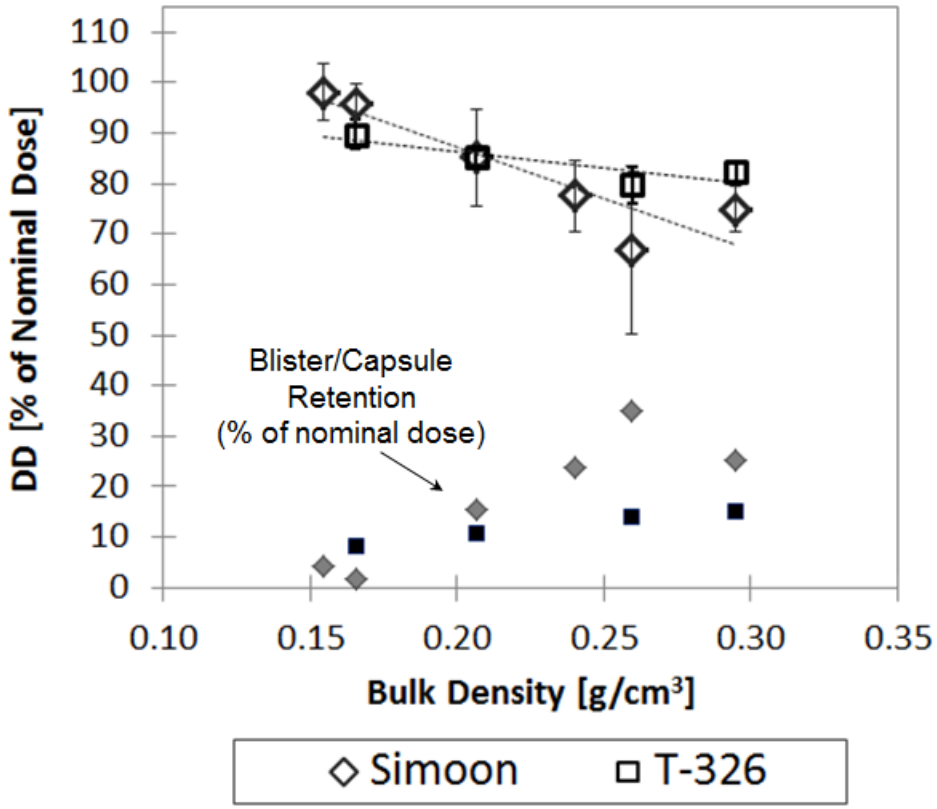

Figure 5.9 Relationship between aerosol performance and bulk density at a 4 kPa pressure drop for delivered dose. Presented as the mean and standard deviation of five replicates.

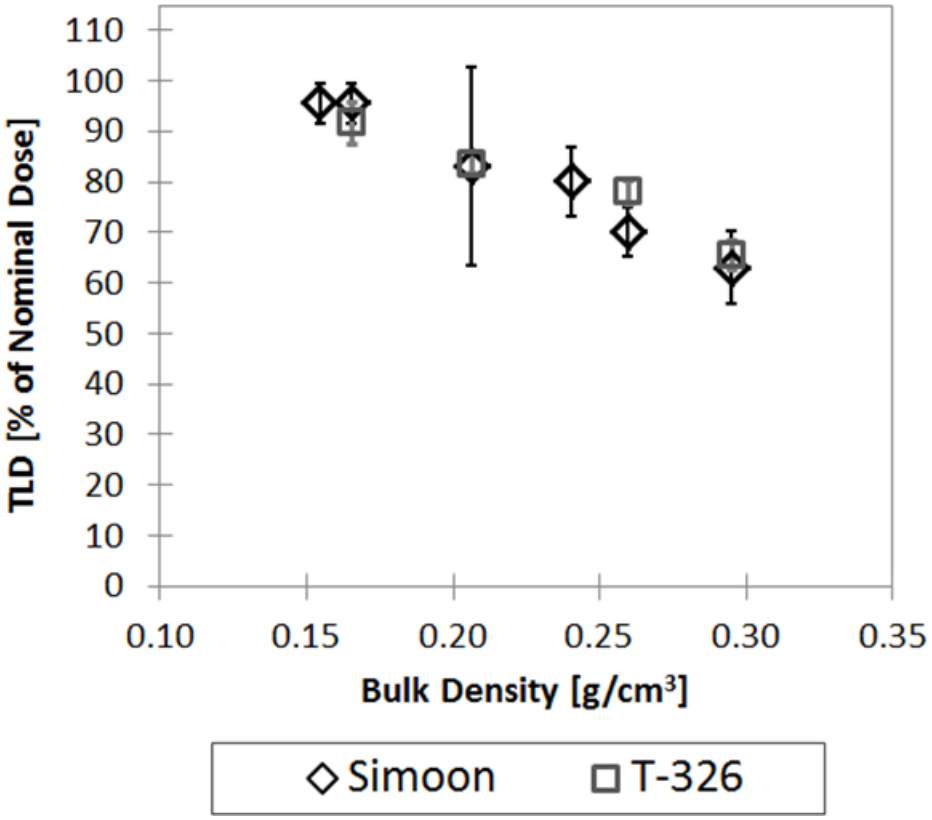

Figure 5.10 Relationship between aerosol performance and bulk density at a 4 kPa pressure drop for *in vitro* total lung dose. Presented as the mean and standard deviation of five replicates.

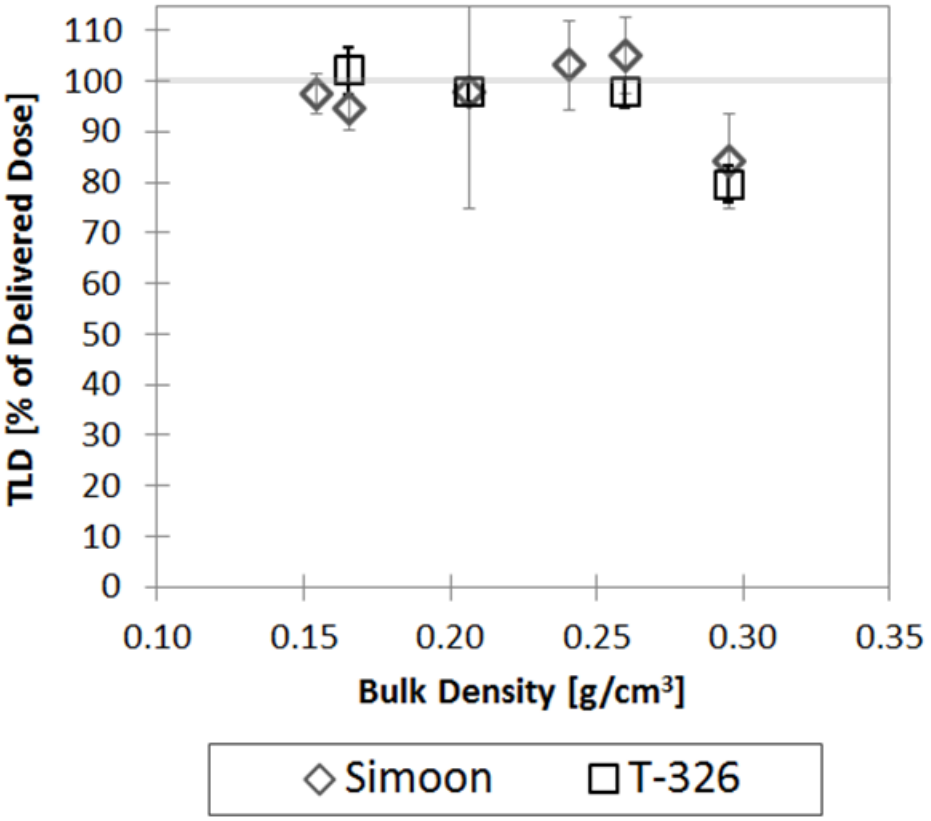

Figure 5.11 Relationship between aerosol performance and bulk density at a 4 kPa pressure drop for *in vitro* total lung dose normalized to delivered dose. Presented as the mean and standard deviation of five replicates.

Figure 5.10 plots the corresponding *in vitro* TLD as measured by the AIT model for the two inhalers. A steep drop in *in vitro* TLD is observed as powder bulk density increases for both inhalers. The drop in the *in vitro* TLD appears to largely reflect the drop in DD. This is further reflected in **Figure 5.11**, which plots the *in vitro* TLD as a percentage of the DD. The low density powders, exhibit an *in vitro* TLD for the Simoon and T-326 inhalers that are comparable to the DD, i.e., there was negligible deposition in the AIT, for bulk density ≤0.26 g/cm^3. That is, the insulin particles are effectively targeted to the lungs.

The effect of flow-rate on dose delivery of insulin inhalation powders was assessed over a range of pressure drops from 2 – 6 kPa. The results of flow-rate testing are presented in **Tables 5.4** and **5.5** and the sequence of bulk density (from low to high) is EXP-C2-05< EXP-C2-04< EXP-C2-06< EXP-C2-07< EXP-C2-03< EXP-C2-02. The results show that the T-326 performance is relatively independent of flow-rate over the full range of pressure drops. The dose delivery performance of the Simoon inhaler is reasonably independent of flow-rate from 2 – 6 kPa, however higher variability was observed for the 2 kPa pressure drop for higher bulk density powders. These differences are once again reflective of the different mechanisms of powder fluidization and dispersion in the two inhalers. Despite these differences, it is clear that for the spray dried insulin inhalation powders studied here, the powder bulk density provides a powerful lever to affect the dose delivery performance with both inhalers, and that the best dose delivery performance for both inhalers is achieved for the insulin powders with the lowest bulk density.

Table 5.4 Effect of inhaler pressure drop (ΔP) and corresponding flow-rate (Q) on DD for six insulin inhalation powders, when tested with the Simoon and T-326 inhalers. Presented as the mean and standard deviation shown in parenthesis of five replicates.

	ΔP	Q	delivered dose (% nominal)					
Inhaler	[kPa]	[L/min]	EXP-C2-02	EXP-C2-03	EXP-C2-04	EXP-C2-05	EXP-C2-06	EXP-C2-07
Simoon (Blister-based)	2	23	65 (6)	61 (13)	80 (35)	96 (3)	88 (6)	80 (7)
	4	33	75 (4)	67 (17)	96 (4)	98 (6)	85 (10)	78 (7)
	6	41	72 (4)	81 (11)	99 (2)	98 (1)	93 (1)	83 (2)
T-326 (Capsule-based)	2	55	84 (2)	75 (5)	88 (4)	Not Tested	85 (5)	Not Tested
	4	78	82 (2)	80 (4)	90 (3)	Not Tested	85 (1)	Not Tested
	6	96	81 (1)	86 (4)	95 (4)	Not Tested	86 (3)	Not Tested

Table 5.5 Effect of inhaler pressure drop (ΔP) and corresponding flow-rate (Q) on *in vitro* TLD for six insulin inhalation powders, when tested with the Simoon and T-326 inhalers. Presented as the mean and standard deviation shown in parenthesis of five replicates.

Inhaler	ΔP [kPa]	Q [L/min]	*in vitro* TLD (% nominal) EXP-C2-02	EXP-C2-03	EXP-C2-04	EXP-C2-05	EXP-C2-06	EXP-C2-07
Simoon (Blister-based)	2	23	63 (11)	64 (18)	82 (22)	97 (5)	91 (3)	79 (12)
	4	33	63 (7)	70 (5)	91 (4)	96 (4)	83 (20)	80 (7)
	6	41	69 (3)	76 (4)	94 (4)	94 (9)	87 (4)	82 (5)
T-326 (Capsule-based)	2	55	74 (3)	74 (5)	90 (1)	Not Tested	80 (4)	Not Tested
	4	78	65 (3)	78 (2)	92 (4)	Not Tested	83 (2)	Not Tested
	6	96	65 (3)	79 (3)	91 (3)	Not Tested	84 (3)	Not Tested

The aerodynamic particle size distributions for campaign-2 powders as determined with the Simoon inhaler at a pressure drop of 4 kPa are presented in **Table 5.6**. With the exception of the larger sized particles obtained in the EXP-C2-02 batch, the remaining powders have an MMAD of about 2 μm. It is worth noting that for batches EXP-C2-04 and EXP-C2-05, virtually the entire nominal dose is sampled on the impactor. That is, the DD is high and deposition in the induction port is low. While comparable MMAD values are sometimes reported for many other pharmaceutical aerosols (Berger and Berger, 2013), the analysis does not account for the size of particles that are lost by impaction in the inhaler and induction port or pre-separator, which often constitutes the major fraction of the delivered dose.

Table 5.6 NGI data obtained for selected powders in the Simoon inhaler at a pressure drop of 4 kPa (33 L/min). Presented as the mean and standard deviation shown in parenthesis of three replicates.

	EXP-C2-02	EXP-C2-03	EXP-C2-04	EXP-C2-05	EXP-C2-06	EXP-C2-07
MMAD (μm)	3.14 (0.09)	1.90 (0.06)	1.78 (0.03)	2.02 (0.04)	2.00 (0.07)	2.26 (0.01)
Fine Particle Fraction <5 μm (% of nominal)	49 (2)	69 (1)	82 (3)	85 (1)	79 (4)	68 (3)
CI Recovery (% of nominal) [a]	60 (1)	74 (2)	87 (4)	93 (2)	84 (4)	74 (4)

[a] Cascade impactor (CI) recovery, which defines as sum of total mass from NGI stage 1 to MOC normalized to nominal dose.

5.4 Discussion

As pointed out by Snyder and Lechuga-Ballesteros (2008), *"The detailed physics of the entire droplet to particle formation process is highly complex and dependent on the coupled interplay between the process variables such as initial droplet size, feedstock concentration*

and evaporation rate, along with the formulation physicochemical properties such as solubility, surface tension, viscosity, and the solid mechanical properties of the forming particle shell". This study explored how variations in feedstock composition and spray drying parameters impact aerosol performance in neat insulin powders for inhalation. Optimal aerosol performance, as assessed by effectively bypassing particle deposition in an anatomical throat model, was achieved for neat insulin powders with a bulk density of ~0.15 to 0.17 $g \cdot cm^{-3}$ and X_{50} less than 2 µm.

The addition of an ethanol co-solvent to an aqueous solution has a significant impact on the physicochemical properties of the solvent system. Solubility of insulin in the feedstock is expected to decrease in the presence of ethanol, resulting in precipitation of insulin earlier in the drying process. Even at mass fractions as low as 5% w/w the addition of ethanol results in significant increases in viscosity and decreases in surface tension, factors that will impact atomization, droplet evaporation, and particle buckling (Khattab et al., 2012). Marty and Tsapis (2008) studied the buckling threshold for drying colloidal droplets in ethanol/water mixtures. The co-solvent mass fraction enabled tuning of the buckling radius and the buckling shell thickness. These factors are expected to impact particle morphology and interparticle interactions.

Attempts were made to qualitatively correlate the observed powder properties to spray drying process and feedstock parameters. The results presented in **Figure 5.12** suggest that bulk density can be modulated by varying ethanol to total solids ratio in the solution feedstock. Low bulk densities were particularly favored when the ethanol to total solids concentration is high.

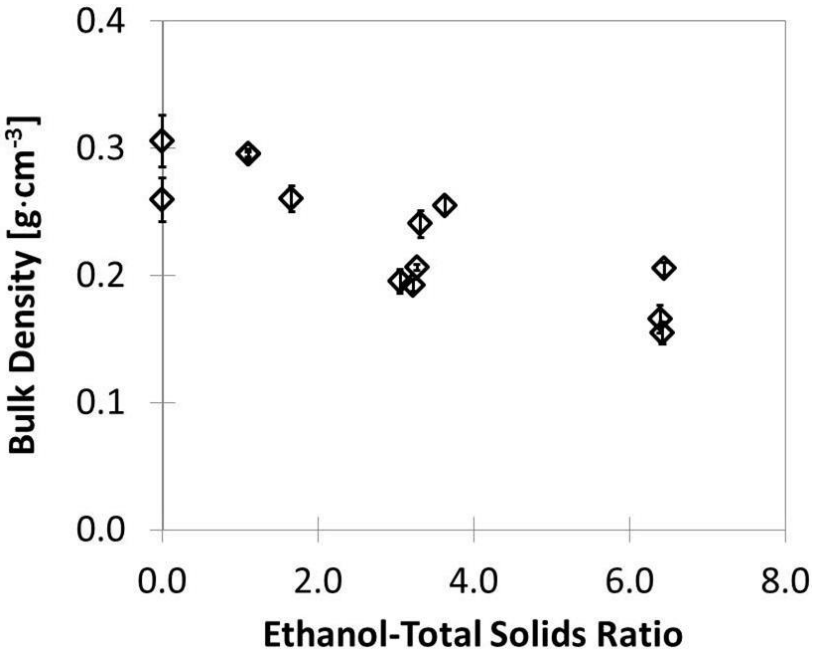

Figure 5.12 Mean powder bulk density scales with ethanol fraction to total solids ratio (error bar represents standard deviation, N = 3 – 5).

The diameter of the spray dried particle is expected to scale with solids content and initial droplet diameter according to Eq. 3:

$$d_g = \sqrt[3]{\frac{C_s \rho_s}{\rho_p}} d_d \qquad (3)$$

where d_d is the initial diameter of the atomized droplet, C_s is total solids in the feedstock, ρ_s is the density of the feedstock solution, and ρ_p is the particle density (Snyder et al., 2008; Vehring 2007). Besides solid concentration, it is well known that the particle size, X_{50}, corresponds to the total gas flow based on the theory of cyclone collection efficiency (Barth, 1956). Combining formulation and spray drying variables, a dimensionless number termed

the Particle Population Density, PPD Eq. (4) was found to correlate with particle diameter of spray dried powders.

$$PPD = \frac{C_s Q_L}{Q_T} \qquad (4)$$

where Q_L is the atomizer liquid flow-rate, and Q_T is the total dryer gas flow-rate. **Figure 5.13** is a plot showing the correlation between X_{50} and PPD. The correlations based on the results from this co-solvent spray drying study with insulin suggest that feedstock and process parameters can be modulated to achieve a desired particle density and size to enable maximum targeting of aerosol to the lungs.

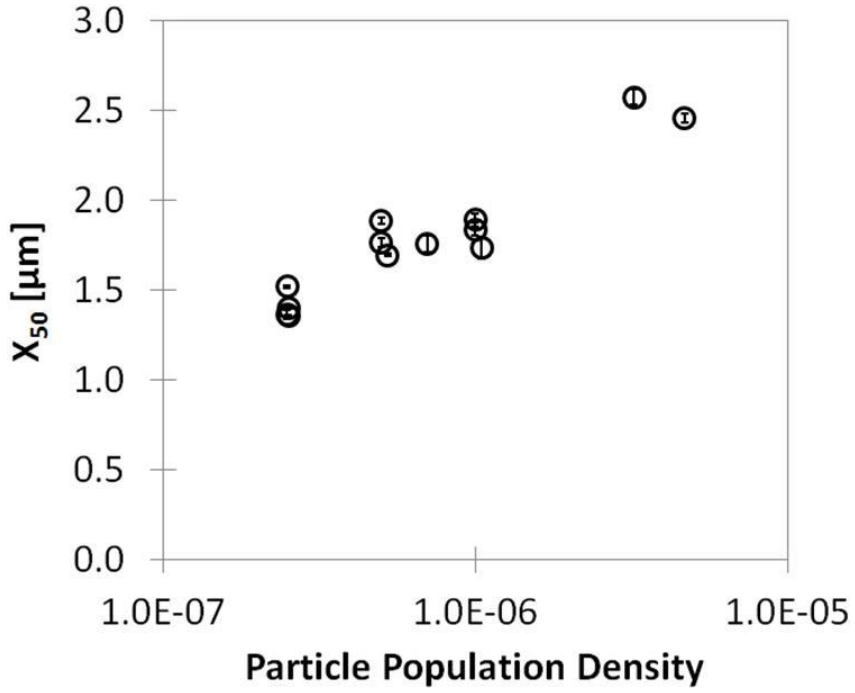

Figure 5.13 Mean X_{50} scales with particle population density parameter (error bar represents standard deviation, N = 3).

As discussed in the introduction, deposition in the mouth-throat is governed by inertial impaction and as such depends critically on the inertial impaction parameter, $d_a^2 Q$. Stahlhofen et al. (1989) studied the impact of variations in $d_a^2 Q$ on regional deposition in the respiratory tract for monodisperse liquid aerosols. No deposition in the mouth-throat was observed for aerosols with $d_a^2 Q < 120$ μm^2·L/min. In the present study, nearly 100% of the DD bypasses deposition in the AIT for lots EXP-C2-04 and EXP-C2-05. Based on the measured MMAD values in TABLE 6 and the test flow-rate (33 L/min), the $d_a^2 Q$ values were 105 and 135 μm^2·L/min, respectively. A significant reduction of deposition in the AIT observed is, therefore, consistent with the results of Stahlhofen *et al.*

Borgström et al. (2006) demonstrated that a significant component of the variability in drug delivery to the lungs results from anatomical differences in a subject's mouth-throat. For current marketed portable inhalers where mean total lung deposition is on the order of 10 – 30%, the mean variability in TLD is approximately 30 – 50%. In the limit where particles are able to entirely bypass deposition in the extrathoracic region, the variability in TLD would by definition, be zero. Hence, significant improvements in dose consistency are anticipated as the drug/device combinations are designed to minimize extrathoracic region deposition. This may be especially important for drugs with a narrow therapeutic index like insulin, or drugs that elicit significant side-effects in the mouth-throat, such as inhaled corticosteroids.

Finally, the small MMAD noted for these aerosols suggests that a significant fraction of the DD will be deposited in the peripheral airways. For proteins like insulin, it has been hypothesized that deposition in the lung parenchyma is critical for achieving effective absorption into the systemic circulation (Patton and Byron, 2007).

5.5 Conclusion

This study explored a particle design space, covering particle size and density, for spray dried insulin microparticles with the aim of enhancing inhalation drug delivery. A co-solvent system comprising small amounts of ethanol added to water in the spray drying feedstock enabled a broad range of powder properties to be achieved. The results demonstrate that by varying the formulation and spray drying parameters it is possible to modulate powder properties and thereby the performance of inhalation powders in dry powder inhalers. Bulk powder data from 13 spray dried insulin powder lots were used to propose predictive correlations relating particle size and density to groupings of feedstock and process variables. *In vitro* dose delivery testing of selected powders with two dry powder inhalers showed that the dose delivery performance was strongly influenced by powder bulk density, with delivery performance improving with decreasing powder density. The *in vitro* performance testing also identified an insulin particle design space where the emitted aerosol is characterized by inertial parameter $d_a^2 Q$ < 120 μm^2·L/min, suggesting that spray dried powders provide a practical means to achieve efficient targeting of the lung with negligible extrathoracic deposition.

5.6 References

1. Al-Ahowair RAM, Tarsin WY, Assi KH, Pearson SB, and Chrystyn H. Can all patients with COPD use the correct inhalation flow with all inhalers and does training help? *Resp. Med.* 2007; **101**: 2395 – 2401.

2. Balducci AG, Cagnani S, Sonvico F, Rossi A, Barata P, Colombo G, Colombo P, and Buttini F. Pure insulin highly respirable powders for inhalation. *Eur. J. Pharm. Sci*. 2015; **51**: 110 – 117.

3. Barth W. Design and layout of cyclone separator on the basis of new investigation. Brennstoff-Warme-Kraft. 1956; **8**: 1 – 9.

4. Berger R and Berger WE. Particle size and small airway effects of mometasone furoate delivered by dry powder inhaler. *Allergy and Asthma Proceedings*. 2013; **34**: 52-58.

5. Borgström L, Olsson B, and Thorsson L. Degree of throat deposition can explain the variability in lung deposition of inhaled drugs. *J. Aerosol Med.* 2006; **19**: 473 – 483.

6. Boraey MA, Hoe S, Sharif S, Miller DP, Lechuga-Ballesteros D, Vehring R. Improvement of the dispersibility of spray-dried budesonide powders using leucine in an ethanol–water co-solvent system. Powder Technol. 2013; 236: 171 – 178.

7. Chew NYK and Chan H-K. Use of solid corrugated particles to enhance powder aerosol performance. *Pharm. Res*. 2011; **18**: 1570 – 1577.

8. Clark AR and Hollingworth AM. The relationship between powder inhaler resistance and peak inspiratory conditions in healthy volunteers – implications for in vitro testing. *J. Aerosol Med*. 1993; **6**: 99 – 110.

9. DeHaan WH and Finlay WH. In vitro monodisperse aerosol deposition in a mouth and throat with six different inhalation devices. *J. Aerosol Med*. 2001; **14:** 361 – 367.

10. Delvadia RR, Hindle MP, Longest PW, and Byron PR. *In vitro* tests for aerosol deposition II: IVIVCs for different dry powder inhalers in normal adults. *J. Aerosol Med.* 2013; **26:** 138 – 144.

11. Dunbar C. Porous particles for inhalation: The science behind their improved dispersibility. *Proc. Respir. Drug Deliv.* 2006; **1**: 307 – 315.

12. Edwards AE, Hanes J, Caponetti G, Hrkach J, Ben-Jebria A, Eskew ML, Mintzes J, Deaver D, Lotan N, and Langer R. Large Porous Particles for Pulmonary Drug Delivery. Science. 1997; 276: 1868 – 1871.

13. Edwards AE, Ben-Jebria A, Langer R. Recent Advances in Pulmonary Drug Delivery Using Large, Porous Inhaled Particles. J. Appl Physiol. 1998; 85: 379 – 385.Finlay WH. The mechanics of inhaled pharmaceutical aerosols: An introduction. *Academic Press*. 2001.

14. Geller DE, Weers JG, and Heuerding S. Development of an inhaled dry-powder formulation of tobramycin using PulmoSphere™ technology. *J. Aerosol Med.* 2011; **24**: 175 – 182.

15. Khattab IS, Bandarkar F, Fakhree MAA, and Jouyban A. Density, viscosity, and surface tension of water+ethanol mixtures from 293 to 323K. *Korean J. Chem. Eng*. 2012; **29**: 812 – 817.

16. Maltz DS, Glusker M, Axford G, Postich M, Rao N, and Ung K. A novel passive dry powder inhaler for unit dose delivery to the deep lung. *Proc. Respir. Drug Deliv*. 2008; **3**: 669 – 674.

17. Maltz DS and Paboojian SJ. Device engineering insights into TOBI® Podhaler®: A development case study of high efficiency powder delivery to cystic fibrosis patients. *Proc. Respir. Drug Deliv. Europe*. 2011; **1**: 55 – 66.

18. Marty G and Tsapis N. Monitoring the buckling threshold of drying colloidal droplets using water-ethanol mixtures. *Eur. Phys. J. E.* 2008; **27**: 213 – 219.

19. Olsson B, Borgström L, Lundbäck H, and Svensson M. Validation of a general *in vitro* approach for prediction of total lung deposition in healthy adults for pharmaceutical inhalation products. *J. Aerosol Med*. 2013; **26**: 1 – 15.

20. Patton JS and Byron PR. Inhaling medicines: Delivering drugs to the body through the lungs. *Nature Rev. Drug Discov*. 2007; **6**: 67-74.

21. Rabinovich YI, Adler JJ, Ata A, Singh RK, Moudgil BM. Adhesion between nanoscale rough surfaces: I. role of asperity geometry. *Journal of Colloid and Interface Science.* 2000; **232**: 10 – 16.

22. Rietema K. The dynamics of fine powder. *Kluwer Academic Publishers*. 1991.

23. Rumpf H. Particle Technology. *Chapman and Hall*. London, 1990.

24. Shekunov BY, Chattopadhyay P, Tong HHY, and Chow AHL. Particle size analysis in pharmaceutics: principles, methods and applications. *Pharm. Res*. 2007; **24**: 203 – 227.

25. Snyder HE and Lechuga-Ballesteros D. "Spray drying: theory and pharmaceutical applications." *Pharmaceutical Dosage Forms: Tablets*. Informa Healthcare. Third Edition 2008; **1**: 227 – 260.

26. Stahlhofen W, Rudof G, and James AC Intercomparison of Experimental Regional Aerosol Deposition Data. *J. Aerosol Med*. 1989; **2:** 285 – 308.

27. Stapleton KW, Guentsch E, Hoskinson MK, and Finlay WH. On the suitability of κ–ε turbulence modeling for aerosol deposition in the mouth and throat: A comparison with experiment. *J. Aerosol Sci*. 2000; **31:** 739 – 749.

28. Ung TK, Axford G, Chan L, Glusker M, Le J, Maltz D, Rao N, Weers JG. Effect of powder release kinetics on the performance of a dry powder inhaler. *Respir. Drug Deliv*. 2012; **3**: 627 – 630.

29. Ung TK, Rao N, Weers JG, Clark AR, and Chan H-K. *In vitro* assessment of dose delivery performance of engineered dry powders for inhalation. *Aerosol Sci. & Tech*. 2014; **48**: 1099 – 1110.

30. Vehring R. Pharmaceutical particle engineering via spray drying. *Pharm. Res*. 2007; **25**: 999 – 1022.

31. Vanbever R, Mintzes JD, and Wang J. Formulation and physical characterization of large porous particles for inhalation. Pharm. Res. 1999; 16: 1735 – 1742.

32. Weers JG, Ung K, Le J, Rao N, Ament B, Axford G, Maltz D, and Chan L. Dose emission characteristics of placebo PulmoSphere® particles are unaffected by a subject's inhalation maneuver. *J. Aerosol Med.* 2013; **26**: 56 – 68.

33. Weers JG, Clark AR, Rao N, Ung K, Haynes A, Khindri SK, Sheryl A, Perry SA, Machineni S, and Colthorpe P. *In vitro–in vivo* correlations observed with indacaterol-based formulations delivered with the Breezhaler®. *J. Aerosol Med*. 2015; **28**: 1 – 13.

34. Weiler C, Egen M, Trunk M, and Langguth P. Force control and powder dispersibility of spray dried particles for inhalation. *J. Pharm Sci*. 2010; **99**: 303 – 316.

35. White S, Bennett D, Cheu S, Conley PW, Guzek DB, Gray S, Howard J, Malcolmson R, Parker JM, Roberts P, Sadrzadeh N, Schumacher JD, Seshadri S, Sluggett GW, Stevenson CL, and Harper NJ. EXUBERA®: Pharmaceutical development of a novel product for pulmonary delivery of insulin. *Diabetes Technol. Ther*. 2005; **7**: 896 – 906.

36. Zhang Y, Gilbertson K, and Finlay WH. *In vivo-in vitro* comparison of deposition in three mouth-throat models with QVAR® and Turbuhaler® inhalers. *J. Aerosol Med*. 2007; **20**: 227 – 235.

Chapter 6

Conclusion

6.1 Summary

A simple adjustment to the insulin feedstock solution (i.e., total solids and ethanol-to-water ratio) is effective at changing the bulk density and size of spray dried insulin particles, which in turn improves their aerosol delivery performance when dispersed by passive dry powder inhalers. The *in vitro* aerosol performance was favored by lower bulk density and smaller equivalent optical diameter of the particles, with deposition in the extrathoracic region anticipated to be significantly reduced. Results suggest that total lung dose of up to 95% of the delivered dose could be achieved with the engineered particle formulations, significantly higher than those for drug products with lactose-based carrier, for which TLD was typically <40% of the DD. The high TLD of the protein microparticles achieved in *in vitro* tests suggest that a remarkably high degree of lung targeting could be achieved with engineered powders, almost completely bypassing deposition in the extrathoracic region.

The selection of ethanol as a co-solvent for spray drying was guided by a screening study presented in **Chapter 2**. Here 5 different co-solvents were initially studied using spray dried insulin particles as a model system. Small amounts of co-solvent added to the insulin aqueous solution feedstock significantly lowered the bulk density of spray dried particles, in comparison to those obtained by spray drying without solvent addition. SEM examination of powder samples showed a mixture of oval and corrugated "wrinkled" particles with solvent addition, versus only wrinkled particles for the case where no solvent was added. While the

addition of co-solvent and lowering of powder density appeared to be related to the appearance of the oval particle morphology, an effort to develop a mechanistic explanation for this phenomenon is beyond the scope of this work. The study focused on correlating powder properties with *in vitro* aerosol performance, and therefore the improved performance was favored for low bulk density insulin powders when delivered with a capsule-based T-326 dry powder inhaler.

Chapter 3 discusses why it was necessary to develop an alternative tool (i.e., Alberta Idealized Throat model) for assessing inhaled drug performance, rather than relying on conventional methods, such as those based on cascade impactors, e.g., Next Generation Impactor. The advantages of the Alberta Idealized Throat (AIT) over standard cascade impactors (i.e., NGI, ACI, and MSLI) are (a) direct measurement of *in vitro* TLD, (b) better at capturing the physics of particle transport and deposition in patient airways, (c) allowing the use of realistic breath profiles when simulating patient use scenarios, and (d) no airflow and volume limitations during testing. Although the AIT has not been adopted as an industry standard, results from *in vitro* testing comparing the AIT and NGI with a panel of engineered powders and 2 marketed products give similar rank order when using the TLD as a metric of product performance.

Several marketed inhalation drug products along with a Novartis prototype inhaler with engineered powder formulation were tested in **Chapter 4** to investigate the effect of ramp-up flow-rate on *in vitro* aerosol performance. The AIT was used in the study as it provides the most practical means to measure the *in vitro* aerosol delivery performance for inhalers with different flow resistances, and for more complex airflow profiles. The results show the effect of flow ramp on DD is relatively small for all DPIs tested in the study. However, greater

variation was observed in the TLD, with the Asmanex® Twisthaler® showing the greatest variation as a function of flow ramp. The flow ramp effect on TLD essentially reflect an underlying flow-rate dependence effect, since different ramp conditions lead to differences in the "effective" flow-rate during the aerosolization event.

Chapter 5 presented a deeper exploration of co-solvent spray drying of inhalable drugs, focused on ethanol as the co-solvent, and insulin as the model inhaled drug. The study explored a particle design space covering density and size, by varying parameters such as ethanol fraction in the aqueous solution feedstock, solids content, and air-to-liquid ratio, the final spray drying campaign with neat insulin was successful in producing powders with bulk density ranging from 0.15 – 0.30 g/cm^3 and particle size ranging from1.36 – 2.58 μm, respectively. An Alberta idealized throat model was used to assess total lung dose for each powder formulation, when delivered from two different dry powder inhalers. *In vitro* test results showed that a high TLD >95% of the delivered dose could be achieved, which suggested that deposition in the extrathoracic region could be reduced to negligible levels. In summary, the study identified a favorable design space for engineered particles, targeting a certain range of micromeritic properties in order to essentially maximize total lung delivery.

6.2 Future work

This thesis demonstrated co-solvent spray drying with small amount of ethanol addition added to the aqueous solution can be used to modulate the bulk density and size of the particles. Results show good correlation between powder properties and *in vitro* aerosol performance of spray dried pure insulin microparticles. A significant finding in this thesis

shows engineered particles could be used to target certain range of micromeritic properties in order to achieve maximum total lung delivery, where *in vitro* TLD was improved and favored for powders with low bulk density and small particle size. Most of the findings here were based on *in vitro* testing using the model throats. *In vivo* proof-of-concept studies to confirm these findings are beyond the scope of the present work, but are acknowledged as a necessary step towards demonstrating the viability of the co-solvent spray drying approach for inhaled drugs.

While this thesis focuses on using ethanol as process aid to control the micromeritic properties of the spray dried particles, other factors to engineer the particles (i.e., use of shell-former excipient or other solvents) should be further explored, as well as application to other biological or small molecule compounds.

Although insulin was a candidate compound used in this research study, the chemical stability and biological activity of the drug product post spray drying was not assessed, as the research is primarily focusing on physical properties (i.e., particle size and density and *in vitro* aerosol performance) of spray dried formulations. The focus of this thesis is not to develop an inhaled insulin product, but to use insulin as a model compound to study the effect of ethanol addition during spray drying of engineered particles, with a view to minimize deposition in the extrathoracic region and maximize total lung delivery.

Other suggestions for future work: This thesis has shown that small amounts of co-solvent addition to aqueous solution feedstock can be used to modulate insulin particle morphology in a direction more favorable for aerosol delivery performance. No attempt has been made to develop a theoretical framework to explain these findings, particularly the mixed morphology

of wrinkled and oval particles associated with the powder samples from co-solvent spray drying. This is partly due to lack of solubility data for insulin in various co-solvent mixtures, which is essential to modeling of particle formation.